Model motora s unutarnjim izgaranjem za ispitnu stanicu

Mustać, Jurica

Master's thesis / Diplomski rad

2018

Degree Grantor / Ustanova koja je dodijelila akademski / stručni stupanj: **University of Zagreb, Faculty of Mechanical Engineering and Naval Architecture / Sveučilište u Zagrebu, Fakultet strojarstva i brodogradnje**

Permanent link / Trajna poveznica: https://urn.nsk.hr/urn:nbn:hr:235:531126

Rights / Prava: In copyright / Zaštićeno autorskim pravom.

Download date / Datum preuzimanja: **2024-03-28**

Repository / Repozitorij:

Repository of Faculty of Mechanical Engineering and Naval Architecture University of Zagreb







UNIVERSITY OF ZAGREB
FACULTY OF MECHANICAL ENGINEERING AND NAVAL ARCHITECTURE

MASTER'S THESIS

Jurica Mustać

Zagreb, 2018.

UNIVERSITY OF ZAGREB
FACULTY OF MECHANICAL ENGINEERING AND NAVAL ARCHITECTURE

MASTER'S THESIS

Mentor:

Prof. dr. sc. Darko Kozarac, dipl. ing.

Student:

Jurica Mustać

Zagreb, 2018.

Izjavljujem da sam ovaj rad izradio samostalno koristeći znanja stečena tijekom studija i navedenu literaturu.

I declare that I have completed this thesis using the knowledge and skills gained during my universities studies and using specified literature.

Jurica Mustać

Zahvala

Prvo bih se zahvalio svome mentoru, profesoru dr.sc. Darku Kozarcu što me prihvatio pod svoje mentorstvo unatoč administrativnim poteškoćama. Također mu se zahvaljujem za pruženu podršku tijekom rada te za sve korisne savjete i natuknice.

Također se zahvaljujem svim kolegama u tvrtki AVL-AST d.o.o. koji su mi svojim savjetima i kritičkim razmišljanjem pomogli tijekom izrade rada.

Posebno se ipak zahvaljujem svojoj obitelji i bližnjima koji su mi bili najveća podrška kroz studij i izradu diplomskog rada.

Acknowledgments

First I'd like to thank my mentor, professor dr.sc. Darko Kozarac for accepting me into his mentorship despite the administrative difficulties. I thank him as well for the provided support during the thesis and for all the useful tips and guidelines.

I also thank all of my colleagues from AVL-AST d.o.o. who, with their advice and critical thinking, helped me during the thesis.

My special thanks go to my family and close ones who have been my biggest support during my studies and writing of this thesis.

SVEUČILIŠTE U ZAGREBU
FAKULTET STROJARSTVA I BRODOGRADNJE
Središnje povjerenstvo za završne i diplomske ispite
Povjerenstvo za diplomske radove studija strojarstva za smjerove:
proizvodno inženjerstvo, računalno inženjerstvo, industrijsko inženjerstvo i menadžment, inženjerstvo materijala te mehatronika i robotika

Sveučilište u Zagrebu Fakultet strojarstva i brodogradnje	
Datum:	Prilog:
Klasa:	
Ur. broj:	

DIPLOMSKI ZADATAK

Student: **JURICA MUSTAĆ** Mat. br.: 0035194969

Naslov rada na hrvatskom jeziku: **Model motora s unutarnjim izgaranjem za ispitnu stanicu**

Naslov rada na engleskom jeziku: **Test bed internal combustion engine simulator**

Opis zadatka:

Test of a vehicle performance, emissions and drivability is during development phase performed by a real Internal Combustion Engine (ICE) set on Engine Test Bed (ETB) and connected with a Real Time Vehicle Simulation (RT-VS). In order to reduce the setup time for connecting the real ICE (on ETB) with RT-VS model the RT-VS has to be prepared in the office environment with a simulation model of ICE. Currently in this process RT-VS uses a mean value model of each component including mean value model of the engine speed and torque. Since in real ICE the crankshaft speed and torque is not constant but oscillates as a consequence of real cycles, in order to obtain the correct engine speed and torque, a more detailed real time engine model (RT-EM) has to be developed.
The new RT-EM has to model all important effects that are responsible for engine torque and engine speed oscillations, e.g. combustion, inertias of crank – slider mechanism elements and distribution of forces in the crank slider mechanism. Finally a control system for engine parameters has to be designed with all of its accompanying subsystems. Based on the objectives of the thesis it is necessary to:
1. Study available literature on ICE design, controls and control unit subsystems.
2. Model the dynamic Slider-Crank mechanism that includes inertia forces and model the combustion process in order to reproduce crankshaft torque generated by the cylinder pressure (use MATLAB/Simulink).
3. Design and implement low-level controllers for air-fuel ratio, boost pressure, EGR and throttle flow (PID control).
4. Design and implement high-level (supervisory) controllers such as idle speed control and cruise control (engine control unit).
5. Compile the model to standard co-simulation model (FMU) including the model parameters.
During thesis preparation one must comply with the rules for preparation of the Master thesis.
It is necessary to list all literature used and received assistance.

Zadatak zadan:
27. rujna 2018.

Rok predaje rada:
29. studenog 2018.

Predviđeni datum obrane:
05. prosinca 2018.
06. prosinca 2018.
07. prosinca 2018.

Zadatak zadao:
prof. dr. sc. Darko Kozarac

Predsjednica Povjerenstva:
prof. dr. sc. Biserka Runje

CONTENT

CONTENT I
LIST OF FIGURES III
LIST OF TABLES V
LIST OF SYMBOLS VI
SAŽETAK X
SUMMARY XI
1. INTRODUCTION 1
1.1. Motivation 1
2. ICE MODEL TYPE SELECTION 4
2.1. Types of ICE models 4
2.1.1. Theoretical and experimental models 4
2.1.2. Mean value and Discrete event models 6
2.2. Characteristics of the developed model 7
3. MODEL DESCRIPTION 8
3.1. Traces model 8
3.1.1. Cylinder energy balance equation 10
3.1.2. Cylinder geometry relations 12
3.1.3. Combustion model 15
3.1.4. Thermodynamic properties of the gas mixture 19
3.1.5. Heat losses 20
3.1.6. Initial conditions 24
3.1.7. Torque calculation 33
3.2. Transient model 38
3.2.1. Altered traces model 40
3.2.2. Indicated engine torque 41
3.2.3. Engine friction 43
3.2.4. Performance 45
3.2.5. Engine inertia 48
3.2.6. Flywheel 50
3.2.7. T-engine or N-engine model 51
3.3. Results validation and comments 54
3.3.1. Traces model results 54
3.3.2. Transient model results 59
4. ENGINE CONTROL SYSTEMS 64
4.1. Idle speed control 65
4.1.1. PI control 66
4.1.2. Sliding mode control introduction 67
4.1.3. SMC design 70
4.1.4. PI Control with an additional simple SMC part 75
4.1.5. Results and performances 77
4.2. Cruise Control 83

5. FMU COMPILATION 86
6. CONCLUSION 89
REFERENCES 91
APPENDICES 93
Appendix A 94
Appendix B 97
NA SI Engine 97
TC CI Engine 100
Appendix C 102

LIST OF FIGURES

Figure 1. An example of AVL testbed environment [2] 2
Figure 2. Types of mathematical process models 5
Figure 3. Cylinder geometry basic relations [8] 12
Figure 4. Four strokes of the engine cycle, cylinder volume defined with the intake value at the start of the cycle, data from Appendix A, Engine 1 15
Figure 5. The Shape of the predefined heat release depending on parameter *m* 17
Figure 6. An example of a Sankey diagram for an ICE [8] 20
Figure 7. Calculated heat transfer coefficient, Woschni method. Data from Appendix A, Engine 1 22
Figure 8. Volumetric efficiency based on (22) 26
Figure 9. Naturally aspirated SI engine intake pressure look-up table 27
Figure 10. Turbocharged CI engine intake pressure look-up table 28
Figure 11. CI engine fuel mass look-up table, data for Appendix A, Engine 2 30
Figure 12. SI engine exhaust pressure look-up table, Appendix A, Engine 1 31
Figure 13. CI engine exhaust pressure look-up table, Appendix A, Engine 2 31
Figure 14. A first-order system approximation of the exhaust stroke 32
Figure 15. A block representation of the developed traces model 35
Figure 16. Calculating and reseting the crank-angle α 39
Figure 17. Values of the crank-angle during several cycles 39
Figure 18. Transient cylinder pressure calculation 40
Figure 19. Torque calculation for a different number of cylinders 42
Figure 20. Detail of the enabled subsystem for a 4_cylinder case 43
Figure 21. Friction mean effective pressure map 44
Figure 22. Mean indicated torque block diagram 45
Figure 23. Reset T block of the mean indicated torque calculation 46
Figure 24. Distribution of engine work using the mean pressure values. In idle, all of the indicated work is spent on friction (mechanical) losses.[8] 46
Figure 25. The dual-mass flywheel dynamics [3] 50
Figure 26. An example of an N model engine speed where a constant value is given as an input to the model 52
Figure 27. Equation (53) in Simulink and the T or N model selection via a switch and a variable 53
Figure 28. The T or N engine model classification 53
Figure 29. Indicated cylinder pressure at 3000rpm and load signal = 1, data from Appendix A, Engine 1 54
Figure 30. Cylinder pressure trace through various engine speeds, load signal = 0.2, thesis model result, data from Appendix A, Engine 1 55
Figure 31. Cylinder pressure trace through various engine speeds, load signal = 0.2, AVL Cruise M model result, data from Appendix A, Engine 1 55
Figure 32. Inertia forces at 3000rpm, oscillating mass is 0.47kg 56
Figure 33. Combined piston forces for at 3000rpm, data from Appendix A, Engine 1 57
Figure 34. Combined piston forces at 3000rpm, data from Appendix A, Engine 2 57
Figure 35. Indicated torque at 3000rpm and load signal = 1, data from Appendix A, Engine 1 58
Figure 36. Indicated torque one cylinder trace at 2000rpm and load signal = 1, thesis model result and AVL Excite result comparison, data from Appendix A, Engine 2 58
Figure 37. Total indicated torque of a 4-cylinder engine at 3000rpm, data from Appendix A Engine 1 59

Figure 38. Shifted cylinder pressure, now the start of the cycle is the compression stroke, data is the same as in Figure 29 60
Figure 39. Indicated torque of a 6-cylinder engine at 3000rpm, data from Appendix A, Engine 3 60
Figure 40. Engine speed oscillations at 3000rpm, data from Appendix A, Engine 1 61
Figure 41. Effect of the dual-mass flywheel concept on the engine speed fluctuations 62
Figure 42. Engine torque fluctuations before and after the dual-mass flywheel, 4 cylinder engine 62
Figure 43. System trajectories converging onto sliding surface *S* [22] 69
Figure 44. Engine load acting upon the flywheel 77
Figure 45. ISC response of Engine 3, data from Appendix A, various control systems 78
Figure 46. Control signal for Engine 3, data from Appendix A, various control systems 78
Figure 47. ISC response of Engine 4, data from Appendix A, various control systems 79
Figure 48. Control signal for Engine 4, data from Appendix A, various control systems 79
Figure 49. ISC response of Engine 2, data from Appendix A, various control systems 80
Figure 50. Control signal for Engine 2, data from Appendix A, various control systems 80
Figure 51. ISC response of Engine 5, data from Appendix A, various control systems 81
Figure 52. Control signal for Engine 5, data from Appendix A, various control systems 81
Figure 53. Imposed engine load during the simulation 84
Figure 54. Cruise control system performance 84
Figure 55. Brake mean engine torque 84
Figure 56. FMI in the Model Connect environment along with the main model parameters 88
Figure 57. Vehicle velocity profile, WLTP 88

LIST OF TABLES

Table 1. Values of parameters α_c and *m* for different engine types 17
Table 2. Indicated torque signal delay table 42
Table 3. Performance of designed control systems, ISC, Engine 3, data from Appendix A 78
Table 4. Performance of designed control systems, ISC, Engine 4, data from Appendix A 79
Table 5. Performance of designed control systems, ISC, for Engine 2, data from Appendix A 80
Table 6. Performance of designed control systems, ISC, Engine 5, data from Appendix A 81

LIST OF SYMBOLS

Symbol	Unit	Description
A	m^2	Nominal piston surface area
A/F	-	Air/Fuel ratio
a_c	m/s^2	Piston acceleration
b	-	System input coefficient
BDC	m	Cylinder bottom dead center
$BMEP$	bar	Brake mean effective pressure
C	-	Vibe parameter
C_1	-	Heat transfer parameter
C_2	-	Heat transfer parameter
C_{fly}	Nm/rad	Flywheel stiffness factor
c_m	m/s	Mean piston speed
c_v	J/(kg K)	Specific heat at constant volume
D	m	Cylinder diameter
D_{fly}	Nm s/rad	Flywheel damping factor
e	rad/s	Tracking error
F	N	Combined forces acting upon the piston
$FMEP$	bar	Friction mean effective pressure
F_g	N	Gas forces
F_{in}	N	Inertia forces
H	m	Cylinder stroke
H_l	MJ/kg	Fuel lower heating value
h	m	Piston path
h_{BB}	J/kg	Specific enthalpy of the blow-by
h_e	J/kg	Specific enthalpy of the mass flowing out of the cylinder
h_i	J/kg	Specific enthalpy of the mass flowing into the cylinder
$IMEP$	bar	Indicated mean effective pressure
J	kg m^2	Engine moment of inertia
J_E	kg m^2	Engine inertia (flywheel section)
J_{fly}	kg m^2	Flywheel moment of inertia
J_{rot}	kg m^2	Rotating part of the engine inertia

K_I	1/rad	PI integral gain
K_P	s/rad	PI proportional gain
K_{SMC}	-	SMC Control gain
L	-	SMC boundary layer width
l	m	Conrod length
m	-	Vibe shape parameter
m_a	kg	Mass of the fresh working substance in the cylinder
m_{BB}	kg	Mass of the blow-by
m_c	kg	Gas mass in the cylinder
$m_{conrod,osc}$	kg	Oscillating part of the conrod mass
$m_{conrod,rot}$	kg	Rotating part of the conrod mass
m_{crank}	kg	Crankshaft mass
m_e	kg	Mass flowing out of the cylinder
m_{exh}	kg	Residual combustion products mass
m_f	kg	Fuel mass in the cylinder
m_i	kg	Mass flowing into the cylinder
m_{osc}	kg	Oscillating mass
m_p	kg	Piston mass
m_{rot}	kg	Rotating mass
n	rpm	Engine speed in rpm
u	-	System control input
p_0	Pa	The pressure at the end of the intake
p_c	Pa	Cylinder pressure
p_{exh}	Pa	Exhaust pressure
p_h	Pa	Housing pressure
p_m	bar	Motored pressure
p_{st}	Pa	Standard pressure
Q_{cl}	J	Heat transferred by cooling
Q_{ev}	J	Fuel evaporation heat
Q_f	J	Fuel heat input
Q_m	J	Heat transferred by friction
Q_{rad}	J	Radiation heat
Q_w	J	Wall heat losses

R	J/(kg K)	Specific gas constant
S	-	Sliding surface
r	m	Crankshaft radius
T_0	K	Cylinder temperature in the intake manifold
T_B	Nm	Brake engine torque
$\overline{T_B}$	Nm	Mean brake engine torque
T_c	K	Cylinder temperature
T_{exh}	K	Residual combustion products temperature
T_F	Nm	Friction torque
T_{fly}	Nm	Engine torque transmitted by the flywheel
T_h	K	Cylinder head temperature
T_I	Nm	Indicated torque
$\overline{T_I}$	Nm	Mean indicated engine torque
T_L	Nm	Engine load
T_l	K	Liner temperature
T_p	K	Piston temperature
T_s	K	Standard temperature
TDC	m	Cylinder top dead center
u	-	System input
V	m^3	Cylinder volume
$V(S)$	-	Lyapunov function
V_0	m^3	Cylinder volume at the end of the intake
V_E	m^3	Total engine displacement
V_H	m^3	Cylinder displacement
V_K	m^3	Cylinder compression volume
v	-	Piston speed
W_b	J	Brake or effective work
W_i	J	Indicated work
W_m	J	Mechanical or friction work
x	-	Mass fraction burned
y	-	Control system output
y_d	-	Desired system output
$\tilde{y}$	-	System tracking error

Z_0	-	Stochiometric A/F ratio
z	-	Number of cylinders
α	rad	Crank angle
α_0	rad	Start of combustion
α_c	rad	Combustion duration
α_w	W/(m^2 K)	Heat transfer coefficient
γ	-	Residual combustion products fraction
ε	-	Cylinder compression ratio
η_b	-	Brake efficiency
η_m	-	Mechanical efficiency
η_v	-	Volumetric efficiency
κ	-	Specific heat ratio
λ	-	Lambda coefficient, equivalence ratio
λ_c	-	Crankshaft radius to conrod length ratio
λ_{ch}	-	Charging efficiency
λ_{smc}	-	SMC positive constant
ρ	-	SMC switching law gain
ω	rad/s	Engine speed
ω_d	rad/s	Desired engine speed
ω_2	rad/s	Rotational speed after the flywheel

SAŽETAK

Da bi se smanjili troškovi razvoja automobilskih motora s unutarnjim izgaranjem, njihovo početno testiranje i nadzor performansi se odvija na testnim stanicama. Pomoću električne kočnice motora i upravljačke jedinice, motor s unutarnjim izgaranjem se može dovesti u bilo koju željenu radnu točku ili priključiti na postojeći matematički model vozila i okoline. Da bi se motor lakše i u kraćem vremenu podesio za testnu stanicu, potrebno je izraditi pouzdani matematički model motora pomoću kojeg će se moći procijeniti karakteristike stvarnog motora.

U prvom dijelu izrade modela motora, definirana je točnost i kompleksnost samog modela. S tim pretpostavkama se odabiru dijelovi dinamike motora koji će se opisati teorijski ili empirijski, a sve sa svrhom provođenja proračuna u realnom vremenu ili čak brže od toga. Opisan je model u domeni kuta zakreta koljenastog vratila te su verificirani rezultati s relevantnim software-om. Nadalje je opisan model u vremenskoj domeni s kojim je moguće pokretati simulaciju kroz neko vremensko razdoblje i povezati s modelima ostatka vozila.

U drugom dijelu rada, izrađeni su relevantni regulacijski sustavi za upravljanje značajkama rada motora, od regulatora brzine vrtnje u praznom hodu do tempomata. Ovi regulacijski sustavi su ključni za završne performanse motora i njegovu stabilnost u željenim radnim točkama. *Sliding mode* regulator je izabran kao nazivni regulator zbog svojih robusnih svojstava i dobrih performansi u raznim radnim točkama.

Na kraju rada, model je preveden u globalno priznati standard za razmjenu matematičkih modela (FMU) koji se izvodi brže od opisanog modela u Simulink-u i ponaša se kao svojevrsna crna kutija. Vidljivi su samo ulazi i izlazi iz modela, dok se sastavu modela ne može pristupiti niti ga izmijeniti.

Ključne riječi: *testna stanica, motor s unutarnjim izgaranjem, model u stvarnom vremenu, upravljački sustav, FMU*

SUMMARY

To reduce the research and development costs of the internal combustion engines (ICE), their initial testing and performance control is conducted on the testbeds. By using eletrical brake with control unit, the ICE can be run at any desired operating point or can even be connected to an existing mathematical model that simulates the rest of the vehicle and the environment. To shorten the time it takes to set up the ICE to the testbed, a reliable ICE model has to be designed in order to accurately calculate characteristics of a real engine.

In the first part of the thesis, the desired accuracy and complexity of the model are defined. With these assumptions, parts of the model that will be described theoretically or empirically are selected in order to enable the model to in real time, or even faster. A crank-angle dependent model is described and the results are verified with the relevant software. Afterwards, the time-dependent model is described, with whom it is possible to run the simulation in the desired time frame and to connect it with the models of the rest of the vehicle.

In the second part of the thesis, the relevant control systems for engine performance are designed, from the idle speed controller to the cruise control system. These control systems are crucial for the final engine performance and its stability in the desired operating points. Sliding mode control was selected as the default controller due to its robust properties and good performance in various engine states.

Finally, the model is compiled to a globally recognized standard for mathematical model sharing (FMU) which runs faster than the model designed in Simulink and acts as a sort of a black box. Only the inputs and the outputs of the model are visible, while the content of the model is inaccessible and unchangeable.

Keywords: testbed, internal combustion engine, real-time model, engine control unit, FMU

PROŠIRENI SAŽETAK

Ovaj diplomski rad je izrađen u suradnji sa tvrtkom AVL - AST d.o.o. iz Zagreba i AVL List GmbH iz Graza s ciljem da se pojednostavni i skrati potrebno vrijeme podešavanja motora s unutarnjim izgaranjem za testnu stanicu.

U današnje vrijeme vozilo se podvrgava raznim testovima i prijeđe brojne kilometre prije nego što se uopće izvede na pravu cestu. Isto vrijedi i za pojedine podsustave vozila. Motor i ostali dijelovi pogonskog sustava se pojedinačno testiraju na posebnim testnim stanicama gdje se dovode u razne radne točke i ocjenjuju njihove performanse. Na temelju podataka dobivenih na testnim stanicama, ponašanje svake od testiranih komponenti se analizira i po potrebi poboljšava. Relevantna testna stanica za ovaj rad je ona na kojoj se testira motor s unutarnjim izgaranjem gdje se pomoću električne kočnice motora, motor s unutarnjim izgaranjem dovodi u željene radne točke. U svrhu skraćivanja vremena potrebnog za podešavanje testne stanice za specifični motor, kroz ovaj rad je razvijen model motora koji što vjernije pokušava replicirati ponašanje pravog motora na testnoj stanici u Matlab/Simulink okruženju. Glavni cilj modela je proračun oscilacija brzine vrtnje i indiciranog momenta sukladno ponašanju stvarnog motora uz nužan uvjet izvođenja modela u realnom vremena.

U prvom dijelu diplomskog rada opisane su razne vrste simulacijskih modela motora s unutarnjim izgaranjem. Ovisno o svrsi za koju se izrađuje i zahtjevima za razinu točnosti modela, postoje različite klase koje rezultiraju s različitim performansama. Odabrani model je izrađen na način da je kombinirano teorijsko i eksperimentalno opisivanje procesa u smislu da se model sastoji od diferencijalnih i algebarskih jednadžbi te eksperimentalno određenih tablica koje sadržavaju vrijednosti određenih varijabli za neke radne točke. Ova je kombinacija rezultirala ispunjavanjem nužnog uvjeta za model, onaj da se model izvodi u realnom vremenu ili čak brže od toga, uz zadovoljavajuću točnost. Razvijeni model računa varijable od interesa (brzina vrtnje motora i indicirani moment) u njihovom realnijem, oscilatornom obliku, za razliku od većine ostalih modela u realnom vremenu koji računaju samo srednje vrijednosti varijabli modela.

Prvo je razvijen takozvani *eng. traces* model u kojem su sve varijable ovisne o kutu zakreta koljenastog vratila te ovaj model služi za proračun tijekom jednog ciklusa motora i to u stacionarnim uvjetima. Uvedene su određene pretpostavke u svrhu pojednostavljivanja računanja modela. Najvažnija od njih je da postoji jedna varijabla stanja (tlak) i da se ona računa samo tijekom takta kompresije i ekspanzije, dok se vrijednosti tlaka za vrijeme usisa i ispuha

zadaju pomoću tablica, ovisno o radnoj točki motora. Dinamika izmjene radnog medija, protok u usisnom i ispušnom kolektoru se zanemaruju.

Zadana je glavna jednažba očuvanja energije za cilindar tijekom taktova kompresije i ekspanzije uz uključnu energiju goriva. Pomoću te jednadžbe računa se indicirani tlak za vrijeme promatranih taktova. Geometrija samog cilindra ovisna je o parametrima motora te je također zadana ovisnost puta, brzine i akceleracije klipa ovisno o kutu zakreta koljenastog vratila. Iz mnoštva modela koji opisuju izgaranje u cilindru izabran je model prema Vibe-u. Ovaj model je najrašireniji i uz relativno malo parametara mogu se definirati glavne značajke izgaranja koje uključuju: oblik i duljinu izgaranja te kut pretpaljenja. Svaki od tih parametara može se mijenjati čime se direktno utječe na trajanje oslobađanja energije goriva, amplitudu i oblik indiciranog tlaka te posljedično na indicirani moment. Također su zadane relacije za izentropski eksponent plina u cilindru, i posljedično za specifični toplinski kapacitet pri stalnom volumenu čije promjene bitno utječu na računanje u modelu. Prijenos topline u cilindru je glavni oblik gubitka energije te se treba adekvatno opisati. Koeficijent za prijenos topline računa se prema Wochni-ju za čiju realizaciju treba najmanje dodatnih parametara što je idealno za razvijani model. Definirane su površine izmjene topline i izračunat je toplinski tok prijenosa topline kroz granice cilindra. Potrebno je izvršiti konverziju toplinskog toka iz ovisnosti o vremenu u ovisnost o kutu zakreta koljenastog vratila.

Početni uvjeti modela podrazumijevaju usisni tlak, masu u cilindru te masu goriva koja sudjeluje u izgaranju. Usisni tlak ovisi o radnoj točki motora, tj. o brzini motora i opterećenju te je zadan preko posebne tablice ovisno o vrsti motora. Pomoću njega računa se masa cilindru. Masa goriva kod „benzinskog“ motora ovisi o masi koja je završila u cilindru, dok masa goriva kod „dizelskog“ motora ovisi o drugoj tablici koja je također ovisna o radnoj točki motora.

Ovako definiran tlak u cilindru rezultira silom plinova koja djeluje na klip. Ona se kombinira se inercijskim silama koje su posljedica oscilatornog gibanja mase klipa i dijela mase klipnjače. Sile inercije ovise o drugoj potenciji brzine vrtnje te na velikim brzinama imaju dominantni utjecaj na oblik indiciranog momenta. Rezultirajući indicirani moment jednog cilindra uslijed kombiniranog djelovanja sila plinova i inercijskih sila superponira se sa indiciranim momentima drugih cilindara. Tako je dobivena krivulja indiciranog momenta motora u nekoj radnoj točki.

Validacija dobivenih rezultata (indiciranog tlaka i momenta) provedena je u certificiranim simulacijskim alatima, AVL Cruise M i AVL Excite te je donesen zaključak da se rezultati razvijenog modela preklapaju sa rezultatima validacijskih alata u zadovoljavajućoj mjeri te da je razvijeni model do ovog stupnja spreman za korištenje. Određeni parametri modela (masa

klipa, radilice, masa goriva kod „dizelskog“ motora) mijenjaju se ovisno o dimenzijama klipa i cilindra.

Razvijeni model preveden je u takozvani *eng. transient* model koji je ovisan o vremenu te je moguće izvoditi simulacije željeni broj ciklusa ili vremenski period u različitim radnim točkama. Nakon određenih modifikacija *traces* modela i postavljene pretpostavke o vezi između trenutne brzine vrtnje i trenutnog kuta koljenastog vratila, model u vremenskoj domeni je spreman za izvođenje.

Indicirani moment jednog cilindra potrebno je preslikati i fazno pomaknuti ovisno o broju cilindara motora. Pomoću bloka u Simulink-u koji fazno pomiče ulazni signal za jednu ili više vrijednosti, ovisno o broju cilindara, realizirano je više fazno pomaknutih signala od kojih svaki pojedini signal predstavlja moment jednog od cilindara. Oni su superponirani kao i na pravoj radilici te je tako dobiven indicirani moment motora.

Pojam indicirano se odnosi na vrijednosti povezane sa procesima u cilindru, prije utjecaja mehaničkih gubitaka. Mehanički gubici predstavljaju skup otpora koji se pojavljuju kroz rad motora i naposljetku trajno snižavaju korisnost cijelog procesa. Uključuju gubitke zbog trenja, snagu koja se troši za pokretanje pomoćnih uređaja u motoru te mogu uključivati rad pumpanja. U ovom radu, ukupni mehanički gubici su predstavljeni sa srednjim efektivnim tlakom trenja koji je također zadan tablično. On se računski pretvara u ekvivalentni moment koji se oduzima od indiciranog momenta, čime se dobiva efektivni moment motora.

Da bi se oscilacije brzine vrtnje točno izračunale, inercija motora i njena varijabilnost mora biti dobro definirana. Opisuje se ovisnost inercije klipnog mehanizma o kutu zakreta koljenastog vratila te uvodi koncept dvomasenog zamašnjaka koji korektno opisuje realnu elastičnu vezu između motora i testne stanice. Elastična veza je opisana sa dvije mase od kojih svaka masa ima pola vrijednosti momenta inercije zamašnjaka i dodatno je definirana sa faktorima krutosti i prigušenja. Prikazani su utjecaji momenta inercije zamašnjaka na izgled krivulje brzine vrtnje te utjecaj na prigušivanje amplituda oscilacija efektivnog momenta.

Razvijeni model do ovog stupnja je takozvani T(oznaka za moment)-model; u smislu da je jedan od ulaza u model željeni moment tereta na koji motor treba odgovoriti, a drugi ulaz oponaša papučicu gasa i definira opterećenje motora. Izlaz iz ovog modela je prigušena brzina vrtnje nakon zamašnjaka. Druga vrsta modela koja se danas primjenjuje u industriji je N(oznaka za brzinu vrtnje)-model. Ulaz u ovaj model je brzina vrtnje, koja može doći ili iz ostatka pogona automobila, ili je definirana električnim motorom na testnoj stanici. Tako je definira brzina vrtnje motora dok je drugi ulazni signal opterećenje motora, isto kao i u T-modelu. Razvijeni

moment pri tom opterećenju i definiranoj brzini vrtnje je izlaz iz N-modela i to nakon što mu se oscilacije priguše na zamašnjaku.

Tema sljedećeg poglavlja je razvoj upravljačkih sustava motora s unutarnjim izgaranjem. Da bi se razvijeni model održao na željenoj brzini izvođenja, neki sustavi za upravljanje se pojednostavljuju (regulacija tlaka prednabijanja i omjera zrak/gorivo) ili zanemaruju (EGR). Razvijeni sustavi uključuju regulaciju brzine vrtnje u praznom hodu te pojednostavljenu verziju tempomata. Regulacija brzine vrtnje u praznom hodu je od presudnog značaja kod suvremenih automobila. Zadaća sustava je da održava što nižu brzinu vrtnje radi smanjenja ukupne potrošnje a da pritom ne pate performanse motora. Sustav treba biti otporan na iznenadne vanjske poremećaje tijekom praznog hoda te omogućavati kontinuiran i ugodan rad motora.

Tri regulatora su predložena za ostvarenje regulacijskog sustava brzine vrtnje u praznom hodu. Prvi je heuristički podešen linearni PI regulator koji je pogodan za gotovo sve upravljačke sustave i ima dobre performanse te služi kao referenca sa kojom se uspoređuju dalje razvijeni regulatori. Druga opcija je robusni nelinearni *eng. sliding mode controller (SMC)* čije je svojstvo da odlično reagira na neopisanu dinamiku i nesigurnosti u modelu te da dobro uklanja vanjske poremećaje. Glavna zamjerka ovog regulatora je izrazito oscilatorno upravljačko djelovanje na koje se djeluje sa nekom vrstom prigušenja. Treća opcija je svojevrsni spoj između dva prije definirana regulatora; PI + SMC regulator gdje je preuzet prije opisani PI regulator te mu je dodana pojednostavljena verija SMC regulatora.

Upravljački sustavi su testirani na raznim referentnim brzinama vrtnje i na više vrsta i veličina motora. Podvrgnuti su iznenadnim poremećajima čime je testirana njihova otpornost na neočekivana opterećenja. Usporedbom performansi prema definiranim evaluacijskim faktorima (integral srednje greške i integral kvadratne greške), SMC je kao sustav sa najboljim performansama izabran kao nazivni regulator za upravljački sustav brzine u praznom hodu.

Isti se regulator primijenio i na upravljački sustav pojednostavljenog tempomata. Tempomat je u ovom radu ekvivalentan sa regulacijom brzine vrtnje kroz veliki spektar brzina uz nametnute poremećaje. Referentna brzina je zadana kao konstanta ili kao krivulja te je testirano njeno praćenje uz nametnute poremećaje koji su također u obliku konstante ili krivulje. Ostvarene su zadovoljavajuće performanse te se korišteni regulator za regulaciju brzine vrtnje u praznom hodu koristi i za pojednostavljeni tempomat.

Završni korak u sklopu diplomskog rada je prevođenje razvijenog modela u globalno prepoznati standard za razmjenu modela, *eng. functional mock-up unit (FMU)*. Potrebno je definirati ulaze i izlaze iz modela. Ulazi ovise o vrsti modela (T ili N model), dok korisnik može definirati proizvoljni broj izlaza. Također je moguće definirati parametre modela čije vrijednosti korisnik

može mijenjati prije izvođenja modela. Parametri definiraju tip i dimenzije motora te neke dodatne opcije (većinom vezane uz izgaranje). Model u FMU formatu je tako svojevrsna crna kutija, korisniku su vidljivi samo ulazi i izlazi te podesivi parametri.

Model kao FMU je naposljetku uključen kao dio kosimulacijskog modela u AVL Model Connect okruženju u kojem se nalaze ostali modeli koji definiraju ostatak vozila (virtualni vozač, ostatak pogona, okoliš). Vozilo je testirano na najnovijem certifikacijskom WLTP ciklusu te je razvijeni model motora uspješno odradio zadatak.

1. INTRODUCTION

This thesis is done in cooperation with AVL – AST d.o.o. from Zagreb and AVL List GmbH from Graz with the purpose of developing a real-time capable model of an internal combustion engine with desired performance and properties.

1.1. Motivation

Over the last couple of decades a newly developed concept, hardware in the loop (HiL), became very popular in research of various industry components which enables faster and more effective development. Hardware in the loop is the emerging idea of combining a real hardware with real-time capable models of the auxiliary components [1]. With constant technological advances and growing processor power, the bulk of industry research is shifted to the virtual domain. Numerous modeling and simulation software products now offer the possibility of merging the real and the virtual world, where the data from a real hardware can be analyzed, processed and acted upon.

The prime example, as well as the focus of the thesis, is the engine testbed. It connects a real internal combustion engine (ICE) with real-time capable models which can describe a variety of engine related functions. Development on testbeds is more cost-efficient than development on a whole vehicle (or certain desired components) and, with accurate and reliable models, a good approximation of a real behavior can be achieved.

Engine testbed (ETB) has become an industry standard for successful research and development of an internal combustion engine, and lately electric motors. Along with the progress of technology, ETBs are becoming increasingly sophisticated and provide a growing amount of data to development engineers. Various technologies are used for a large scope of different measurements that include precise monitoring of cylinder pressure, gas-particle movement, exhaust gas composition, brake torque etc.

In addition, ETBs reduce the R&D costs significantly as the engines rarely leave them until their performances meet the desired criteria. In that way, engines run countless kilometers and are subjected to various loads, imitating the road conditions as much as possible. Engineers are able to monitor the important data and act on them, either by redesigning a specific part or tuning a subsystem of the engine control unit (ECU).

Along with the ETB, other parts of the engine powertrain are also continuously researched, tested and redesigned. Everything is done to ensure that every component of the complicated

system works as desired once the vehicle reaches the stage where it is tested on a real road and eventually sold to customers.

An ETB environment is shown in Figure 1 below.



Figure 1. An example of AVL testbed environment [2]

As ETBs become an essential part of every OEM, there is a tendency to also improve the surrounding systems. The load that is asserted to the ETB has to be a realistic approximation of the conditions that the vehicle would encounter in a regular driving situation. Therefore, reliable models which would encompass the vehicle as a whole (except the engine), need to be designed and they, in most of the cases, consist of a drivetrain model, driver model, engine control unit, road and surroundings, thermal management etc. The models need to be able to run in real time as they are connected to a real-time ICE set on an ETB.

Adapting the designed models and real ICE in a working system is a challenging task. A method to make this task easier is to develop a model of the ICE that would reliably describe the behavior of the real ICE. The model also has to be able to run in real-time and has to provide the desired data.

First, the engine model needs to be designed using appropriate software (e.g. Matlab/Simulink) along with a model of the engine control system. This leads us to a concept named Model in

the loop (MiL). This means nothing more than that the engine and the control system are represented as a virtual picture of the real parts [1].

One way to reliably describe the behavior of the real ICE is to insert the previously designed model in a virtual (simulated) HiL environment. Virtual HiL environment is a concept where a powerful machine imitates the engine behavior with the help of a designed engine model. It then communicates with its surroundings in the same way as a real engine would, via some of the standardized communication protocols (e.g. CAN). The surroundings, in virtual HiL case, are other real-time capable models which exchange data back to the engine also via CAN. The virtual HiL simulations run in real time and enable the engineers to have a detailed look into the engine operation and to enable faster prototyping without even having to place a real engine on a testbed.

The current ICE model that is used in the Virtual HiL environment is a mean value model, with only the mean values of the relevant variables calculated. The objective of this thesis is to develop an ICE model (with accompanying control systems) that will accurately describe the engine performance throughout its operating points. The relevant performance consists of the proper calculations of the engine speed and indicated torque fluctuations. These fluctuations are then transmitted further down the driveline; in the ETB case, to the elastic connection with the electric motor (the „dyno“) that provides the load. Data from the virtual HiL environment is to be used to improve the behavior of the real HiL setup and shorten the setup time.

An ICE model needs to be designed from these guidelines. The developed model has to be able to describe a range of engine types and sizes. Upon the model completion, its usage should provide the desired benefits to the users.

2. ICE MODEL TYPE SELECTION

The automotive industry is one of the largest industries in the world. As such, every part of it is brought almost to perfection in regard to cost efficiency and sustainability. ICEs are still the power source of the majority of the automotive powertrains. Although hybrid and electric vehicles are lately coming into fashion, the ICE is still ruling the market, at least for the time being. The research and development of the ICE is, as already mentioned, taking place on engine testbeds.

It can be assumed that the testbed is a very delicate (and expensive) system. Therefore it has to be handled carefully leading to a lengthy setup time. Once the ICE is set up on the engine testbed (ETB), it is ready to be connected to the desired inputs. Today the ICEs are commonly tested on the certificated driving cycles (NEDC, WLTP). Vehicle data, drivetrain and road data are contained within (usually several) models prepared in office. The aforementioned models need to be capable of running real-time as they are to be connected to a real engine on a testbed. The electric brake motor („the dyno“) provides the load, calculated from the real-time models, to the real ICE. To reduce the setup time of the ETB and the real-time models, a real-time ICE model needs to be prepared in office and has to satisfy the before mentioned model requirements.

2.1. Types of ICE models

To properly address the engine model requirements, one must be aware of the existing methods of ICE modeling. In the following section, a classification of the models will be performed with respect to [1]. The temporal behavior of multiple-domain systems, such as an internal combustion engine, can be described with mathematical models of the static and dynamic behavior of the system components or the processes. In the case of the ICE, models span several physical areas including mechanics, thermodynamics and electricity. It is obvious that any legitimate engine model would be a highly complicated one and so we can divide them into two groups; models based on theoretical modeling and models based on experimental modeling.

2.1.1. Theoretical and experimental models

Theoretical modeling usually follows a methodology of setting up the relevant equations [1]. These equations are:

- Balance equations for stored masses, energies and momentum,

- Constitutive equations of special elements,
- Phenomenological equations, if irreversible processes are involved and
- Connection equations.

By summarizing the above equations a theoretical model is obtained with a specific structure and certain parameters. The parameters of the model can be distributed or lumped. Distributed parameters exhibit spatial dependency and therefore lead to partial differential equations while the lumped parameters depend only on time and lead to a model with ordinary differential equations. Depending on the model needs and accuracy, either one of the parameter types can be used. The theoretical model is often linearized for simplification.

By experimental modeling, also called process identification, the mathematical model is obtained from measurements [1]. Input and output signals from a real system are measured and a mathematical relationship is established between the two.

Theoretical and experimental modeling mutually complete themselves. Either one is used for different applications. Theoretical (slower) modeling is rather used for the simulation of a realistic dynamical behavior while an experimental model can be used for a quick control system design or a fault detection.

A summed-up representation can be seen in Figure 2.

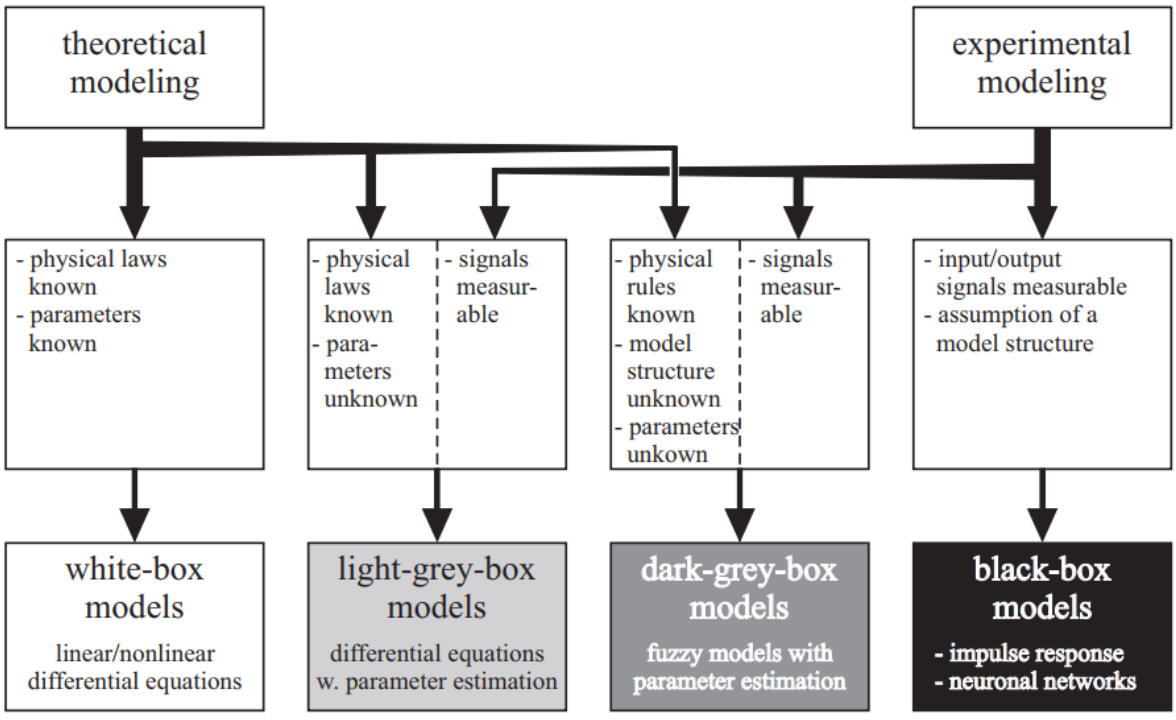


Figure 2. Types of mathematical process models

The model presented within this thesis would be a „light-grey-box“ model. The critical condition of a real-time simulation does not allow the possibility of a purely theoretical model as that model would be too complex and would have a large real-time factor. The model also will not be purely experimental as mathematical relationships within the model are mostly known. The ones that are not known or are too time-consuming to calculate will be mapped in an empirical way as shown later in the thesis.

2.1.2. Mean value and Discrete event models

An additional important feature of the presented model must be chosen. According to [3], there are two types of ICE models in respect to taking the reciprocating motion of the engine into account. They can be defined as follows:

- Mean value models (MVM): continuous models, which neglect the discrete cycles of the engine and assume that all processes and effects are spread out over the engine cycle and
- Discrete event models (DEM) or Cylinder-by-cylinder engine model (CCEM): models that explicitly take into account the reciprocating behavior of the engine.

In MVM, time is the independent variable, while in DEM, the crankshaft angle is the independent variable [3]. Often, DEMs are formulated assuming a constant engine speed.

In MVM, the reciprocating behavior is captured by introducing delays between cylinder-in and cylinder-out effects. For example, the torque produced by the engine does not respond immediately to an increase in the manifold pressure. The new engine torque will be active only after the induction-to-power (IPS) delay:

$$\tau_{IPS} = \frac{2\pi}{\omega_e} \quad \textbf{(1)}$$

has elapsed (assuming a four-stroke engine) with ω_e denoting engine speed. Good examples of MVMs can be found in [4] and [5].

As the engine model presented in this thesis will be a cylinder-by-cylinder engine model, this class of models will be described in greater detail. The DEMs are needed in the following cases: [3]

- When the system representation, and therefore the subsequent controller realization, is simpler in the crank angle domain,
- When the cylinder-individual effects have to be analyzed, e.g., single-cylinder air/fuel control, misfire detection with engine speed measurements, etc.

In the case of this thesis, the DEM is required to accurately capture the engine torque and speed oscillations and amplitudes which are crank-angle dependent. The developed DEM will be based on the calculated cylinder pressure.

2.2. Characteristics of the developed model

As mentioned in the previous section, the developed model will be a discrete one with the focus on accurately capturing the realized cylinder pressure and the resulting engine performance. The imperative condition is that the model needs to be real-time capable, meaning that the surrounding dynamics (intake manifold dynamics and gas exchange process in particular) would be modeled with the help of experimental data. In the next chapter, the developed model will be explained in detail.

3. MODEL DESCRIPTION

In the following section, the structure and details of the developed model will be discussed. The developed model can be divided into two versions, a traces (basic) model and a transient model.

The traces model calculates the desired variables over one engine cycle only and is usually used to observe only the steady-state dynamics. Only four stroke ICEs are considered within this thesis meaning one engine cycle lasts two crankshaft revolutions (720 degrees or 4π radians). Every calculated variable in the traces model is crank-angle dependent. The traces model is used to verify the developed model against an external, verified set of data and this kind of model cannot run in a transient simulation.

The transient model, on the other hand, is a model specifically designed to run in a simulation that can last an unlimited number of cycles with changing operating points. It can be created from a converted traces model, including several assumptions and simplifications which will be described during this section. Every calculated variable in this model is time-dependent.

The traces model and its structure will be discussed first since it is the model from which the transient model will later be formulated.

3.1. Traces model

The structure of the traces model will be defined first. If one would go with a purely theoretical path into modeling an internal combustion engine, a complex set of differential equations would have to be defined to accurately describe the dynamic behavior. The model would be divided into several parts with state variables connecting these parts and interacting with each other. These parts (in order of the airflow throughout the engine) are:

- Throttle dynamics (if a Spark ignition (SI) ICE is modeled),
- Intake manifold dynamics – mass flow and heat exchange dynamics,
- Gas exchange process – charging efficiency of the engine, exhaust gas fraction, inlet and exhaust valve opening,
- Cylinder dynamics – compression, combustion and expansion with all of the dynamics included (combustion rate, blow-by flow, heat exchange, etc),
- Exhaust manifold dynamics – exhaust gas composition, air/fuel control, catalyst
- If the engine is turbocharged or has an exhaust gas recuperation (EGR), these dynamics have to be included too and the model becomes even larger and more complex.

A control system that supervises and guides the engine behavior must not be neglected as it also introduces time delays, e.g.:

- Electronic throttle control (ETC) - control of the electric motor that sets the throttle angle,
- Fuel injectors control,
- Boost control – varying the angle of turbine blades on the turbocharger leads to a modifiable boost pressure in the intake manifold,
- EGR valve control – modifying the exhaust gas recirculation affects the exhaust gas composition and engine power,
- Idle speed control (ISC) – maintaining the desired engine speed while the engine is in idle, etc.

As one can see from the previous two lists, a purely theoretical model would be an accurate one, albeit a slow one. The critical condition of the model to be developed is its real-time factor which needs to be less than one, leading to a necessary model simplification. The simplifications are as follows:

- The developed model can be defined as zero-dimensional or single-zone [1],[11]. It is assumed that the cylinder dynamics can be considered as a lumped parameter process, such that the gas states are not space-dependent (they are only time-dependent), and that the laws for ideal gases can be applied.
- There will be only one state variable, the cylinder pressure, meaning that the model will contain only one ordinary differential equation. Later in the transient model, more state variables will be added (engine speed and speed after the flywheel). They will be connected with the algebraic relationships which will be defined throughout the thesis.
- The initial conditions of the model will be set at the end of intake and the start of compression. The cylinder pressure will be calculated only during the compression, combustion, and expansion strokes. During the intake and the exhaust stroke, the cylinder pressure will be set at the values defined in the initial conditions.
- The initial conditions of the cycle will depend on the engine speed and the engine load defined with the load signal. These two variables will serve as inputs to a number of look-up tables with experimentally gathered data. The look-up tables will output several variables which will define the behavior of the cycle. These are: intake and exhaust pressure, trapped mass and fuel mass.

- The realized cylinder pressure (predefined and calculated as noted above) is forwarded to the indicated torque calculation. Gas and inertial forces acting upon the crankshaft are calculated and converted to indicated torque.
- The intake port pressure will be defined via look-up tables, whether it is a modified pressure after the throttle (SI engines) or a boosted pressure after the compressor (SI and Compression ignition (CI) engines). That pressure would not be calculated because the dynamics that would need to be described would be slowing the simulation even further (electronic throttle and turbocharger control and dynamics).
- The Air/Fuel (A/F) ratio of the SI engine will be set to its stoichiometric value and is presumed that an A/F control system exists and is keeping the ratio at the desired value.
- Exhaust gas recuperation (EGR) will not be described as it affects the exhaust gas composition which not of the interest in this thesis. It also affects the engine power but in no great measure.

The model needs to be designed in Matlab/Simulink environment and verified against certified results. The certified results will be collected from the AVL Cruise M and AVL Excite software and its example models regarding ICE modeling, with their default parameters altered to match the developed model.

In the following sections, the details and structure of the developed model will be further clarified.

3.1.1. Cylinder energy balance equation

A detailed description of the traces model structure will begin at the heart of the model, the cylinder dynamics, and spread further from there. A constitutive equation for the considered closed system leads from [6]:

$$\frac{d(m_c \cdot u)}{d\alpha} = -p_c \cdot \frac{dV}{d\alpha} + \frac{dQ_f}{d\alpha} - \sum \frac{dQ_w}{d\alpha} - h_{BB} \frac{dm_{BB}}{d\alpha} + \sum \frac{dm_i}{d\alpha} h_i - \sum \frac{dm_e}{d\alpha} h_e \qquad \textbf{(2)}$$

where:

- m_c is the gas mass in the cylinder,
- u is the specific internal energy of the cylinder,

- α is the crank angle,
- p_c is the cylinder pressure,
- V is the current volume of the cylinder,
- Q_f is the fuel heat input,
- Q_w are the wall heat losses,
- h_{BB} is the specific enthalpy of the blow-by,
- m_{BB} is the gas mass of the blow-by,
- m_i is the mass flowing into the cylinder
- h_i is the specific enthalpy of the mass flowing into the cylinder,
- m_e is the mass flowing out of the cylinder,
- h_e is the specific enthalpy of the mass flowing out of the cylinder.

Since the observed cylinder dynamics will only cover compression, combustion, and expansion, energy from the gas exchange will be ignored. Energy from the blow-by will also be disregarded with the aim of keeping the equation as simple as possible. This leads to the basic form of the previous equation:

$$\frac{d(m_c \cdot u)}{d\alpha} = -p_c \cdot \frac{dV}{d\alpha} + \frac{dQ_f}{d\alpha} - \sum \frac{dQ_w}{d\alpha} \quad \textbf{(3)}$$

Depending on the chosen state variable to be solved (cylinder temperature or pressure), the above equation can be analyzed in two ways. The first one is the equation below in which the state variable is the cylinder pressure [7]:

$$\frac{dp_c}{d\alpha} = \frac{R}{c_v \cdot V}\left(-\left(1 + \frac{c_v}{R}\right) \cdot p_c \cdot \frac{dV}{d\alpha} + \frac{dQ_f}{d\alpha} - \sum \frac{dQ_w}{d\alpha} \right) \quad \textbf{(4)}$$

where:

- R is the specific gas constant,
- c_v is the specific heat at constant volume.

The second method to analyze the equation (3) is to make cylinder temperature a state variable:

$$\frac{dT_c}{d\alpha} = \frac{1}{m_c \cdot c_v}\left(-\left(\frac{mRT_c}{V} \right) \cdot \frac{dV}{d\alpha} + \frac{dQ_f}{d\alpha} - \sum \frac{dQ_w}{d\alpha} \right) \quad \textbf{(5)}$$

where:

- T_c is the cylinder temperature.

In either way, the other variable is calculated using the ideal gas law equation:

$$p_c \cdot V = m_c \cdot R \cdot T_c \quad \textbf{(6)}$$

and assuming that the specific gas constant R has a constant value of 287 J/(kg K) throughout the simulation. As mentioned before, the selected state variable is the cylinder pressure. The initial state of the integrator is the inlet pressure at the start of the compression with a value defined from the experimental data. Cylinder temperature is calculated with the help of the ideal gas law equation (6).

3.1.2. Cylinder geometry relations

In the figure below, the basic cylinder geometry relations for an inline engine are shown.

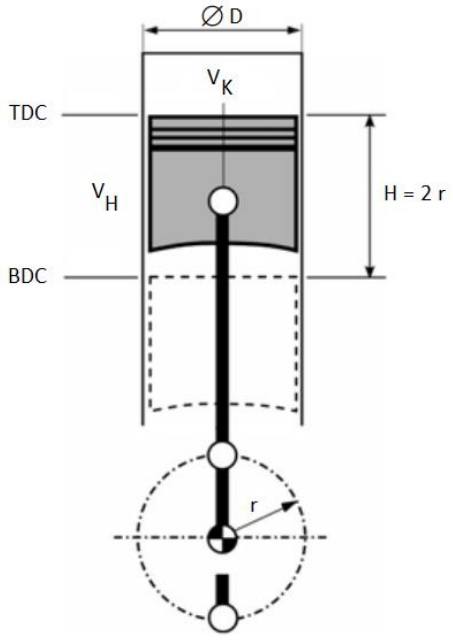


Figure 3. Cylinder geometry basic relations [8]

Where:

- D is the cylinder diameter,
- r is the crankshaft radius,
- H is the cylinder stroke,
- TDC is the cylinder top dead center,
- BDC is the cylinder bottom dead center,
- V_H is the cylinder displacement and
- V_K is the cylinder compression volume.

Cylinder displacement is defined as the swept volume between the TDC and BTC during one engine stroke and the piston offset is not taken into consideration. The ratio between the maximum volume and the minimum volume of the cylinder is defined with the compression ratio ε. Other relations that can be derived from the expressions above are as follows:

$$V_H = \frac{D^2 \cdot \pi}{4} \cdot H = V_{\max} - V_{\min}$$

$$V_E = V_H \cdot z$$

$$V_{\min} = V_K \qquad \textbf{(7)}$$

$$V_{\max} = V_H + V_K = V_H \cdot \frac{\varepsilon}{\varepsilon - 1}$$

$$\varepsilon = \frac{V_{\max}}{V_{\min}} = \frac{V_H + V_K}{V_K}$$

Where:

- z is the number of cylinders,
- $V_{\min}$ is the minimum cylinder volume, equal to the compression volume,
- V_E is the total engine displacement,
- $V_{\max}$ is the maximum cylinder volume and
- ε is the compression ratio.

The cylinder volume changes during the stroke (i.e. from its maximum value at BDC to its minimum value at TDC and vice versa) and needs to be described with an appropriate equation which needs to be crank-angle dependent. That equation is derived from [9] and with certain simplifications is used in the following form:

$$V(\alpha) = r \cdot \left(1 - \cos(\alpha) + \frac{\lambda_c}{4}(1 - \cos(2\alpha)) \right) \cdot A \qquad \textbf{(8)}$$

$$\lambda_c = \frac{r}{l}$$

Where:

- l is the conrod length,
- λ_c is the crankshaft radius to conrod length ratio,
- A is the cylinder/piston surface area

So, the total cylinder volume at any crank angle α is:

$$V = V(\alpha) + V_K \qquad \textbf{(9)}$$

and the derivative of volume against crank angle is:

$$\frac{dV}{d\alpha} = r \cdot A \cdot \left(\sin(\alpha) + \frac{\lambda_c}{2} \cdot \sin(2\alpha) \right) \qquad \textbf{(10)}$$

As can be seen from the previous equations, it is assumed that the starting stroke of the cycle is the intake, and the variables related to this assumption are defined accordingly. It means that the cylinder defined with the above relations has the nominal ignition time at 360 crank-angle degrees (CA), the end of compression and start of the expansion, and with ignition time defined like that, the cylinder has its place defined in the firing order of the engine. In the figure below, cylinder volume trace is shown. The data for its calculation can be found in Appendix A, Engine 1.

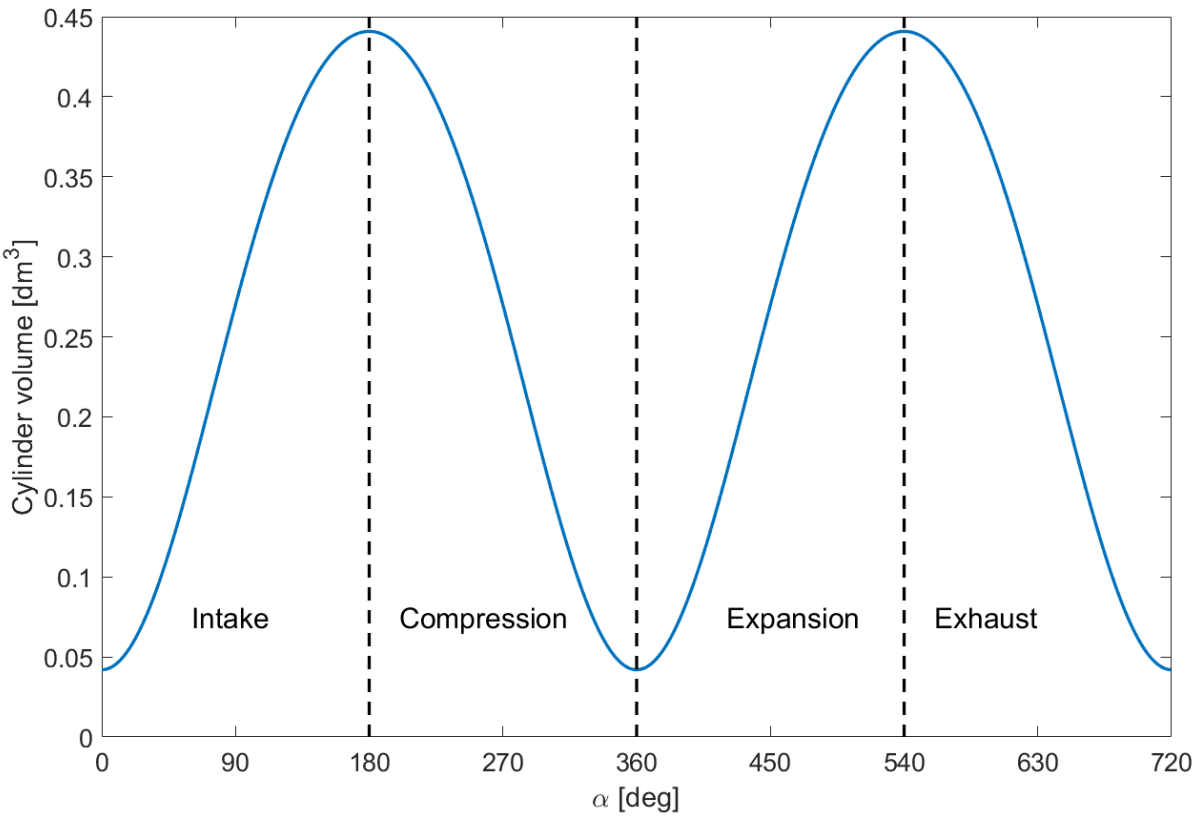


Figure 4. Four strokes of the engine cycle, cylinder volume defined with the intake value at the start of the cycle, data from Appendix A, Engine 1

3.1.3. Combustion model

A model of combustion in an internal combustion engine is probably the hardest and most complicated part of any engine model. Due to the very large energy exchange between the fuel and gas elements and the processes that accompany it happening in a very short timeframe, it is very hard to accurately capture the exact characteristics of the combustion itself. If one would go down the path of theoretically and accurately describing the events that happen in the scope of a couple of milliseconds, a number of features and properties of the combustion would have to be known. The exact composition of the gas in the cylinder, the velocity of the flame front spread and properly defining the gas-particle kinetics that describes their movement within the cylinder are just a couple of items that would have to be modeled in detail. It almost goes without saying that these models are relatively slow and cannot be possibly considered as a part of a real-time capable model.

A different, empirical approach then needs to be considered. According to [10], there are three categories in which the various engine combustion models can be grouped:

- Zero-dimensional models,
- Quasi-dimensional models and
- Multi-dimensional models.

Zero-dimensional models are then further categorized into [10]:

- Single-zone models,
- Two-zone models and
- Multi-zone models.

The above classification can also be applied to engine models in general. In fact, it was already applied at the start of the section 3.1., defining the developed model to be zero-dimensional and single-zone.

In single-zone models, the working fluid in the engine is assumed to be a homogeneous thermodynamic system, meaning that a single value of the cylinder pressure and the temperature is distributed evenly throughout the cylinder [11].

The Vibe function is the most popular empirical model of an approximated and predefined heat release. It can be applied to single-zone and multi-zone models and has the following shape according to [6]:

$$\frac{dx}{d\alpha} = \frac{-C}{\alpha_c} \cdot (m+1) \cdot y^m \cdot e^{C \cdot y^{(m+1)}}$$

$$y = \frac{\alpha - \alpha_0}{\alpha_c} \qquad \textbf{(11)}$$

Where:

- x is the mass fraction burned,
- C is the Vibe parameter with a value of -6.9 for complete combustion,
- m is the Vibe shape parameter which determines the shape of heat release,
- α_c is the combustion duration and
- α_0 is the crank angle at the start of combustion.

In Figure 5 below, one can see how the shape of the predefined heat release changes during the combustion, depending on the value of the Vibe shape parameter *m*.

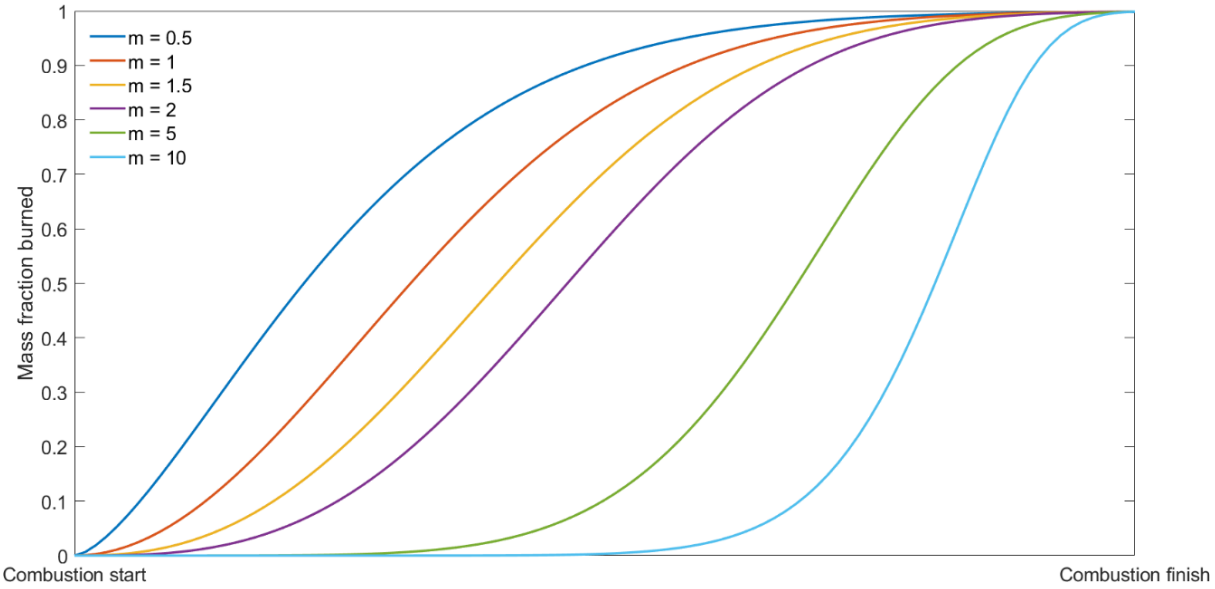


Figure 5. The Shape of the predefined heat release depending on parameter *m*

The values of the parameters *m* and α_c have been empirically collected for different types of internal combustion engines and can be defined as in Table 1. From [8]:

Table 1. Values of parameters α_c and *m* for different engine types

Engine type	Properties	RPM	α_c [°CA]	*m*
Gasoline engine	2-valve engine	1500	60	2.3
		5000	65	0.9
	4-valve engine	1500	50	2.5
		5000	55	2.1
	Fast burn concept	1500	45	2.6
		5000	50	2.6
Diesel engine with chamber injection for passenger cars	Naturally aspirated	nominal	90	0.5
		30% nominal	65	0.5
	Turbocharged	nominal	90	1
		30% nominal	65	0.8

	Turbocharged intercooled	nominal	90	1.1
		30% nominal	65	0.8
Diesel engine with direct injection for passenger cars	Naturally aspirated	nominal	80	0.4
		30% nominal	55	0.4
	Turbocharged	nominal	75	0.9
		30% nominal	55	0.7
	Turbocharged intercooled	nominal	75	1
		30% nominal	55	0.7
Diesel engine with direct injection for trucks	Naturally aspirated	nominal	70	0.5
		50% nominal	55	0.6
	Turbocharged	nominal	70	1.1
		50% nominal	55	0.8
	Turbocharged intercooled	nominal	75	0.9
		50% nominal	60	1
	Mid-speed engines	nominal	65	1

The heat release from the fuel, as defined in (3) and using (11) can be written in the following form:

$$\frac{dQ_f}{d\alpha} = H_l \cdot m_f \cdot \frac{dx}{d\alpha} \quad \textbf{(12)}$$

where:

- H_l is the fuel lower heating value and
- m_f is the fuel mass in the cylinder.

According to [12], the heating value of the fuel is the quantity of the heat produced by its combustion at constant pressure and under normal conditions. The lower heating value of a fuel assumes that the water product of combustion is at vapor state and the heat of vaporization is not recovered and this value is usually taken for engine calculation.

3.1.4. Thermodynamic properties of the gas mixture

Although the gas mixture within the cylinder is assumed to be an ideal gas, its properties still change significantly during the cycle. That's why its thermodynamic properties have to be properly defined in order to assure that the collected results can be trusted.

The specific gas constant of the mixture, *R*, does not change significantly during the cycle and stays roughly around the value of 287 J/(kg K) and the same value is applied for air and for the mixture [8].

The specific heat ratio (κ) on the other hand, changes significantly and that change has to be properly described. Differential equations that would accurately describe the change exist but are unnecessary in the scope of this thesis. Experimental model is the solution again, with a possible method described in [8]:

$$\kappa = 1.405 - \frac{0.5}{10000} \cdot T_c - a \cdot x \qquad \textbf{(13)}$$

where *x* is defined in (11) and T_c is the current cylinder temperature. The parameter *a* depends on the engine type and can be defined as:

- Gasoline engine $a = 0.05$
- High speed diesel engine $a = 0.04$
- Low speed diesel engine $a = 0.03$

Another equation for κ proved to be more accurate during the validation of the developed model with the certificated software. The equation details can be found in [13]. That equation is used in the model and has the following form:

$$\kappa = 1.38 - 8 \cdot 10^{-5} \cdot (T_c - 300) \qquad \textbf{(14)}$$

As seen in (3), the specific heat at constant volume has to be calculated, which can is done easily with the following expression:

$$c_v = \frac{R}{\kappa - 1} \qquad \textbf{(15)}$$

3.1.5. Heat losses

Heat transfer affects engine performance, efficiency, and emissions [7]. For a given mass of fuel within the cylinder, higher heat transfer to the combustion walls will lower the average combustion gas temperature and pressure, and reduce the work per cycle transferred to the piston. Lower exhaust gas temperature also affects the available recoverable energy by the turbocharger. Thus, specific power and efficiency are affected by the magnitude of engine heat transfer; engine performance drops with larger heat transfer. On the other hand, cylinder gas temperatures of the spark ignition engines can grow higher than 2500K leading to higher rate of generation of NO_x gasses [8]. The maximum metal temperatures of the combustion chamber are limited to much lower values leading to heat fluxes with values up to 10 MW/m^2. This kind of stress to the cylinder structure, unless properly handled, can lead to an overall decrease in performance. Whether it is fatigue cracking, deterioration of the lubricating oil film, piston and liner distortion etc. The importance of heat transfer is then clear. The heat can be transferred by the following modes: conduction, convection, and radiation.

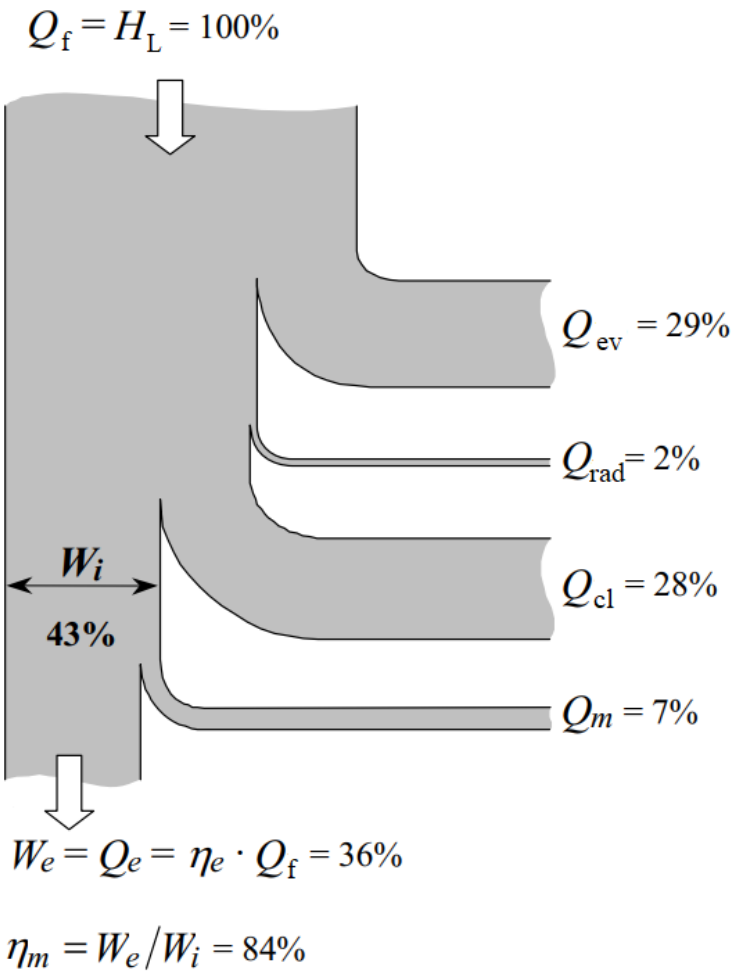


Figure 6. An example of a Sankey diagram for an ICE [8]

In Figure 6 above, an example of the Sankey diagram of an internal combustion engine is shown where the energy flow during one cycle can be seen clearly. The notations are as follows:

- Q_f is the fuel heat input,
- Q_{ev} is the fuel evaporation heat,
- Q_{rad} is the radiation heat,
- Q_{cl} is the heat transferred by cooling,
- Q_m is the heat transferred by friction and other mechanical losses,
- $W_{i,e}$ is the indicated/effective work,
- $\eta_{e,m}$ is the brake/mechanical efficiency.

In the next part of the section, a model that will capture the total heat losses within the cylinder will be selected. This part of the model will also be described empirically as the theoretical model would be too complex. Many empirical models have surfaced over the years of developing the ICE. The most popular of them is the Woschni model from the scientist of the same name, developed in the late seventies, and this model will be used within this thesis, in the form from [6]:

$$\alpha_w = 130 \cdot D^{-0.2} \cdot p_c^{0.8} \cdot T_c \cdot \left[C_1 \cdot c_m + C_2 \cdot \frac{\frac{V_E}{z} \cdot T_0}{p_0 \cdot V_0} \left(p_c - p_m \right) \right]^{0.8}$$

$$c_m = \frac{2 \cdot H \cdot n}{60} \qquad \textbf{(16)}$$

$$V_0 = \frac{V_E}{z} + V_K$$

where:

- α_w is the heat transfer coefficient,
- C_1 is an empirical constant with the value of 2.28,

- c_m is the mean piston speed,
- T_0 is the temperature of the gas mixture in the intake manifold;
- p_0 is the pressure of the gas mixture at the end of intake,
- V_0 is the volume of the gas mixture at the end of intake,
- n is the engine speed in rpm,
- C_2 is an empirical constant with the value of 0.00324 for direct ignition (DI) engines and 0.00622 for indirect ignition engines (IDI) and
- p_m is the motored pressure in [bar].

Other models of the heat transfer coefficient exist, but they require more input data than this model provides.

An example of the calculated heat transfer coefficient during compression, combustion, and expansion with the Woschni method can be seen in Figure 7.

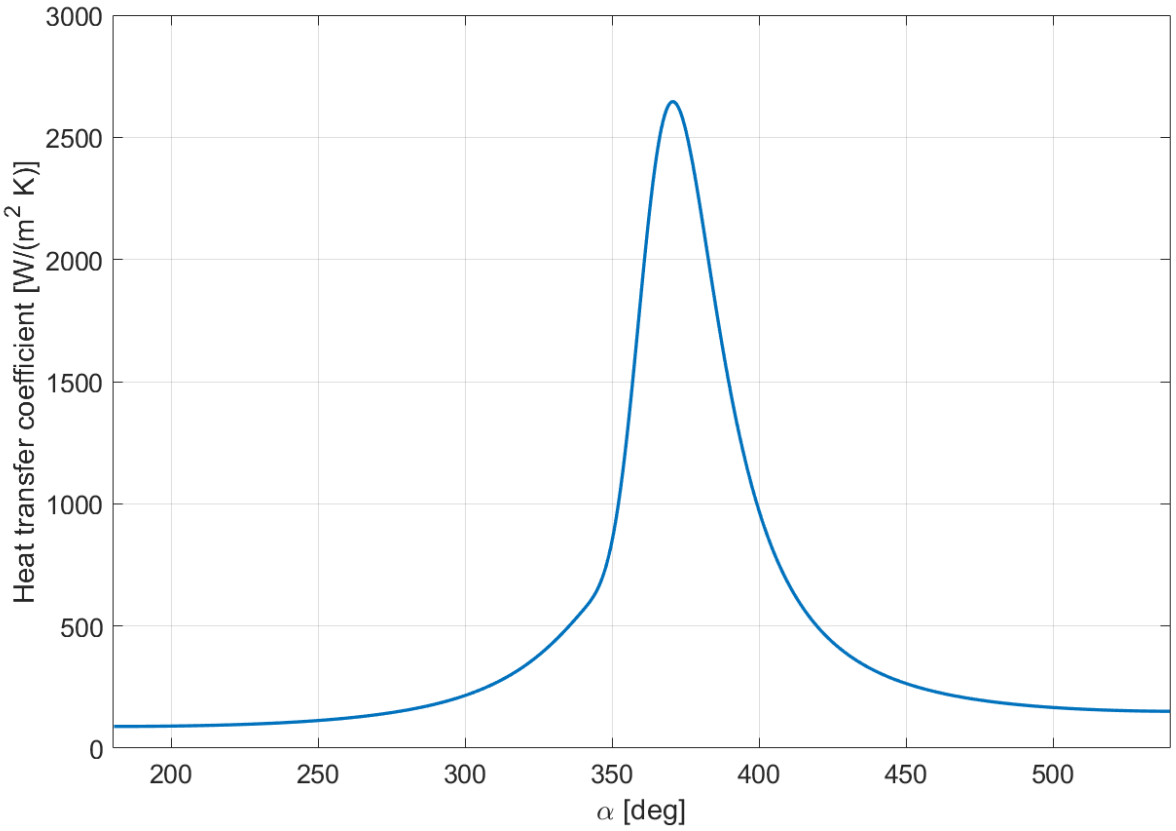


Figure 7. Calculated heat transfer coefficient, Woschni method. Data from Appendix A, Engine 1

A safeguard is introduced in the heat coefficient model. Part of the expression in (16), where the motored pressure is reduced from the cylinder pressure, serves to describe the additional effect of the turbulences to the value of the heat coefficient. These turbulences appear when cylinder pressure is larger than the motored pressure. When the motored pressure is larger than the cylinder pressure, that part of the expression is set to 0. Motored cylinder pressure is modeled as an isentropic process.

Calculated cylinder heat transfer coefficient is then inserted in the following equation for total heat transfer with empirical coefficients to different surfaces:

$$\frac{dQ_w}{dt} = \alpha_w \cdot \left[\left(T - T_p\right) \cdot 1.01A + \left(T - T_h\right) \cdot 1.4A + (T - T_l) \cdot A_l \right] \quad \textbf{(17)}$$

where:

- T_p is the temperature of part of the piston in contact with the gas mixture,
- T_h is the cylinder head temperature,
- T_l is the liner temperature and
- A_l is the liner surface.

The following equation for the liner temperature is also taken from [6] and has the following form:

$$T_l = T_{TDC} \cdot \frac{1 - e^{-c \cdot x}}{c \cdot x}$$

$$c = \ln\left(\frac{T_{TDC}}{T_{BDC}}\right) \quad \textbf{(18)}$$

$$x = \frac{h + \frac{V_K}{A}}{\frac{V_0}{A}}$$

where:

- h is the piston path and is calculated with the following equation:

$$h = r \cdot \left(1 - \cos(\alpha) + \frac{\lambda_c}{4}(1 - \cos(2\alpha)) \right)$$

$$A_i = \left(h + \frac{V_K}{A} \right) \cdot D \cdot \pi \qquad \textbf{(19)}$$

As can be seen from (17), the calculated heat losses are time-dependent. Since the traces model is crank-angle dependent, the heat release must be converted to a crank-angle dependency to successfully incorporate it into the model. It is done by dividing the calculated heat release with the current angular speed.

$$\frac{dQ_w}{dt}, \left[\frac{J}{s}, W \right]$$

$$\frac{dQ_w}{dt} \cdot \frac{1}{\omega} = \frac{dQ_w}{d\alpha} \qquad \textbf{(20)}$$

$$\left[\frac{J}{s} \right] \cdot \left[\frac{s}{rad} \right] = \left[\frac{J}{rad} \right]$$

With the heat losses defined, every part of the equation (3) is dealt with. But before moving on to the torque calculation section, the initial conditions of the model must also be defined.

3.1.6. Initial conditions

Initial conditions of the model refer to the initial values of the relevant variables to the cylinder dynamics. Initial values are defined at the crank-angle when the intake ends and the compression starts. Those variables within this model are:

- intake pressure
- trapped mass within the cylinder,
- fuel mass.

Exhaust pressure is also defined via look-up tables and his realization will be described later on.

There is no intake and exhaust valve overlapping, intake valves are open only during the induction and the exhaust valves are open only during the exhaust stroke.

In the previous sections, it was mentioned that the gas exchange process would not be theoretically described and that the initial values of the relevant variables defined above will be interpolated from the previously defined look-up tables. The majority of the look-up tables will receive engine speed and engine load as their input, then forward the relevant output to further calculations. Engine load is defined as a load signal, usually given as an input to an engine model and coming from a driver model.

Before the first look-up table has been discussed, a term *charging efficiency* will be explained. Cylinders draw the air/air-fuel mixture from the intake manifold during the intake stroke and at the and of the stroke, a certain amount of gas is vacuumed into the cylinder. That amount of gas is called fresh working substance. That amount largely depends on the intake manifold pressure, less on the engine speed and is rarely equal to the referent value.

Charging efficiency is defined as the coefficient between fresh working substance (not including the residual combustion products), after the intake valve closing, and the referent mass that would fit into the cylinder displacement volume under standard conditions (standard pressure and temperature) [8]. Standard conditions are defined with a certified norm (ISO, DIN, SAE).

$$\lambda_{ch} = \frac{m_a}{m_{ref}}$$

$$m_{ref} = \frac{p_{st} \cdot V_H}{R \cdot T_{st}} \qquad \textbf{(21)}$$

where:

- m_a is the fresh working substance,
- λ_{ch} is the charging efficiency,
- m_{ref} is the referent mass,
- p_{st} is the standard pressure and
- T_{st} is the standard temperature.

The typical values for the charging efficiency are:

- naturally aspirated four-stroke engines – $0.8 \ldots 1.1$,

- with charged engines λ_{ch} is always > 1 and can be approximated with the ratio between the pressure after the compressor and the standard pressure.

The specific gas constants *R* of the air and the gas mixture in the cylinder have very similar values and so a single value is considered [8].

The first look-up table that will be discussed will describe the effect of volumetric efficiency of the engine. As stated before, the charging efficiency of the cylinder depends mostly on intake manifold pressure, but in less measure also on engine speed. Volumetric efficiency describes the pumping capability of the cylinder in regard to engine speed because no matter how big the intake pressure is in the intake manifold, at higher RPMs there is simply not enough time to draw the same amount of air as at lower RPMs. The volumetric efficiency is denoted with η_v and is described with the following equation from [4] and graphically shown in Figure 8.

$$\eta_v = -2.55 \cdot 10^{-8} \cdot n^2 + 0.0001425 \cdot n + 0.75145 \quad \textbf{(22)}$$

where:

- η_v is the volumetric efficiency and
- n is the engine speed.

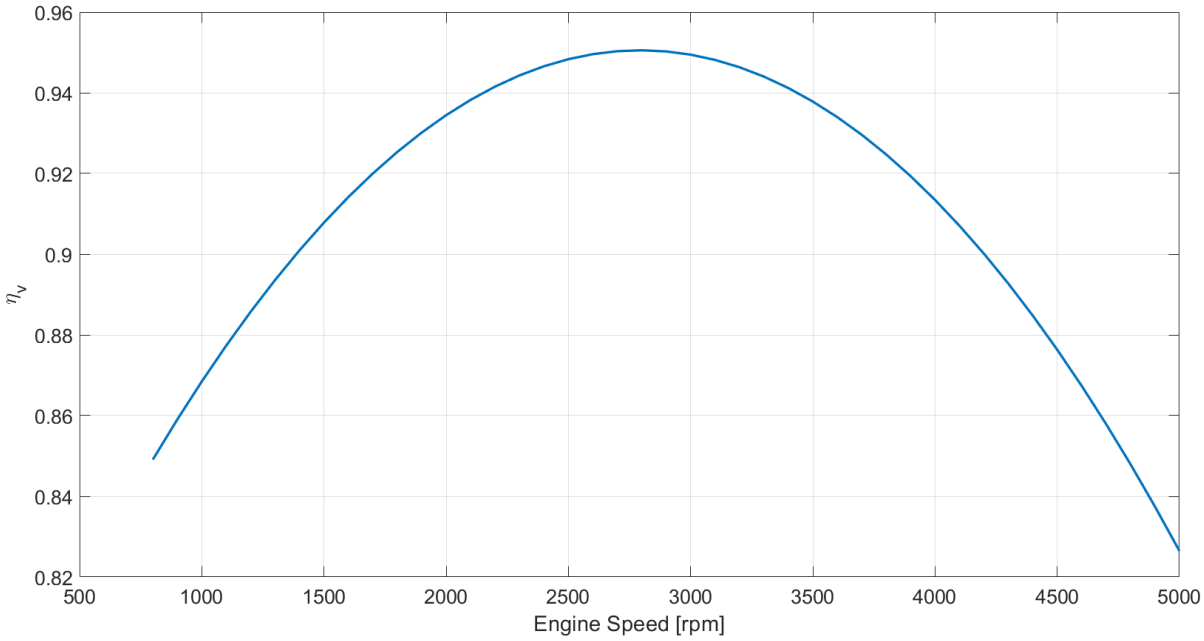


Figure 8. Volumetric efficiency based on (22)

Intake pressure is the relevant cylinder variable which will be used to calculate the cylinder trapped mass. If the intake manifold model was described theoretically, intake pressure would depend on the intake pipes geometry, flow coefficients, throttle angle (SI engines), turbocharger dynamics, etc. Instead, it has been described with a two-dimensional look-up table depending on the engine speed and load signal. Two maps are included within the model, one for the naturally aspirated SI engine and one for a turbocharged engine (CI or SI). If the engine defined would be a naturally aspirated CI engine, only the map describing volumetric efficiency would be used as there would be no throttle in the intake pipes to modify the intake pressure.

The look-up table concerning a naturally aspirated SI engine is shown in Figure 9. The data for the table is gathered from the results of an AVL Cruise M simulation of the engine with the same parameters as will be used within the model (Appendix A, Engine 1).

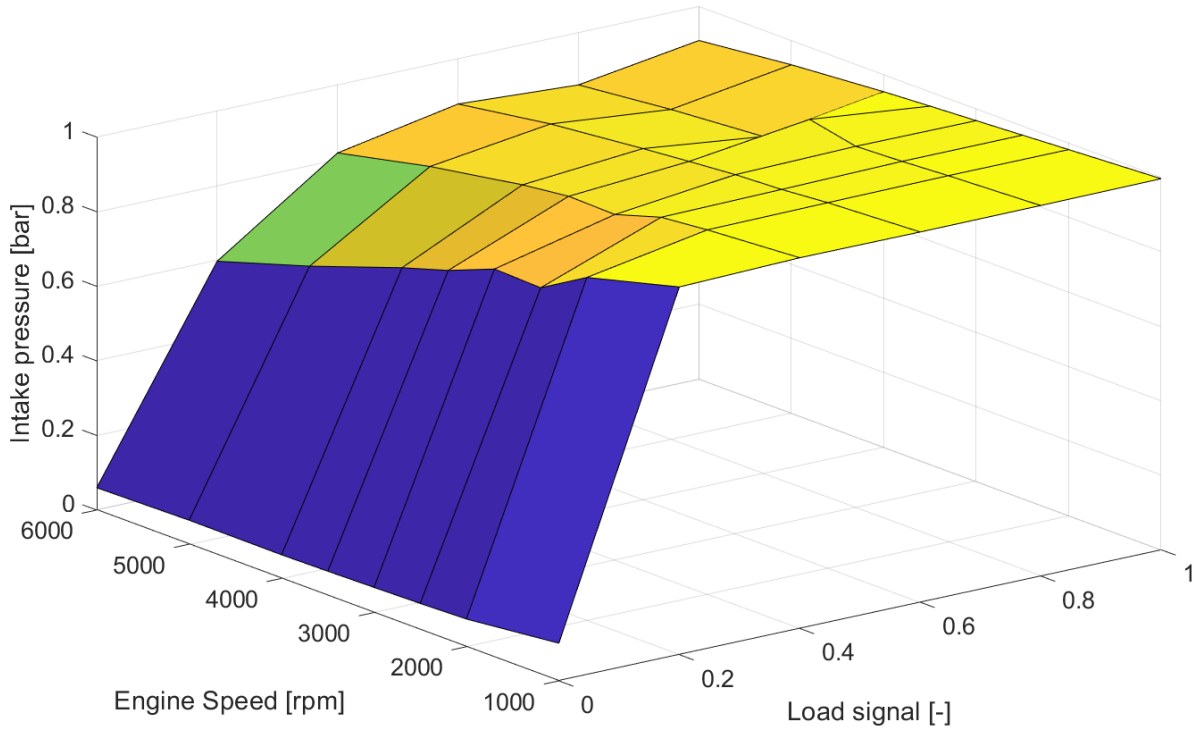


Figure 9. Naturally aspirated SI engine intake pressure look-up table

As one can see from the figure above, the intake pressure curve for a naturally aspirated SI engine depends largely upon the Load signal on its lower values. On the higher values of the Load signal, however, the curve almost draws a line as the pressure drop resulting from the throttle position is not significant. The explanation for this phenomenon is found in [16]. The throttle plate is an effective flow restriction only for small throttle angles (small engine loads). As the load is increased (larger throttle angles), the pressure drop over the throttle plate is small

and opening the throttle further doesn't have any noticeable effects on the intake pressure at that engine speed. In other words, the engine is operating under full throttle intake pressure with the throttle angles well below 90 degrees (where 0 degrees is closed throttle and 90 degrees is full open throttle). The air flow is then determined by the engine speed alone.

Intake pressure curve for a turbocharged engine will be observed next. The intake pressure in a turbocharged engine corresponds to the pressure generated after the compressor. The pressure generated by the compressor, on the other hand, follows from the speed the turbine is rotating. The rotating speed of the turbine can be controlled by varying the angle of the turbine blades, effectively controlling the pressure after the compressor. The blades angle control and the turbocharger dynamics would further complicate the calculations, leading to the look-up table solution. The generated lookup table also depends on the engine speed and load signal and the data also comes from an AVL Cruise M simulation of an engine with the equivalent parameters (Appendix A, Engine 2) and can be seen in Figure 10.

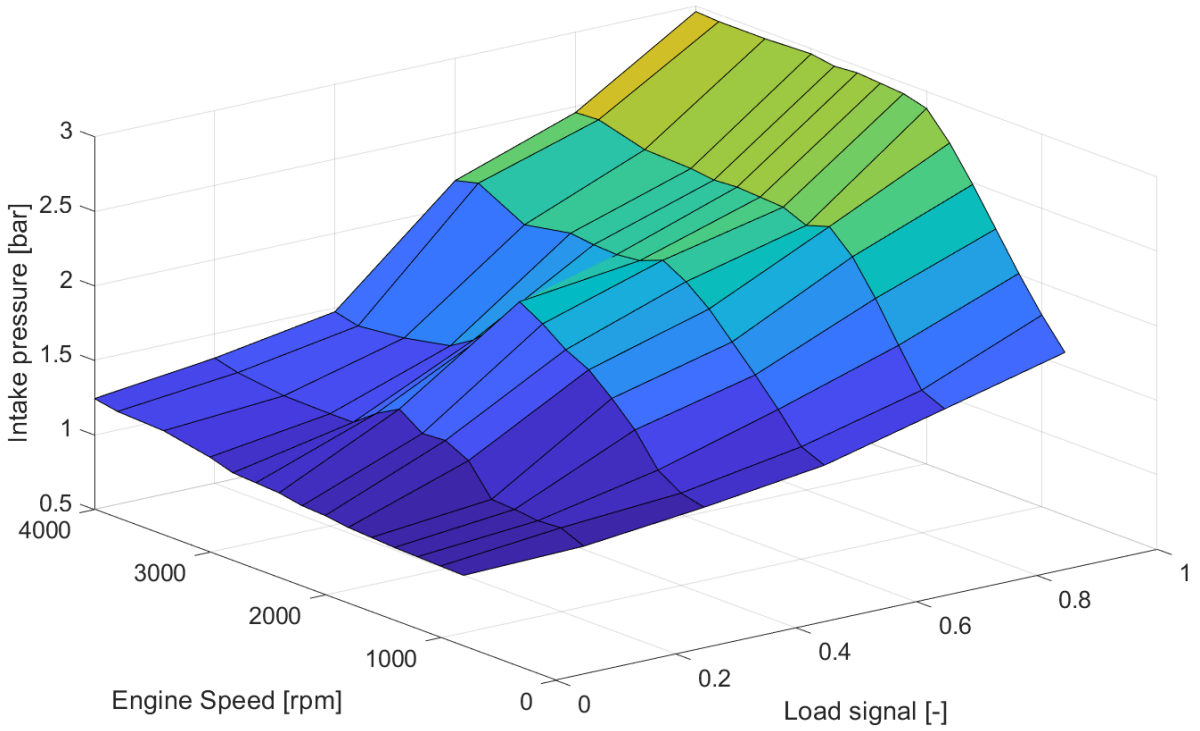


Figure 10. Turbocharged CI engine intake pressure look-up table

From the output of the two above look-up tables, using the ideal gas law equation and utilizing the mapped volumetric efficiency, the fresh working substance of the cylinder is calculated:

$$m_a = \frac{p_0 \cdot V_H}{R \cdot T_0} \cdot \eta_v \tag{23}$$

Air/fuel control is a control system within the engine that ensures that a proper value of the air/fuel ratio is realized. Air/fuel ratio is the ratio between the masses of air and the fuel and its stoichiometric value is around 14.6. The stoichiometric value determines the optimal ratio between air and fuel which ensures that when that value is realized, all of the fuel will burn, i.e. there will be enough oxygen for the fuel to burn. Air/fuel ratios with a lower value than the stoichiometric value imply a rich gas mixture, while the ratios with larger value imply a lean mixture. Either one has different effects on engine performance [8].

$$A/F = \frac{m_a}{m_f}$$
$$\lambda = \frac{A/F}{Z_0} \tag{24}$$

where:

- A/F is the A/F ratio,
- Z_0 is the stoichiometric ratio and
- λ is the equivalence ratio.

In SI engines, A/F control system keeps λ at the optimal value (1) where the SI engine has the best performance [8]. To avoid modeling of the A/F control system, it is assumed that the system is present and that it ensures that the value of λ stays around 1. Leading from this assumption, one can then calculate the fuel mass that is injected before/in the cylinder.

$$m_f = \frac{m_a}{\lambda \cdot Z_0} \tag{25}$$

In CI engines, most of the operating points have a lean mixture with λ values more than 1. The injected fuel mass is usually determined from the engine speed and load and such a realization

will also take place within this thesis. In the case of CI engines, the A/F control system has the following tasks [4]:

- Prevention of the CI engine smoking at full load, which was typical of the older CI engines and
- Correction and adaptation of the injected fuel mass in the low load and idle speed area where a fine coordination between fuel injectors, EGR valves and the turbocharger is required to pass the strict ecological norms

A look-up table of the injected fuel mass depending on the engine speed and load signal will be shown next. It will determine the mass of fuel injected in the cylinder and along with the value calculated in (23), a CI value of λ will be calculated. If the value does not satisfy the imposed regulations, a different amount of desired fuel is passed to the injectors which will satisfy. The look-up table is shown in Figure 11.

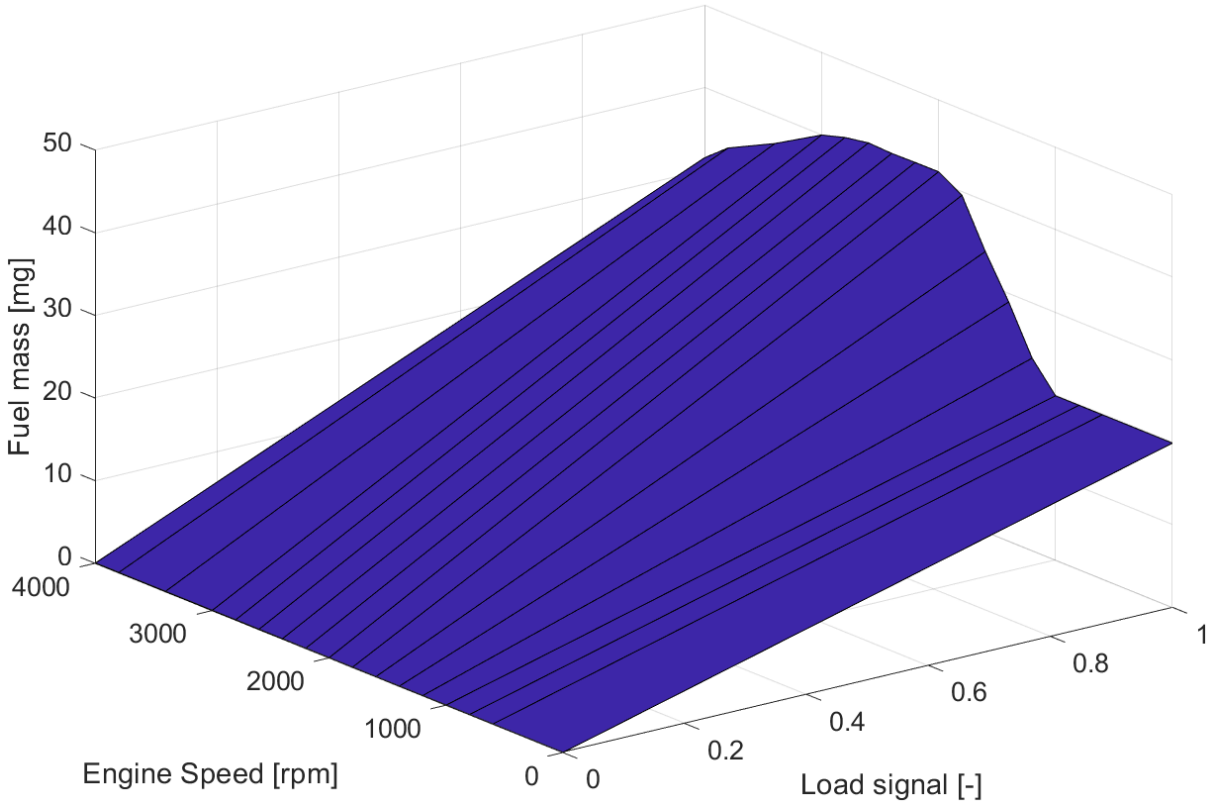


Figure 11. CI engine fuel mass look-up table, data for Appendix A, Engine 2

To additionally ensure the accuracy of the developed model, exhaust pressure will also be given via look-up tables from Cruise M. SI naturally aspirated exhaust pressure is given in Figure 12.

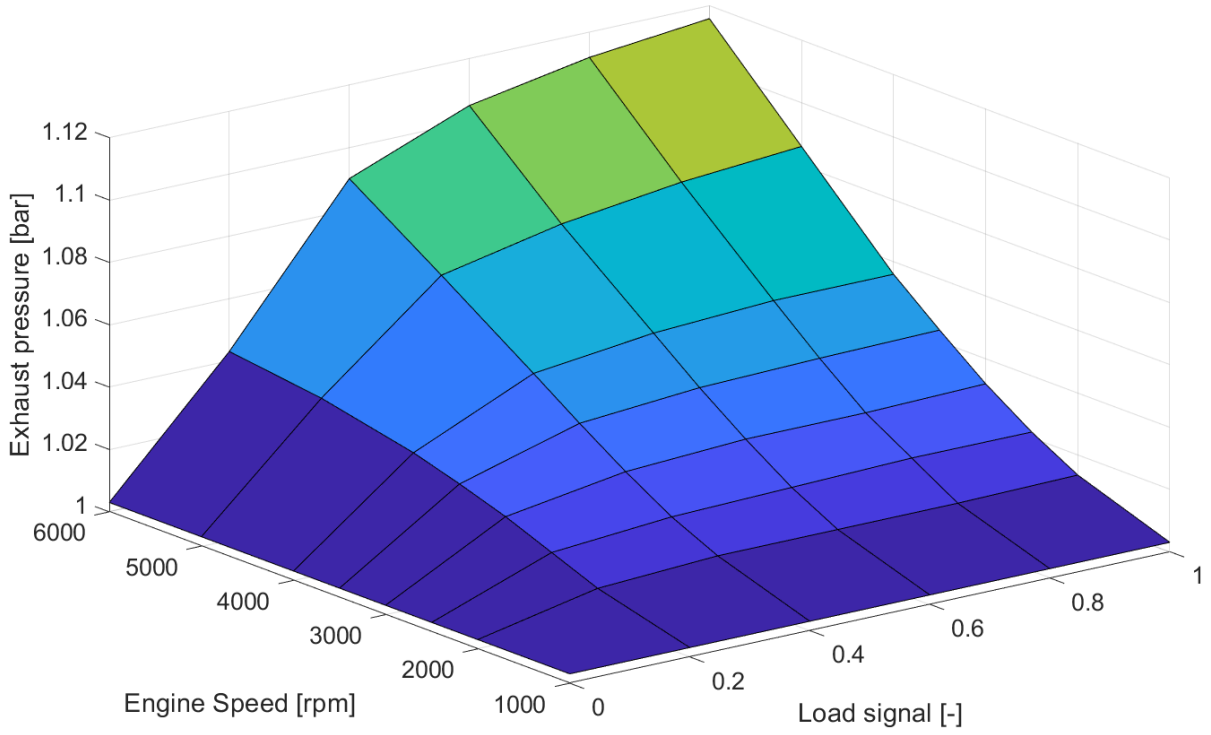


Figure 12. SI engine exhaust pressure look-up table, Appendix A, Engine 1

CI turbocharged exhaust pressure look-up table is given in Figure 13 from data from Cruise M.

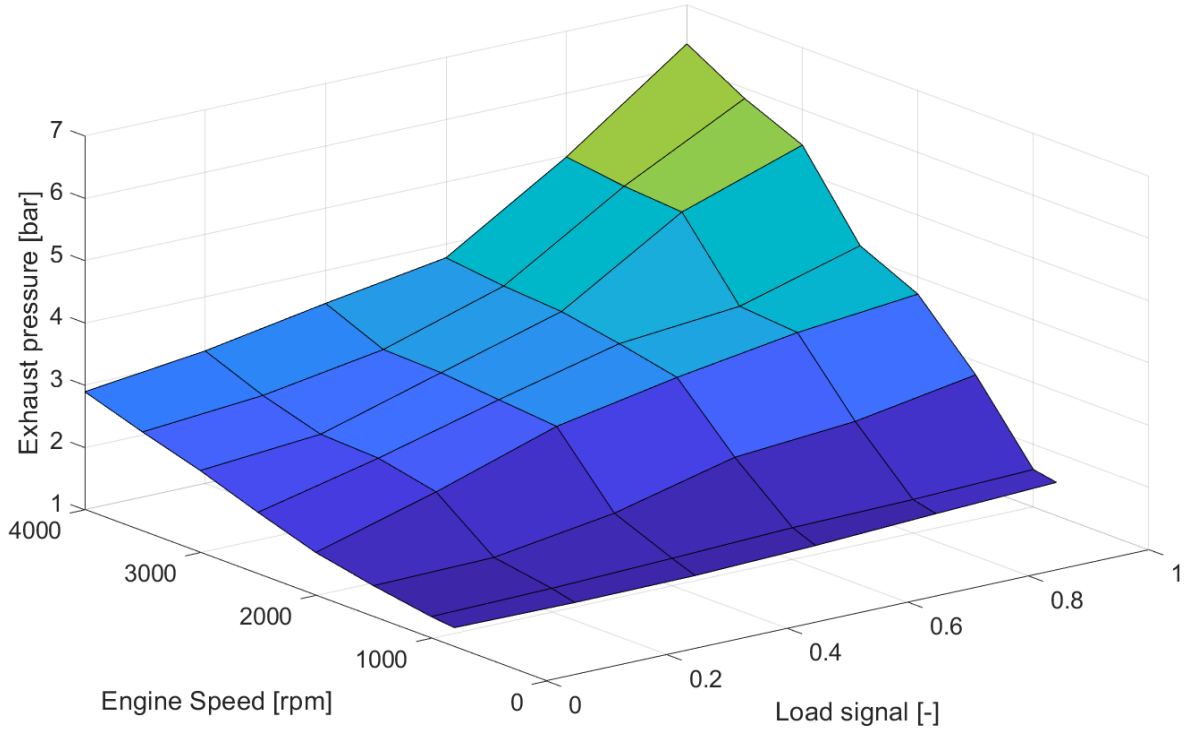


Figure 13. CI engine exhaust pressure look-up table, Appendix A, Engine 2

The exhaust pressure, as defined in the two above look-up tables, is defined as the cylinder pressure at the end of the exhaust stroke. It means that the pressure calculated at the end of the

expansion with (3) has to be modified to the value defined in the look-up tables. It will be done by incorporating a first-order system as seen in Figure 14.

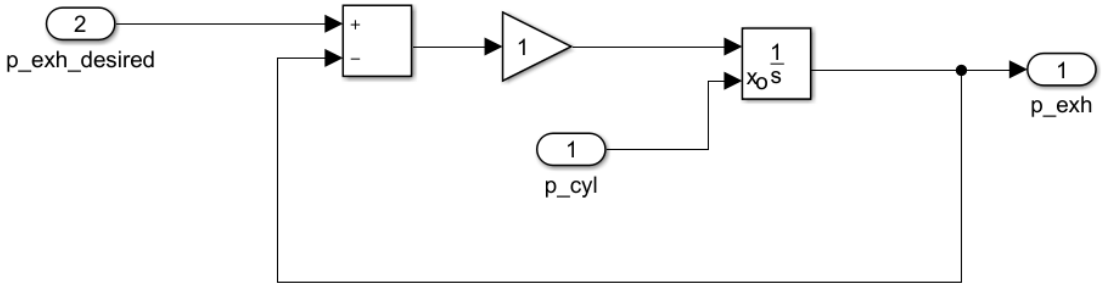


Figure 14. A first-order system approximation of the exhaust stroke

Once the expansion has finished, the above system will be enabled. Initial condition for the integrator is the pressure at the end of the expansion, and with the first-order system above, the cylinder pressure reaches the desired exhaust pressure as defined in Figure 12 and Figure 13. The effect is visible in Figure 29.

Finally, the mass trapped in the cylinder consists of the freshly inducted working substance calculated in (23) and the residual combustion products from the previous cycles, if EGR does not exist. In that case, residual combustion products are the exhaust gasses that are not washed out during the gas exchange process [8]. They occupy the compression volume and their mass can be described as:

$$m_{exh} = \frac{p_{exh} \cdot V_K}{T_{exh} \cdot R} \tag{26}$$

where:

- m_{exh} is the residual combustion products mass,
- T_{exh} is the residual combustion products temperature and
- p_{exh} is the exhaust pressure

This leads to total trapped mass in the cylinder at the start of the compression:

$$m_c = m_a + m_{exh}$$

$$\gamma = \frac{m_{exh}}{m} \quad \textbf{(27)}$$

where:

- γ is the residual combustion products fraction

3.1.7. Torque calculation

Two terms will have to be defined before proceeding to the torque calculation section. The term *indicated* encompasses all of the variables connected with the events within the cylinder and consequently related to them (indicated cylinder pressure, work, torque). The term *brake* or *effective* is established for the variables forwarded further down the powertrain, meaning they are observed with the mechanical efficiency in mind [7].

Combining the defined cylinder intake and exhaust pressures from the initial conditions with the calculated cylinder pressure from (3), a trace of the indicated cylinder pressure from one cycle can be described.

The indicated cylinder pressure is then subtracted with the housing pressure which yields the resulting acting pressure on the piston head surface. The force acting on the piston resulting from the gas pressure can be described as:

$$F_g = \left(p_c - p_h \right) \cdot A \quad \textbf{(28)}$$

where:

- p_h is the housing pressure and has a default value of 1 bar.

As defined in the thesis task, the inertia (mass) forces of the oscillating piston also have to be taken into account for the definition of the resulting torque. First, the piston acceleration needs to be defined. Its equation is derived from the piston path equation in (19), is crank-angle dependent and has the following form [9]:

$$a_c = r \cdot \omega^2 \cdot \left(\cos(\alpha) + \lambda_c \cdot \cos(2\alpha)\right) \quad \textbf{(29)}$$

The oscillating mass can be defined as the piston mass and approximately one-third of the conrod mass [9]. That mass, with the previously defined acceleration, yields the cylinder inertia forces:

$$F_{in} = -m_{osc} \cdot a_c$$
$$m_{osc} = m_p + m_{conrod,osc} \quad \textbf{(30)}$$

where:

- m_{osc} is the oscillating mass,
- m_p is the piston mass,
- $m_{conrod,osc}$ is the oscillating part of the conrod mass.

It can be seen from the previous equations that the inertia forces depend quadratically on the engine speed, meaning that they have an increasing effect on the total piston forces as the RPMs rise.

Gas and inertia forces are not the only forces acting upon the piston, but the rest of them does not have a significant impact on the indicated engine torque and their analysis is more concerned towards the engine balancing. The combined (gas and inertia) forces acting upon the piston can be expressed as:

$$F(\alpha) = F_g(\alpha) + F_{in}(\alpha) = \left(p_c(\alpha) - p_h\right) \cdot A + F_{in} \quad \textbf{(31)}$$

where:

- $F(\alpha)$ is the combined force acting upon the piston, crank-angle dependent

The realized combined forces are colinear to the piston oscillating axis. The piston is, however, connected to the crankshaft via the conrod and the indicated torque is calculated from the tangential force acting upon the crankshaft over the crankshaft radius *r*. A relationship has to be established that will connect the realized combined forces acting upon the piston with the

tangential force acting upon the crankshaft, for a defined engine layout, which is the inline engine. From [9], the indicated torque has the following form:

$$T_I(\alpha) = F(\alpha) \cdot r \cdot \sin(\alpha) \cdot \left(1 + \frac{\lambda_c \cdot \cos(\alpha)}{\sqrt{1 - \lambda_c^2 \cdot \sin^2(\alpha)}} \right) \quad \textbf{(32)}$$

where:

- T_I is the indicated torque, crank-angle dependent

With this, the traces model is completed. All of the crank angle dependent variables have been described and their effect on the developed model explained. The traces model results and comments are part of the section 3.3.1. A clear representation of the developed model can be seen in Figure 15.

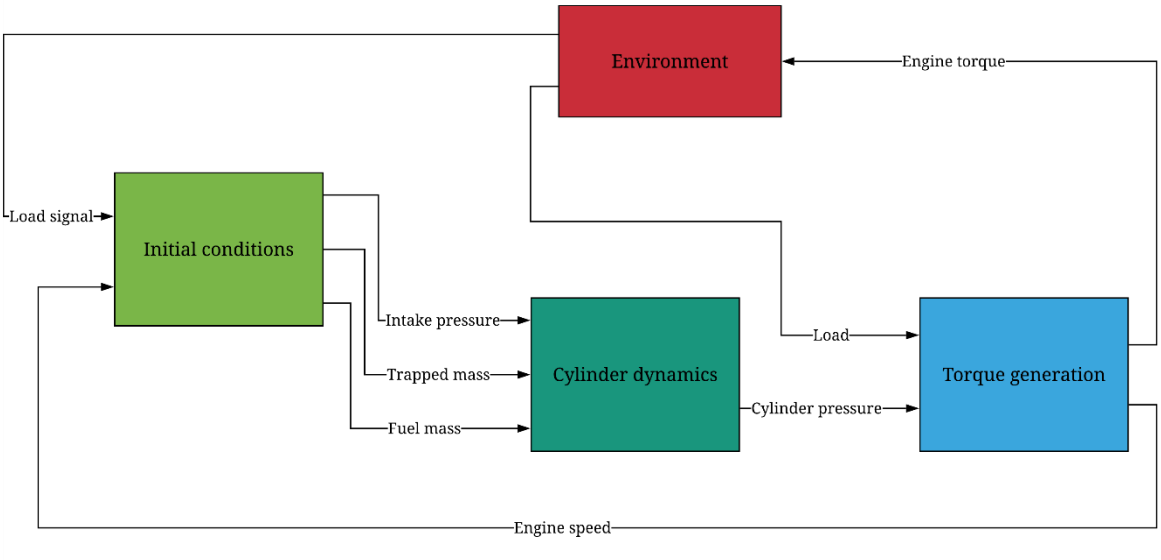


Figure 15. A block representation of the developed traces model

Finally, the sizing of the model needs to be performed as the model needs to represent a variety of the engine sizes. Most of the engine parameters already depend on the engine model input parameters (cylinder diameter, engine displacement, number of cylinders and compression ratio). Other parameters of the model are presumed constant for the sake of simplicity (crankshaft radius to conrod length ratio, housing pressure, specific gas constant, the temperature of the fresh substance, the temperature of the residual combustion products, cylinder head temperature, liner temperature and piston temperature). But some model parameters and variables need to be defined accordingly to the engine/cylinder size/parameters.

The first example is the piston mass. An empirical expression is found to accurately estimate the piston mass depending on the piston diameter. The data for the expression was collected through various sources and has the following form:

$$m_p = 7.958 \cdot D - 0.3631 \quad \textbf{(33)}$$

The oscillating part of the conrod mass is presumed to have two-thirds of the piston mass, leading to:

$$m_{osc} = m_p + m_{conrod,osc} = m_p \cdot \left(1 + \frac{2}{3}\right) \quad \textbf{(34)}$$

An empirical expression was also used for calculating the crankshaft mass, the data collected from the AVL Excite software:

$$m_{crank} = 6.66 + 5.33 \cdot z \quad \textbf{(35)}$$

where:

- m_{crank} is the crankshaft mass

Mass of the conrod rotating part is assumed, a mentioned before, as the two-thirds of the total conrod mass. In the equation above, one-third of the conrod mass (the oscillating part) is assumed to have the value of two-thirds of the piston mass, leading to the conclusion that the rotating part of the conrod has the mass value of:

$$m_{conrod,rot} = \frac{4}{3} \cdot m_p \quad \textbf{(36)}$$

where:

- $m_{conrod,rot}$ is the rotating part of the conrod mass.

Making the total rotating mass equal to:

$$m_r = m_{crank} + z \cdot m_{conrod,rot} \quad \textbf{(37)}$$

where:

- m_r is the total rotating mass of the engine

In this way, the relevant masses are defined through the piston diameter and the number of cylinders, which are general model input parameters and thus keeping the required number of engine parameters at a minimum.

An additional parameter that needs to be modified depending on the engine size is the fuel mass for the CI engine. In the case of the SI engine, fuel mass is calculated from the inducted fresh substance mass. That mass already depends on the engine size (engine displacement) and the intake pressure shown in Figure 9 has a similar shape for all engine sizes. The look-up table on Figure 11 however, was defined for a 0.4-liter cylinder. This data will then be scaled with the factor that is equal to the ratio of the cylinder volume to be simulated, and the 0.4-liter cylinder the look-up table refers to. For example, if the cylinder volume to be simulated is 0.5-liter, the scaling factor for the look-up table would be 1.25.

Next, the transient model will be presented.

3.2. Transient model

The developed traces model (crank-angle dependent) now needs to be converted to a transient model (time-dependent). The transient model can be simulated for a desired period of time and be subjected to a variety of input signals to test the model performance under all conditions and different operating points. In the traces model, the engine speed was kept constant with a false assumption in the case of simplicity. The false assumption was that the engine speed does not vary significantly during one cycle. That is not the case in the transient model so first, an important assumption has to be made. Time and crank angle are connected via engine speed:

$$\alpha = \omega \cdot t \tag{38}$$

Differentiating the above expression yields the following result:

$$d\alpha = \omega \cdot dt + d\omega \cdot t \tag{39}$$

The important assumption is that the second part of the expression above can be ignored with the argument that the change of engine speed in the scope of two simulation time steps is very small. The support to this argument comes from the fact that for the model to be accurate, it needs to run at 10 kHz, so the size of one timestep is 0.1 ms. This leaves us with:

$$d\alpha = \omega \cdot dt \tag{40}$$

This assumption makes it easier to calculate the current crank angle in regard to the current simulation time. A simple integrator in the Simulink environment is required to calculate the current crank angle, with the output value of the integrator reset to zero every time the integrated crank angle crosses the one cycle duration value (4π radians or 720 crank-angle degrees for a 4-stroke engine). The realized concept can be seen in Figure 16 and the concept results in Figure 17.

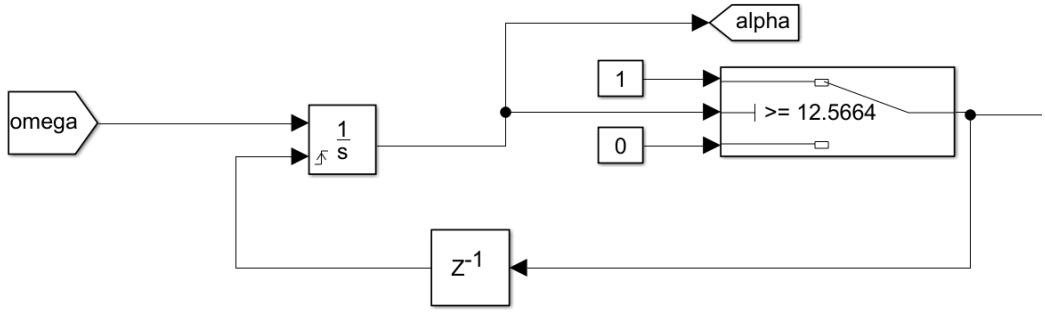


Figure 16. Calculating and reseting the crank-angle α

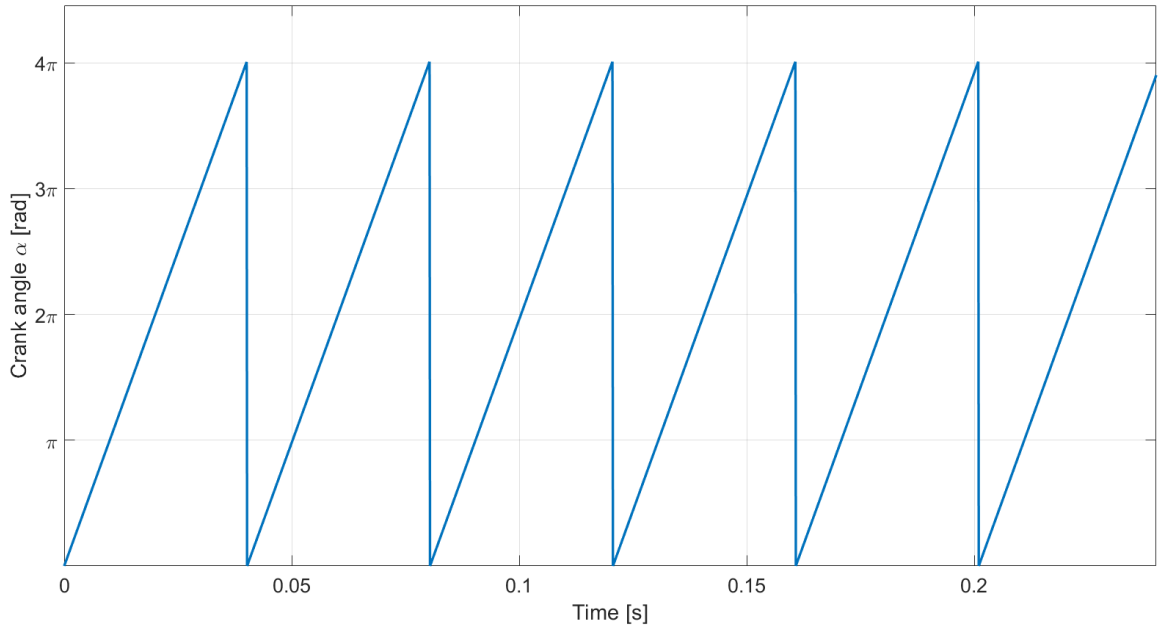


Figure 17. Values of the crank-angle during several cycles

The engine was set to a speed of 3000rpm. It means that it is rotating 50 times a second. It takes two engine rotations to complete one engine cycles for a four-stroke engine. It means that there are 25 cycles per second at 3000rpm, or:

$$25\frac{cycles}{s} = \frac{1}{25}\frac{s}{cycle} = 40\frac{ms}{cycle} \tag{41}$$

Comparing that result to the figure above, one can conclude that the devised way of calculating the current crank angle is satisfactory. The calculated current crank angle is forwarded to the altered traces model and to the other parts of the transient model that require its value.

The initial conditions as discussed within the developed traces model remain the same and their values are refreshed only at the beginning of every new cycle. Those values, different every

new cycle as the load signal and the engine speed change, are then also forwarded to the altered traces model.

3.2.1. Altered traces model

The previously developed traces model has to be altered to support its integration within the transient model. First, all of the signals that are leading into an integrator have to be modified because the original traces model was developed in the crank angle domain and the transient model integrates in the time domain. In this case, only one integrator exists within the model, the one that calculates the current cylinder pressure value. The modification is shown in Figure 18.

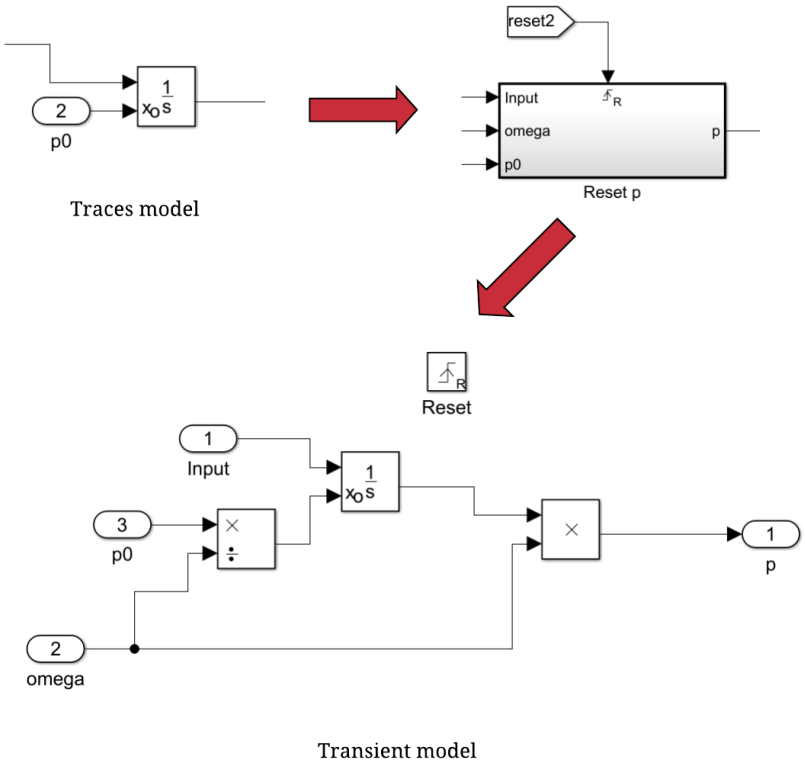


Figure 18. Transient cylinder pressure calculation

To clarify the figure above, in the traces model, the calculated cylinder pressure is crank-angle dependent and its integration was executed in the crank-angle domain. Therefore, if the cylinder pressure is to be calculated in the same way in the transient model, where the integration is executed in the time domain, one must modify the signal to be integrated. The process is described through the following equations.

$$p_c(\alpha) = \int \frac{dp_c(\alpha)}{d\alpha} d\alpha \qquad \textbf{(42)}$$

Using (40) and inserting it into the equation above, calculated cylinder pressure is now time-dependent:

$$p_c(t) = \omega \cdot \int \frac{dp_c(\alpha)}{d\alpha} dt \quad \textbf{(43)}$$

and has to be reset every new engine cycle, therefore the reset block and the reset signal. The initial condition of the integrator is the intake pressure, mapped from the initial conditions that are also ran at the start of every new engine cycle. The initial condition also has to be divided with the engine speed to become time-dependent.

Another modification to the traces model was made. In the traces model, the calculated cycle began with the induction, moved to compression and expansion, and finished with the exhaust stroke. The modification was made to start with the compression first, with the initial conditions already set at the compression start, as explained in section 3.1.6.

Next, the process of torque calculation for multiple cylinders will be discussed.

3.2.2. Indicated engine torque

The indicated torque, as explained in (32), is the result of the calculated cylinder pressure and the inertia forces of a single cylinder only. To expand the model to include multiple cylinders, one can take different paths.

Another block/s in Simulink can be made which will output the indicated torque from a cylinder which will have a different ignition time, and with that, its own place in the engine firing order during one engine cycle. Within that block, a whole different set of settings and parameters could be made, e.g. redefining the combustion parameters as defined in section 3.1.3, forcing a misfire, etc. But additional problems would occur:

- each additional cylinder would slow down the simulation even further,
- a method would have to be devised to simulate only the previously defined number of cylinders and to follow the firing order.

A simpler way is presented. The signal of the calculated indicated torque would be delayed for an appropriate amount of time considering the number of cylinders and according to the following table. A maximum of six cylinders is supported (with a simple possibility to add more) and every one of them has the same characteristics.

Table 2. Indicated torque signal delay table

Number of cylinders	Signal delay
1 - cylinder engine	0
2 - cylinder engine	2π
3 - cylinder engine	$\left[\frac{4}{3}\pi, \frac{8}{3}\pi\right]$
4 - cylinder engine	$[\pi, 2\pi, 3\pi]$
5 - cylinder engine	$\left[\frac{4}{5}\pi, \frac{8}{5}\pi, \frac{12}{5}\pi, \frac{16}{5}\pi\right]$
6 - cylinder engine	$\left[\frac{2}{3}\pi, \frac{4}{3}\pi, 2\pi, \frac{8}{3}\pi, \frac{10}{3}\pi\right]$

Simulink realization of the problem is shown in the figure below.

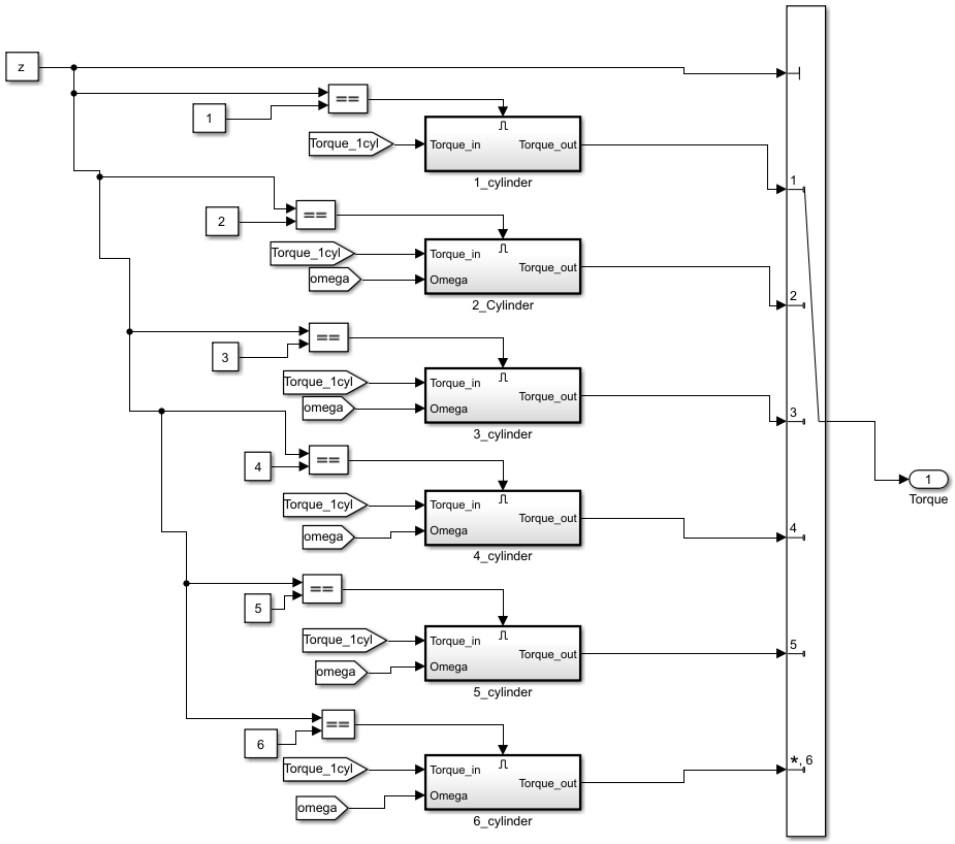


Figure 19. Torque calculation for a different number of cylinders

As can be seen in the figure above, the appropriate subsystem is enabled when the value of the predefined number of cylinders (*z*) responds to the value dedicated to that particular subsystem. Also, the number of cylinders determines which port of the multi-port switch would be forwarded further into the simulation. A 4-cylinder subsystem would be further shown for an example of how the indicated torque for multiple cylinders is realized.

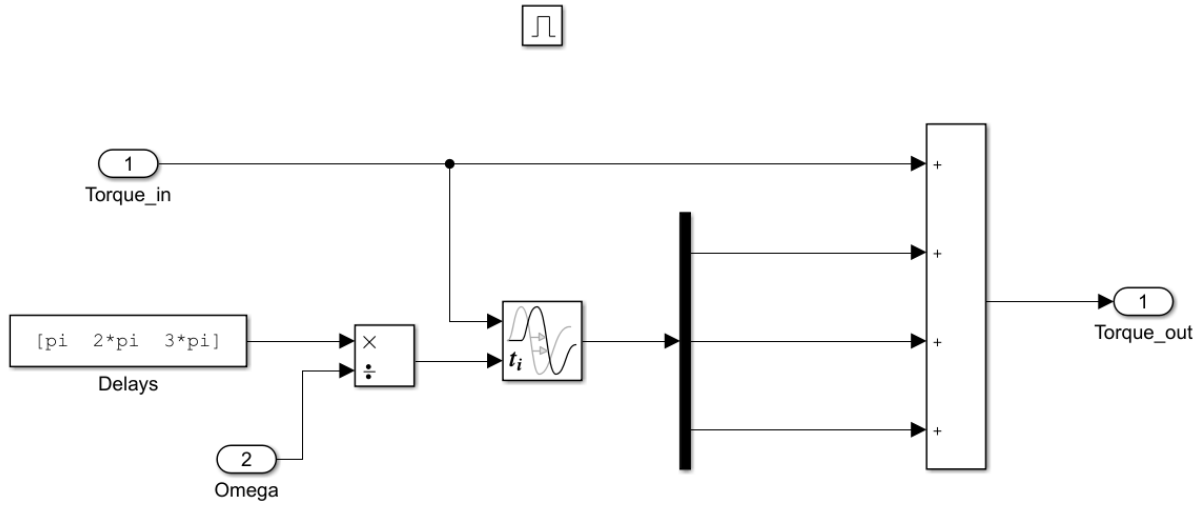


Figure 20. Detail of the enabled subsystem for a 4_cylinder case

Torque is forwarded into a variable transport delay block. The other input of the variable transport delay block is the vector of delays. The default vector of delays is divided by the current value of the engine speed to calculate the equivalent duration of the delay in simulation time. The variable transport delay block outputs as many signals as the size of the vector of the delays. They are then superposed together, just like individual cylinder torques are acting together upon a real crankshaft.

3.2.3. Engine friction

Not all the work transferred to the piston from the gases contained inside the cylinder (the indicated work) is available at the crankshaft for actual use. That portion of the work transferred which is not available is usually termed *friction* or *mechanical* work [7]. The friction work (or power) fraction of the indicated work (power) varies between 5-10% at full load and 100% at idle. These numbers are sufficient for the topic to be of great importance to the engine design and modeling. Friction work is usually expended as follows:

- to draw the fresh mixture through the intake system and into the cylinder, and to expel the burned gases from the cylinder and out to the exhaust system. This is called pumping work.
- to overcome the resistance to relative motion of all the moving parts of the engine. This includes the friction between the piston rings, piston skirt and cylinder wall, friction in the crankshaft and camshaft bearings, friction in valve mechanism, gears etc.
- to drive the engine accessories; the fan, water pump, AC, oil pump, fuel pump, etc.

There have been many attempts to properly describe the friction work in an SI or Ci engine. A good starting point is a set of equations from [7], although that set of equation relates to the engines designed some time ago. As time and technology progresses, significant contributions have been made in order to reduce the engine friction. This lead to the point that in most of the cases, friction maps for individual engines are made. They usually depend on the engine speed and load, and one of them will be used as a reference point for describing the engine friction. The map was taken from a reference engine model in AVL Cruise M which is also used for validation purposes and can be seen in the figure below.

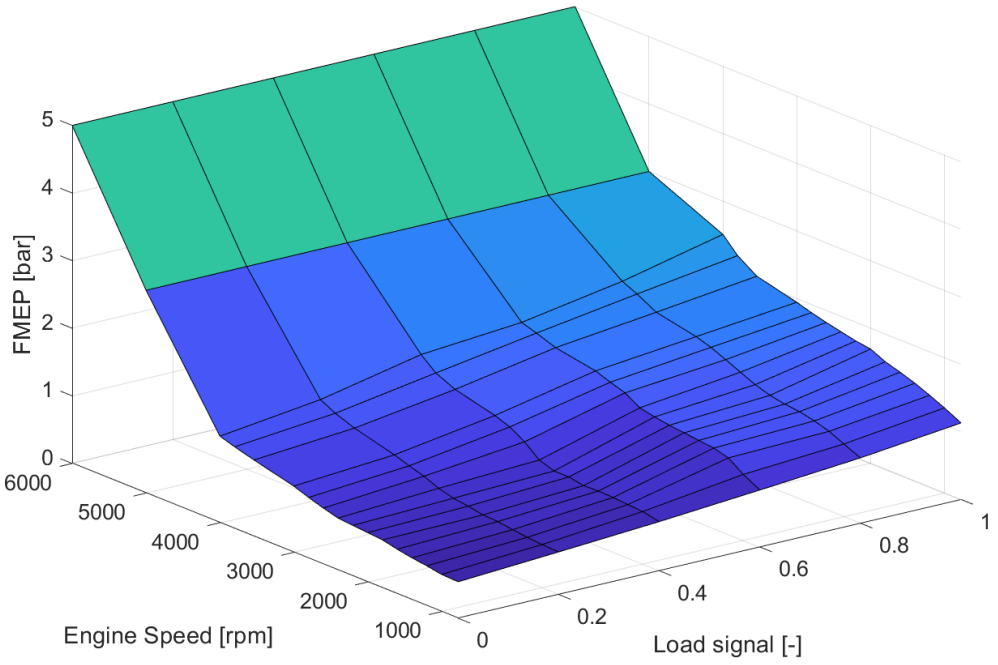


Figure 21. Friction mean effective pressure map

Friction mean effective pressure (FMEP) can be converted to an equivalent friction torque with the following equation:

$$T_F = \frac{10^5 \cdot FMEP \cdot V_E}{4 \cdot \pi} \tag{44}$$

where:

- $FMEP$ is friction mean effective pressure and
- T_F is friction torque.

3.2.4. Performance

To have a better insight into the engine performance, a mean value of the indicated torque must be calculated first. Mean indicated torque value corresponds to the mean value of the indicated torque curve as described in (32) during one engine cycle. The desired variable will be calculated with the following equation [9]:

$$\overline{T_I} = \frac{\int_0^{\frac{4\cdot\pi}{z}} T_I(\alpha) \cdot d\alpha}{\frac{4 \cdot \pi}{z}} \tag{45}$$

where:

- $\overline{T_I}$ is the mean indicated torque

The equation above needs to be realized within the developed transient model. The designed solution is shown in the figure below.

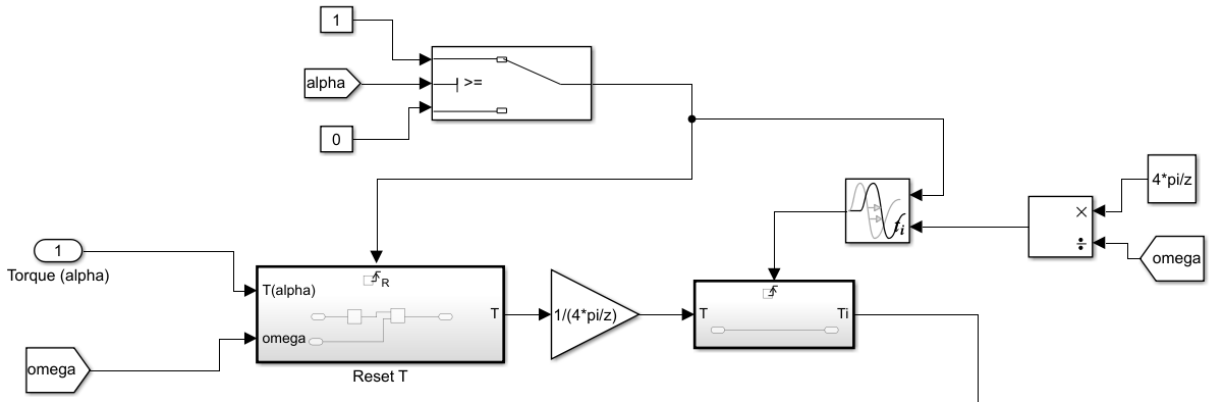


Figure 22. Mean indicated torque block diagram

And within the Reset T block:

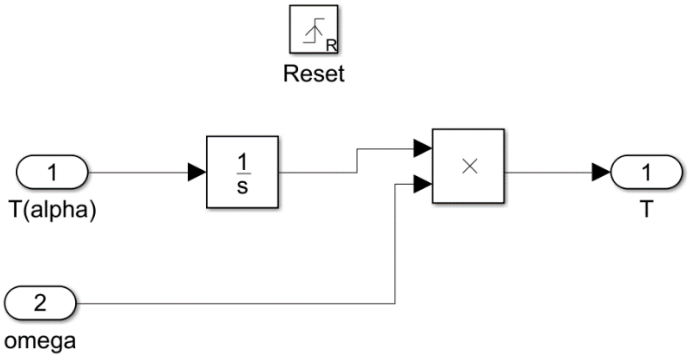


Figure 23. Reset T block of the mean indicated torque calculation

The figure above is similar to Figure 18, where the cylinder pressure derivative (also α dependent) was integrated in the time domain and then multiplied with the current engine speed value to calculate the real value. That value is then divided with the denominator from (45) and the mean value of the indicated torque is calculated. Since it is a cycle related variable, it is reset whenever the crank angle value reaches the end of the cycle and updated only after the current cycle ends (thus the delay block).

The indicated mean effective pressure is a variable that indicates the engine load and performance independently of the engine type. First, a term of indicated work needs to be defined. It can be defined as the surface of a rectangle in the cylinder indicator diagram (p-V diagram) where the base is the engine displacement volume and the rectangle height is the indicated mean effective pressure [8]. The previous definition can be more easily understood through the following figure.

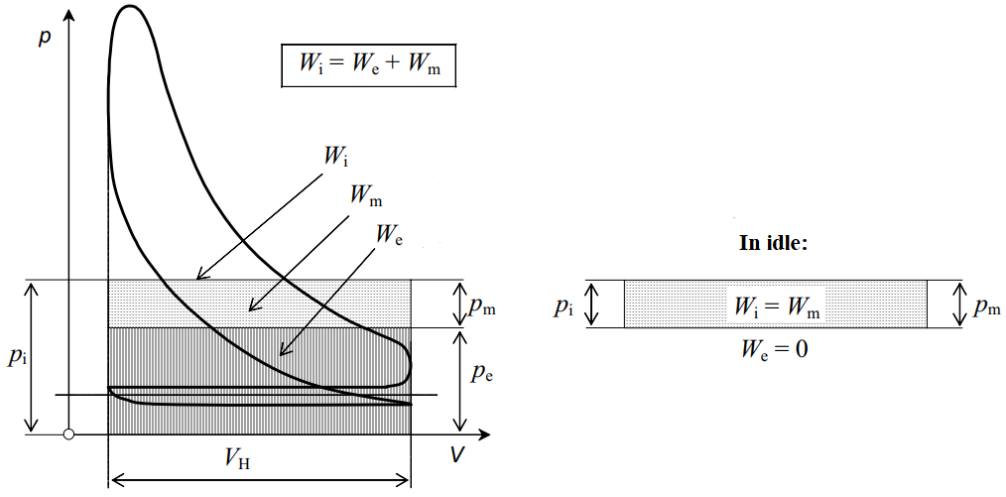


Figure 24. Distribution of engine work using the mean pressure values. In idle, all of the indicated work is spent on friction (mechanical) losses.[8]

where:

- W_i is the indicated work, calculated from the events in the cylinder,
- W_m is the mechanical or friction work, as defined in the previous section and
- W_b is the effective or brake work, value at the engine clutch.

Indicated mean effective pressure (p_i or IMEP) can be calculated from the value of indicated work (as seen in Figure 6) if the indicated efficiency was known or estimated. In this thesis, however, since the mean indicated torque was calculated in one of the previous sections, IMEP is given through the following equation, without the need of estimating indicated efficiency:[8]

$$IMEP = \frac{4 \cdot \pi}{V_E \cdot 10^{-5}} \cdot \overline{T_I} \quad \textbf{(46)}$$

where:

- $IMEP$ is indicated mean effective pressure.

Along with the *FMEP* defined above, brake mean effective pressure is given as:

$$BMEP = IMEP - FMEP \quad \textbf{(47)}$$

where:

- $BMEP$ is the brake mean effective torque

BMEP has similar values in engines of different sizes and purposes and represents a measure of engine load [8]. Increasing the engine load, the brake mean effective pressure is also increased.

Mechanical efficiency of the engine can be defined as:

$$\eta_m = \frac{BMEP}{IMEP} \quad \textbf{(48)}$$

where:

- η_m is the mechanical efficiency

and has zero value when idling because all of the indicated work is spent on mechanical/friction work. Brake efficiency:

$$\eta_b = \frac{W_b}{Q_f} = \frac{BMEP \cdot 10^5 \cdot V_H}{m_f \cdot H_l} \quad \textbf{(49)}$$

where:

- η_b is the brake efficiency

3.2.5. Engine inertia

Finally, when the indicated engine torque has been calculated and engine friction for current engine speed and load defined, brake or effective engine torque dependent on α and mean brake engine torque can be given as:

$$T_B(\alpha) = T_I(\alpha) - T_F$$
$$\overline{T_B} = \overline{T_I} - T_F \quad \textbf{(50)}$$

where:

- T_B is the brake torque and
- $\overline{T_B}$ is the mean brake torque.

Brake engine torque is the input to the governing engine dynamic equation:

$$J(\alpha) \cdot \frac{d\omega}{dt} = T_B(\alpha) - T_L \quad \textbf{(51)}$$

where:

- $J(\alpha)$ is the engine moment of inertia and
- T_L is the engine load.

To properly carry out the tasks given in the thesis, the engine's moment of inertia needs to be properly described. In most of the literature, the moment of inertia is given as a constant. In this

thesis it would not be the case as the proper description of the engine inertia's variable properties has an effect on the calculated engine speed oscillations.

Described moment of inertia has to present the variable impact that the reciprocating movement of the piston mechanism has on the total engine inertia. The moving masses are the piston, gudgeon pin, piston rings, conrod and other smaller parts of the mechanism. Their variable distance to the crankshaft center axis introduces a crank-angle dependent change of the engine inertia which is reduced to the crankshaft center axis itself. A detailed approach to the describing that change can be found in [15], but is too detailed for the developed model as it needs the values of every moving mass in the mechanism. Two approaches to defining the total engine inertia will be considered within this thesis.

The first approach is considering the rotating masses' inertia as constant (crankshaft, part of the conrod mass and the flywheel) and all lumped into a single value. Dedicated equation comes from [14] and is equal to the simplified form of the equation in [15].

$$J(\alpha) = J_{rot} + \sum_{i=1}^{z} m_{osc,i} \cdot v_i(\alpha)^2 = J_{rot} + \sum_{i=1}^{z} m_{osc,i} \cdot \left[r\left(\sin(\alpha) + \frac{\lambda_c}{2} \cdot \sin\left(2 \cdot \alpha\right) \right) \right]^2$$

$$J_{rot} = m_{rot} \cdot r^2 + J_{fly} \qquad \textbf{(52)}$$

$$m_{rot} = m_{crank} + z \cdot m_{conrod,rot}$$

where:

- J_{rot} is the rotating part of the engine inertia
- J_{fly} is the flywheel inertia
- $v(\alpha)$ is the piston velocity, crank angle dependent.

Instead of calculating the oscillating inertia of each cylinder and also selecting the number of inertias being calculated depending on the number of cylinders, the same approach as with the indicated engine torque is used. Only the inertia of one cylinder is calculated, from the second part of (52), and then the signal would be delayed in the same way as seen in Figure 19. The calculated and the delayed inertia are also superposed and added to rotating inertia value. Above defined inertia is inserted into (51) and from there, with calculated brake torque and imposed

load, engine speed can be integrated. Because of the oscillating behavior of the indicated torque and reciprocating cylinder inertia, engine speed is also fluctuating.

3.2.6. Flywheel

The second approach defines the flywheel as a dual-mass flywheel and this approach will be used in the thesis. The dual-mass flywheels are becoming a part of the middle-class cars more and more regularly, no more reserved only for premium-class cars. With them, it is also possible to describe the torque transfer more accurately, whether the transfer is happening from the engine to the driveline, or from the engine to the testbed. The latter case is crucial for this thesis and the flywheel model described in this section will try to describe two behaviors as one; effect of the flywheel and the effect of the elastic connection between the engine and the testbed. The dual-mass flywheel consists of two rotational masses connected by a spring-damper system. Their application results in a considerable reduction of torsion oscillations from the engine to the driveline [1]. The brake torque and the engine speed have a very oscillating behavior. The purpose of the flywheel is to reduce the engine speed fluctuations that consequently appear from the oscillating effective torque [9],[17]. It absorbs energy during the power stroke and distributes it during the exhaust, intake, and compression strokes. The transmission of the torque spikes developed by the engine will be reduced to the driveline and will also enable the sudden loads to be imposed on the engine without stalling it. The flywheel or torque converter (automatic transmission) mass is crucial in controlling the engine speed fluctuations, but it cannot be too large as then it has a negative effect on the engine transient operations.

The dual-mass flywheel's dynamics can be more easily understood from the figure below, while the mathematical description follows after from [3].

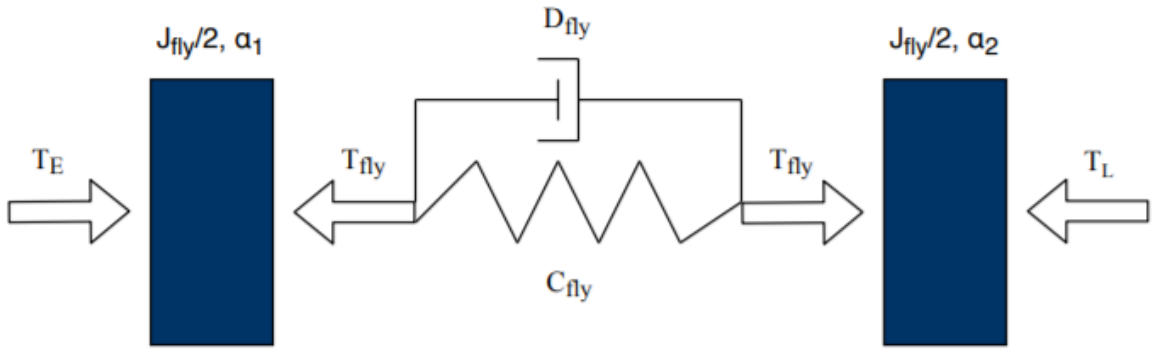


Figure 25. The dual-mass flywheel dynamics [3]

Each of the rotational masses has approximately one half of the total dual-mass flywheel inertia. This results in the following set of equations [3]:

$$J_E \cdot \dot{\omega}_1 = \left(J_{osc} + m_{rot} \cdot r^2 + \frac{J_{fly}}{2} \right) \cdot \dot{\omega}_1 = T_E - T_{fly}$$

$$T_{fly} = (\omega_1 - \omega_2) \cdot D_{fly} + (\alpha_1 - \alpha_2) \cdot C_{fly} \quad \textbf{(53)}$$

$$\frac{J_{fly}}{2} \cdot \dot{\omega}_2 = T_{fly} - T_L$$

where:

- J_E is the engine inertia as defined in the equation above
- $\omega_1 = \omega$ is the engine speed,
- T_{fly} is the engine torque transmitted by the flywheel,
- ω_2 is the shaft speed after the flywheel,
- D_{fly} is the flywheel damping factor and
- C_{fly} is the flywheel stiffness factor.

3.2.7. T-engine or N-engine model

At the end of the developed model section, a final classification to an engine model is to be clarified; whether a developed model is a T or an N type. In the all growing and developing industry of automotive simulations, another classification of the engine model emerged and it depends on the environment the engine model will be connected to. Whether it's a real testbed or a drivetrain model, the inputs and outputs of the developed model have to be defined, along with their connection to that model.

The model that has been discussed so far is a T-engine model. T comes from *torque* and it means that the torque is the relevant input to the model. That torque is the engine load in (51) and represents the load that the engine is subjected to throughout the simulation. It is the load that comes from the wheels and is transferred through the drivetrain to the engine clutch and the engine itself. It depends on the aerodynamic and rolling resistance, road slope, and vehicle

speed, but that is not the subject of the current thesis. The resulting engine load is then the input to a T model. The other input is the engine load signal and is defined by an artificial driver or a speed controller. The defined load signal will, at the current engine speed, produce a certain amount of indicated torque. That torque is, as already described, reduced by the defined engine friction (at current engine speed and load signal). The resulting effective torque is imposed on the flywheel, where its fluctuations are reduced. The load is also acting upon the flywheel and the resulting dynamics, as explained in (53), define the engine speed before and after the flywheel. That speed is the output of a T model.

It is simple to modify the current model to become an N model. N comes from the notation for *engine speed*. In this kind of a model, the speed is given as an input into the model. Engine speed before the flywheel is then calculated with (53) and thus all of the engine speed related variables within the model are then dependent on the speed input. Same as before, the other model input is the engine load signal which will, with the imposed engine speed, determine the calculated engine indicated torque. It will again be reduced by the engine friction and the torque after the flywheel is the output of an N model.

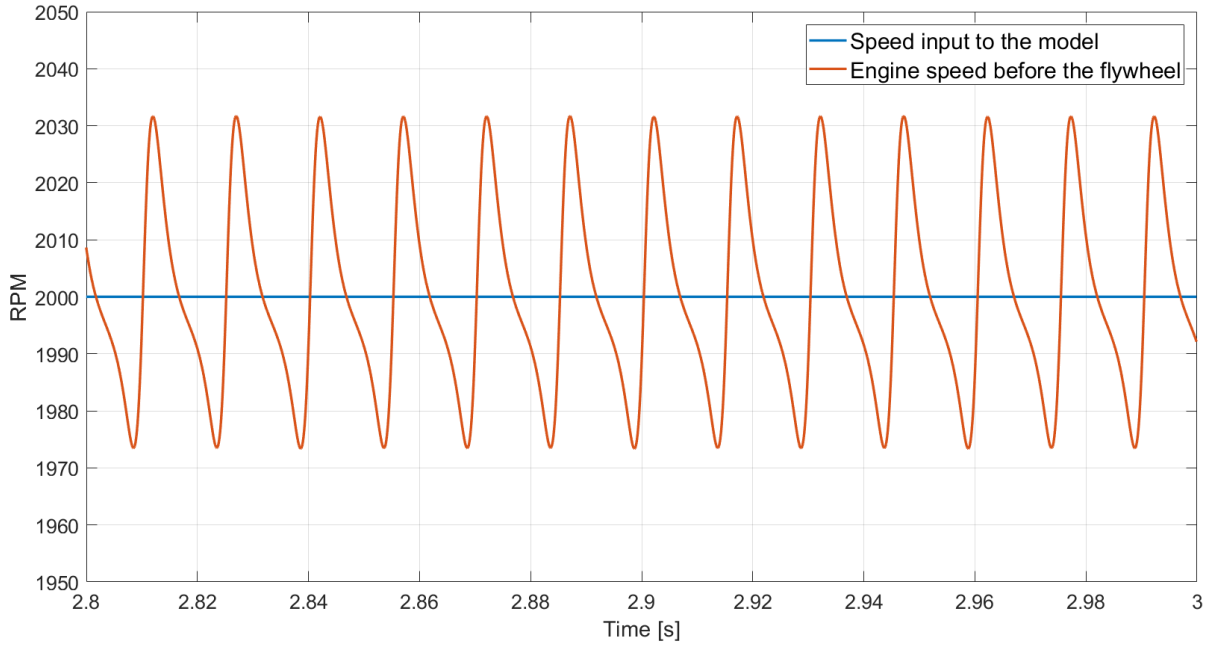


Figure 26. An example of an N model engine speed where a constant value is given as an input to the model

The selection of the model to be simulated is determined with a simple variable and a switch, leading to an even greater level of model diversity.

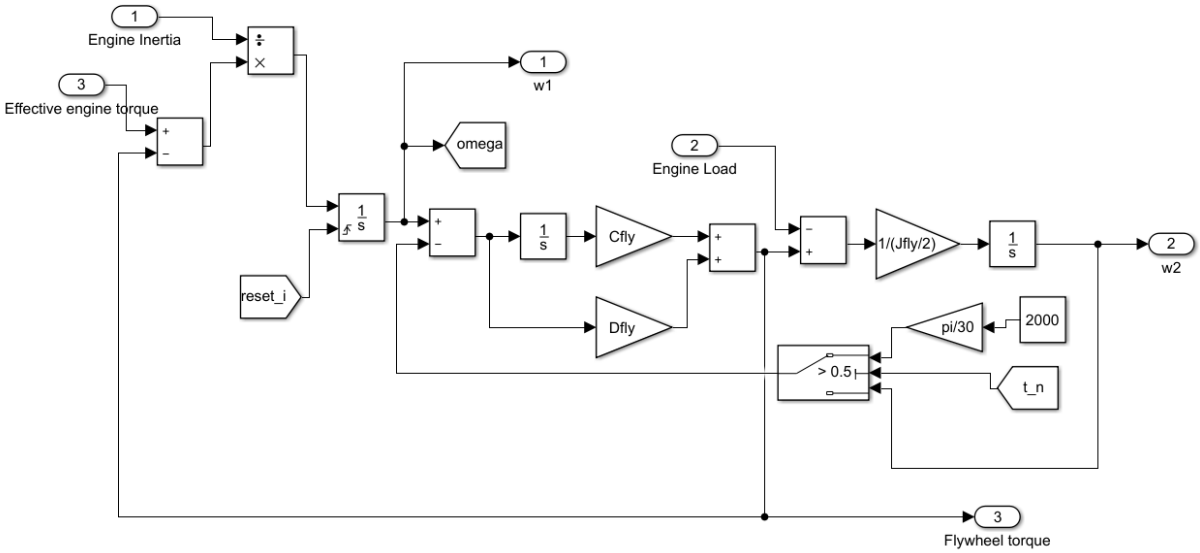


Figure 27. Equation (53) in Simulink and the T or N model selection via a switch and a variable

The model selection depends on the simulation needs and the types of the other available models. The classification is also shown in the figure below.

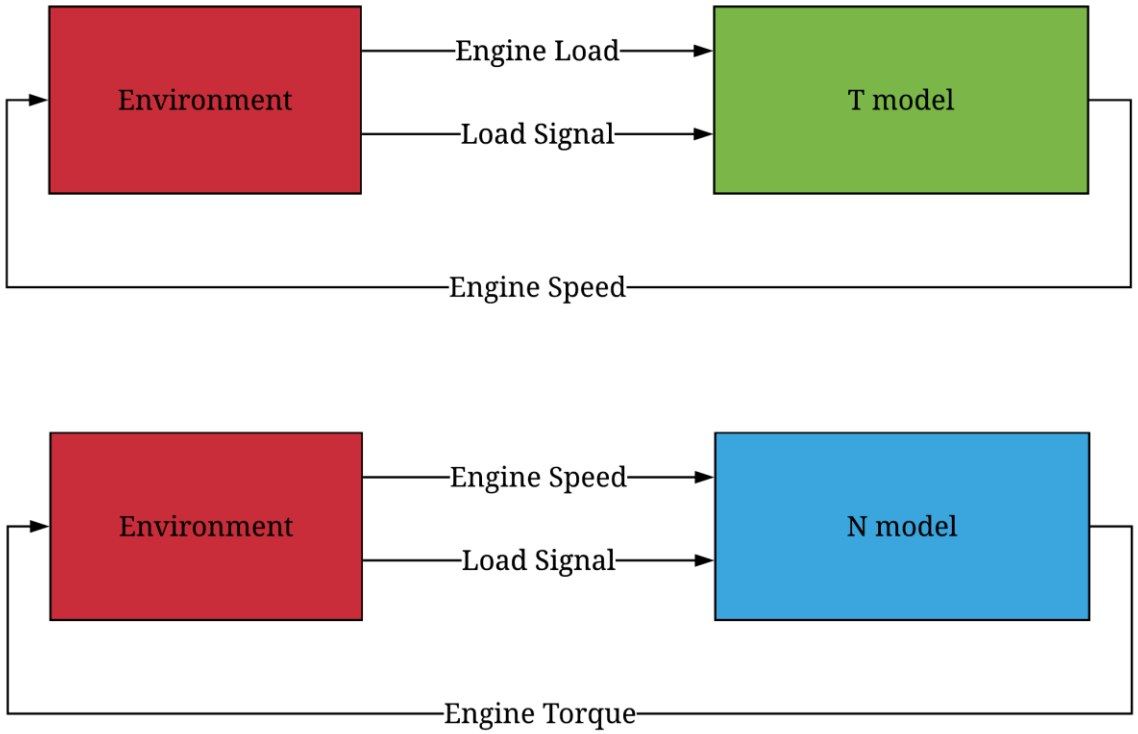


Figure 28. The T or N engine model classification

3.3. Results validation and comments

In this section, results of the traces and the transient simulations will be depicted. They are verified, validated and commented. The model and specific engine parameters are defined in Appendix A.

3.3.1. Traces model results

The traces model will be processed first, starting with the cylinder pressure trace. Combining the defined cylinder intake and exhaust pressures from the initial conditions with the calculated cylinder pressure from (3), a trace of the indicated cylinder pressure from one cycle can be depicted in Figure 29.

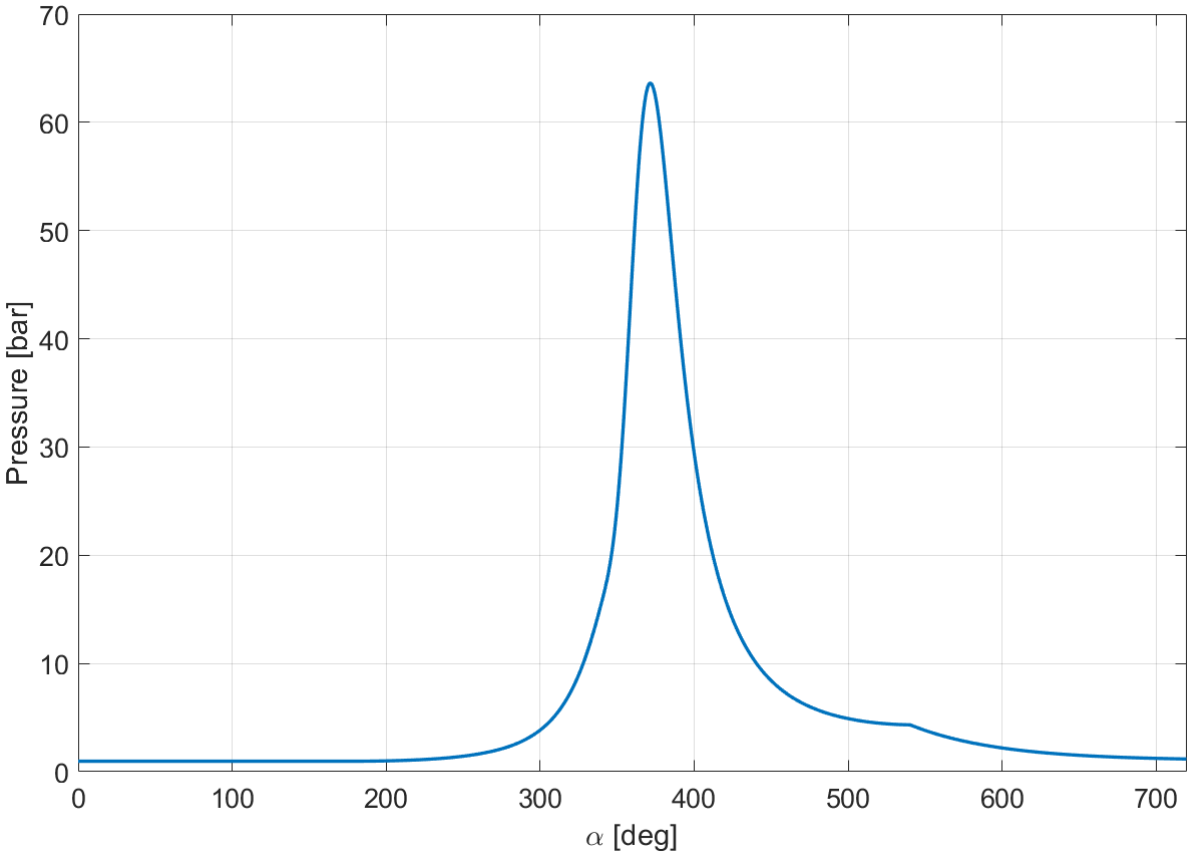


Figure 29. Indicated cylinder pressure at 3000rpm and load signal = 1, data from Appendix A, Engine 1

Let us break down the cylinder pressure calculation with reference to the figure above. Cylinder pressure has the value defined from Figure 9 or Figure 10 for the first 180 crank-angle degrees (until the end of intake). After that, the pressure is calculated accordingly to (3). Then, from the beginning of the exhaust (540 crank-angle degrees), the pressure smoothly reaches the defined exhaust pressure as explained in Figure 14.

The above trace is now validated against the results from the AVL Cruise M for multiple engine speeds.

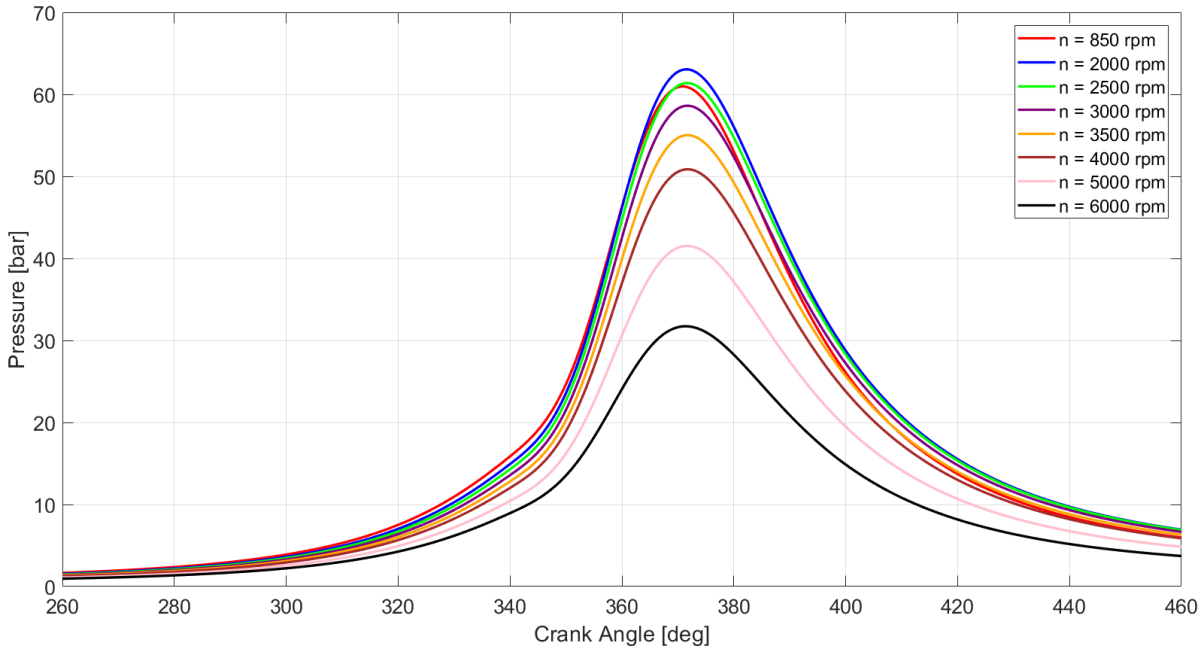


Figure 30. Cylinder pressure trace through various engine speeds, load signal = 0.2, thesis model result, data from Appendix A, Engine 1

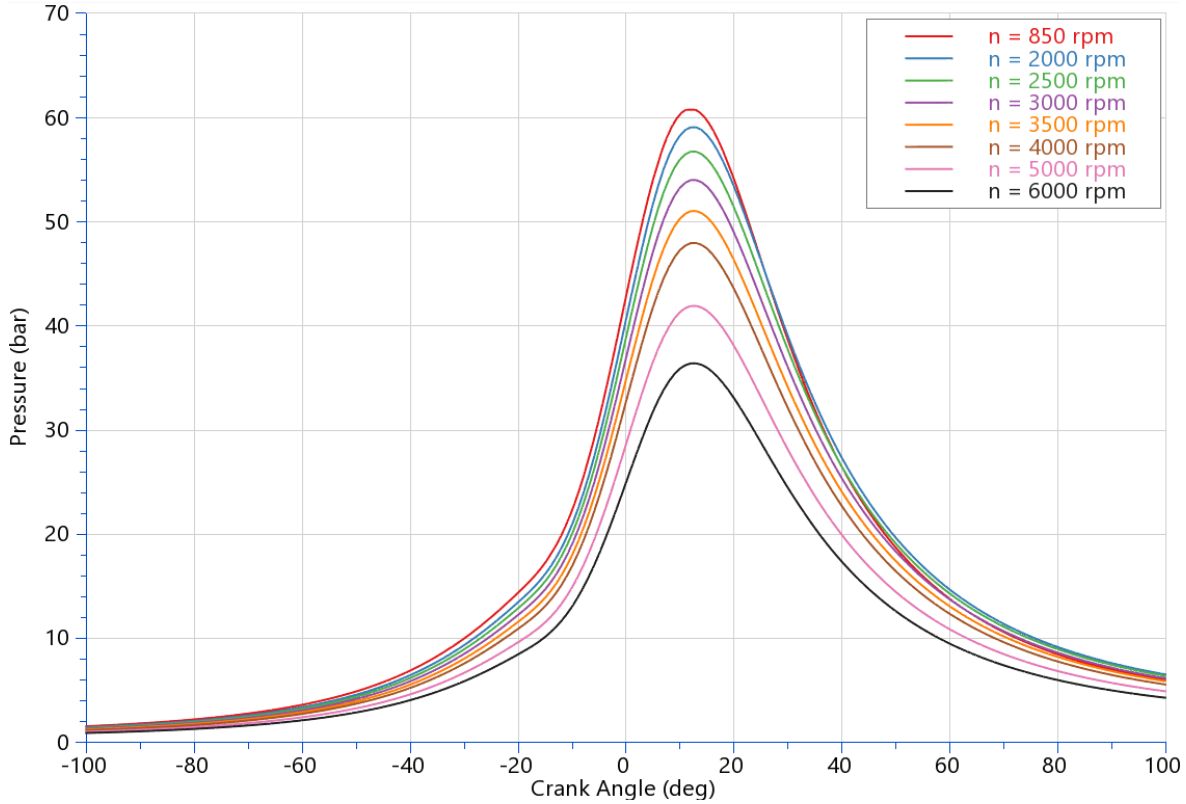


Figure 31. Cylinder pressure trace through various engine speeds, load signal = 0.2, AVL Cruise M model result, data from Appendix A, Engine 1

Other validation results are displayed in Appendix B. Validation results are divided into two parts, one for the spark ignition (SI) model, and one for the compression ignition (CI) model. Each of them was validated in the Cruise M environment and defining the equivalent (but more detailed) engine model in Cruise M with the same parameters as used in the developed model, of course wherever there was an option to. In the scope of this thesis, the disparity between the results of the two model is allowed to be no larger than about 15%. As can be seen from the results, the two models do not differ more than that. The main cause of the emerging mismatches, among many simplifications, is that in the thesis model, volumetric efficiency was defined according to Figure 8 and its effects had their impact on the thesis results.

According to (30), inertia forces can be depicted in the figure below.

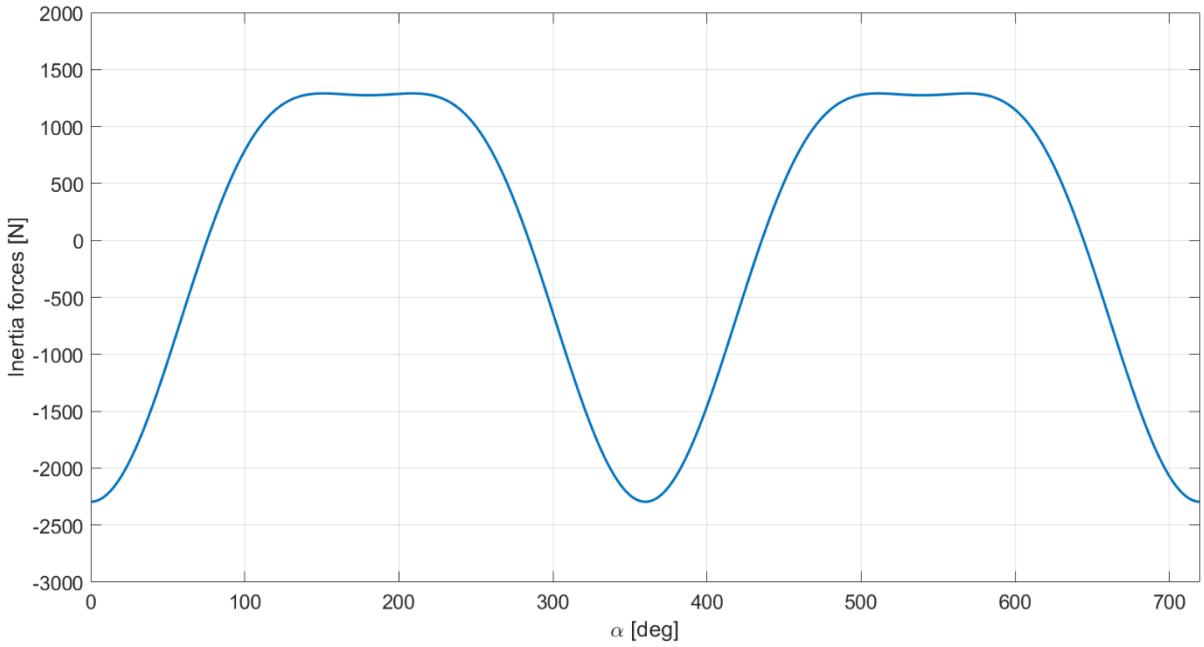


Figure 32. Inertia forces at 3000rpm, oscillating mass is 0.47kg

From the figure above, it is clear that the inertia forces have a zero mean and they don't affect the final mean value of the indicated torque, but nonetheless, their impact lies in the amplitude of the torque oscillations.

Above inertia forces are combined with the gas forces resulting from the cylinder pressure. The inertia forces have a greater impact on the SI engines due to the gas forces at CI engines being significantly larger due to the greater cylinder pressure. But nevertheless, inertia forces become dominant as soon as the engine speed reaches high values. Combined forces for an SI and CI engine are shown in Figure 33 and Figure 34 respectively.

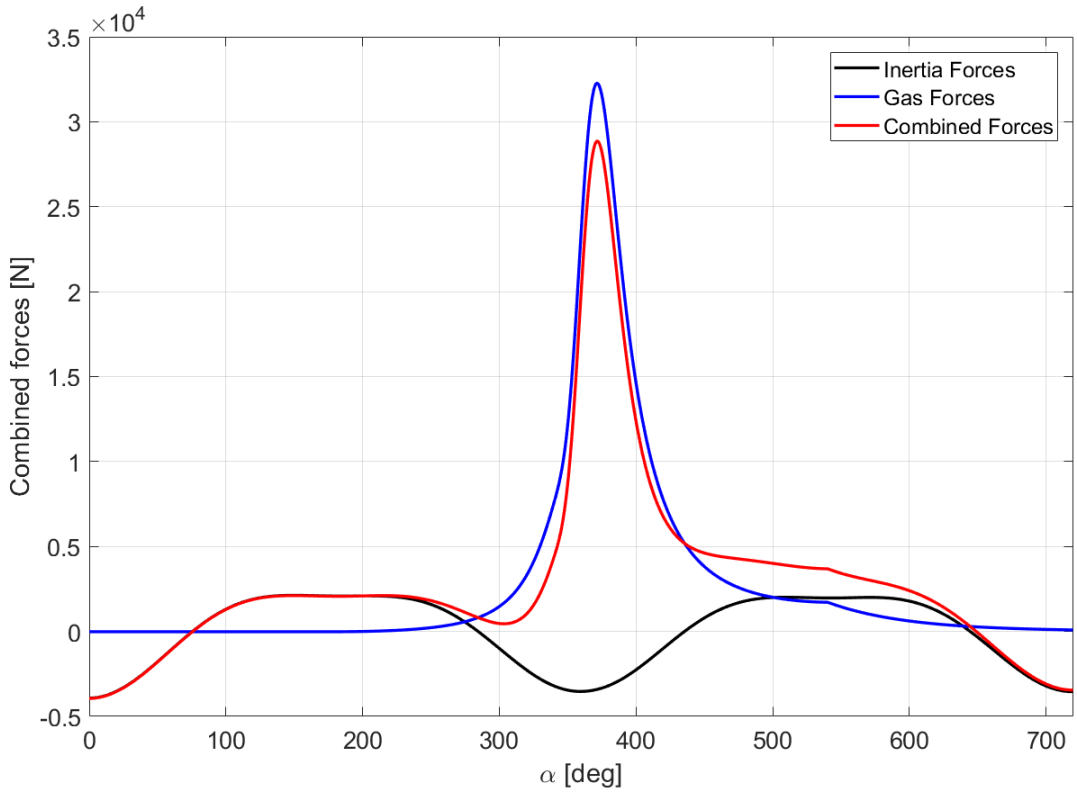


Figure 33. Combined piston forces for at 3000rpm, data from Appendix A, Engine 1

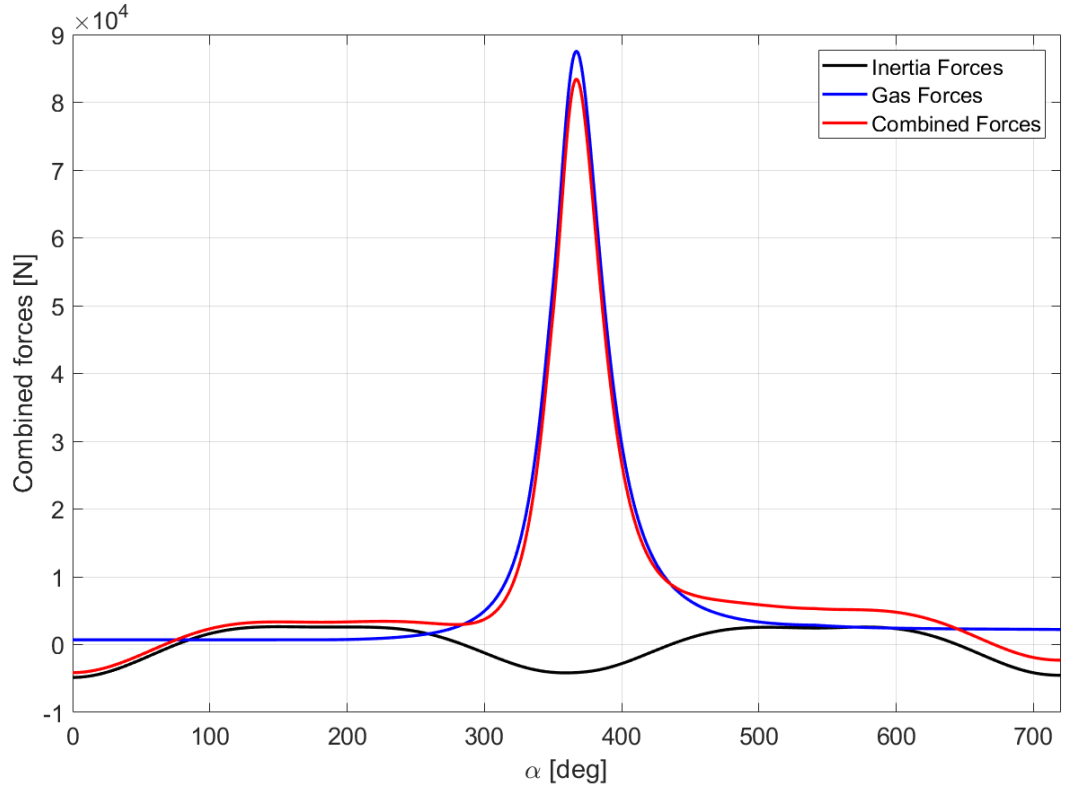


Figure 34. Combined piston forces at 3000rpm, data from Appendix A, Engine 2

Following the equation (32) and with the combined forces data, indicted torque of one cylinder can be calculated. The results are depicted in figure below.

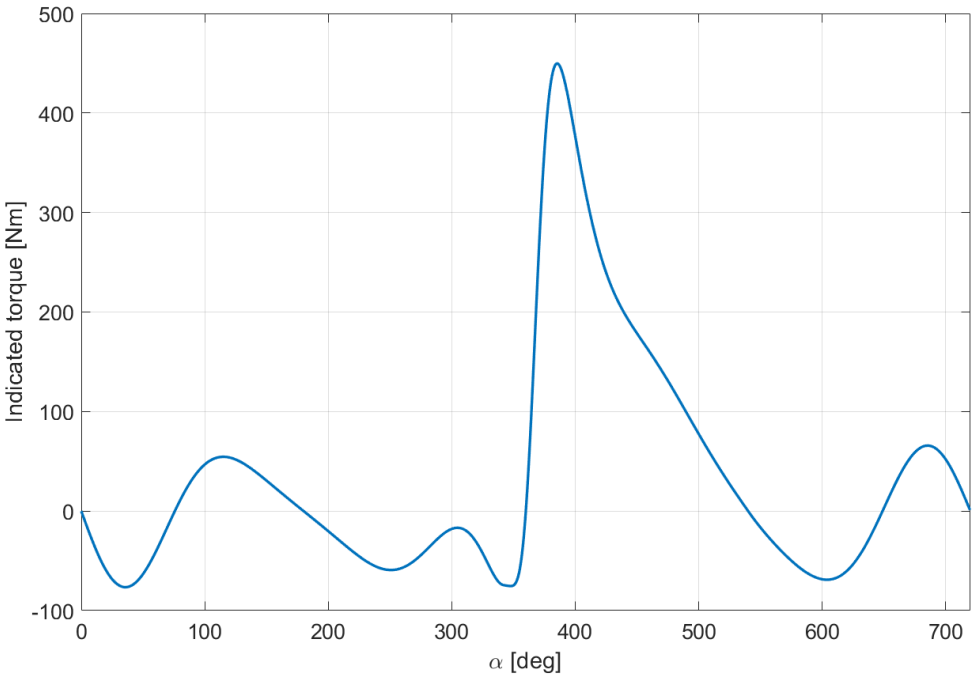


Figure 35. Indicated torque at 3000rpm and load signal = 1, data from Appendix A, Engine 1

In Figure 35, a trace of the indicated torque of an NA SI engine at 3000rpm is displayed. Depending on the engine speed, inertia forces will have greater or lesser effect on the shape of the indicated torque, leading to different pulsations of the engine speed. Validation of this result is conducted in AVL Excite and depicted in figure below.

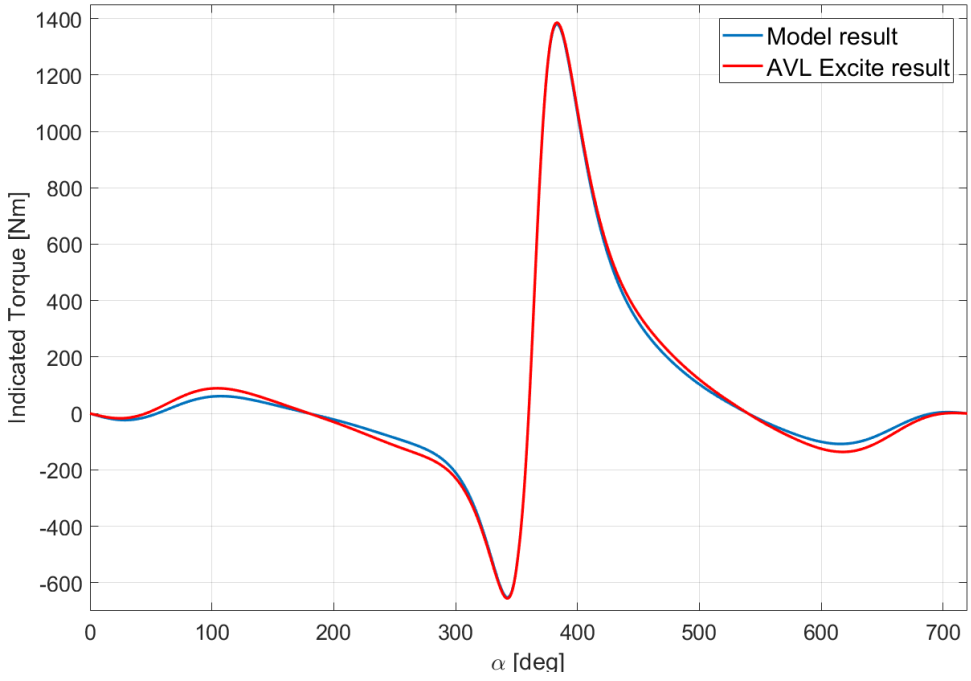


Figure 36. Indicated torque one cylinder trace at 2000rpm and load signal = 1, thesis model result and AVL Excite result comparison, data from Appendix A, Engine 2

From the figure above it can be seen that the indicated torque calculation was done correctly, considering the results from AVL Excite. Other validation results are displayed in Appendix C in more detail.

In the case of a 4-cylinder engine, the cylinders are fired every 180 crank-angle degrees. Combining the calculated indicated torque of the one cylinder from the figure above with the indicted torques from the three remaining cylinders, spaced 180 degrees, one can determine the total indicated engine torque, as seen in figure below.

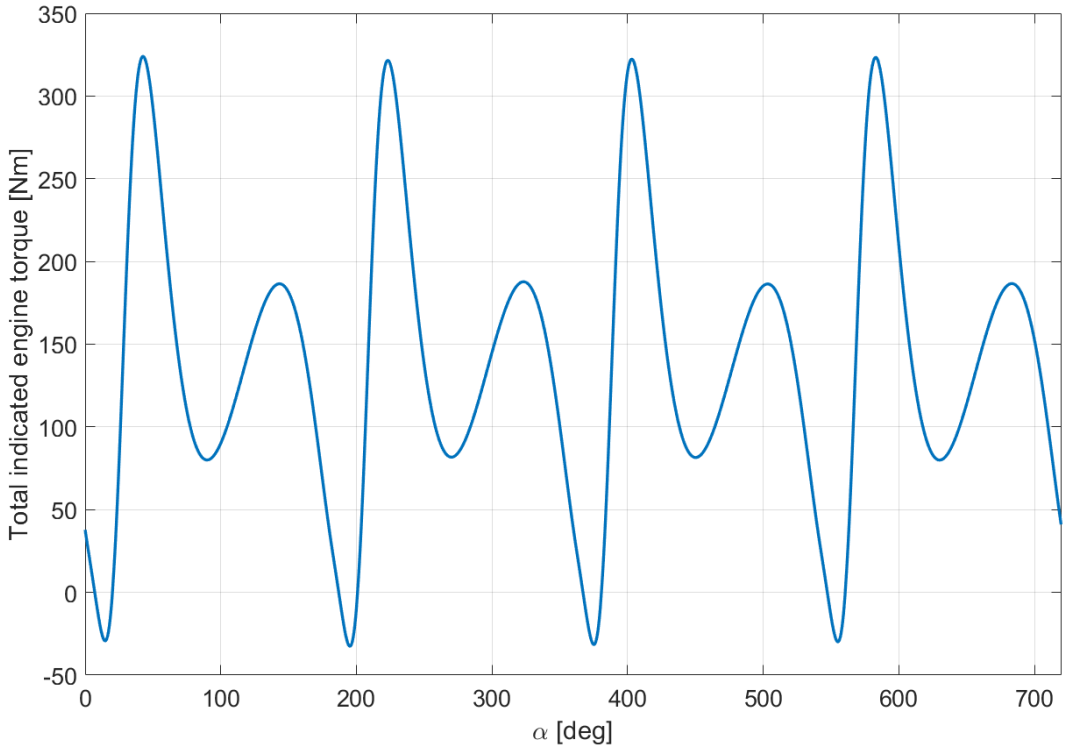


Figure 37. Total indicated torque of a 4-cylinder engine at 3000rpm, data from Appendix A Engine 1

3.3.2. Transient model results

One of the traces model modifications was shifting the start of the cycle to the start of compression, as already described at the end of the section 3.2.1. The modification can be seen in Figure 38 and to accomplish it, several changes to the calculations regarding the crank-angle related variables had to be made (cylinder volume, cylinder volume differential, ignition time, etc.)

The indicated torque, as seen in Figure 35 is also shifted accordingly, but its mean value remains the same.

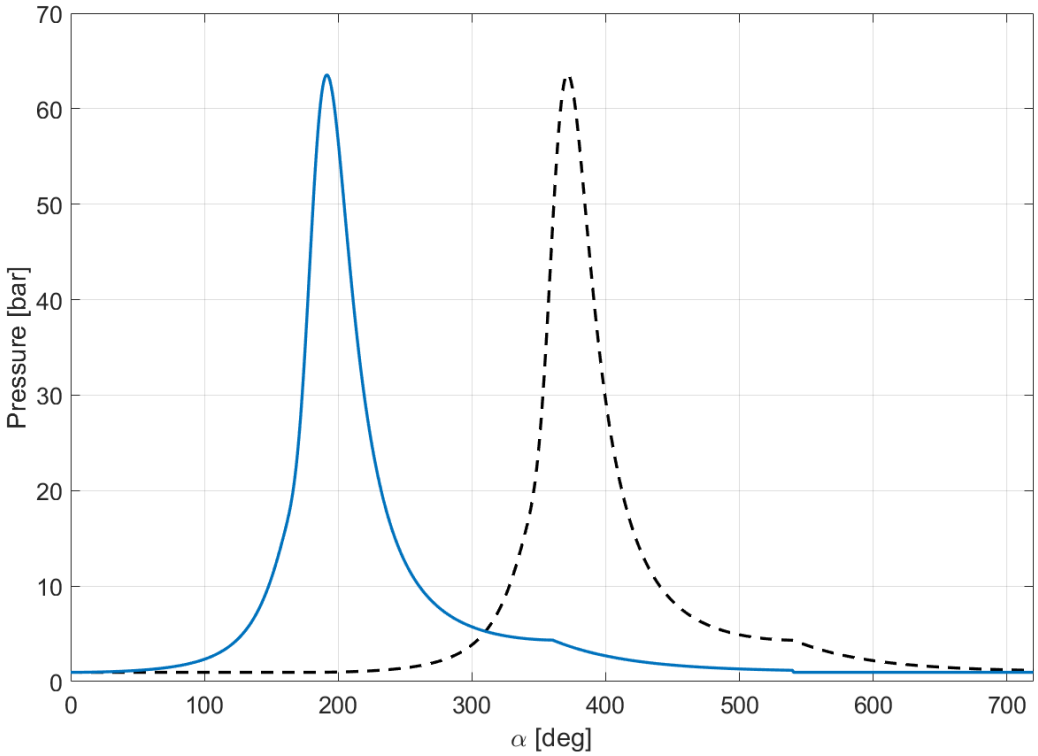


Figure 38. Shifted cylinder pressure, now the start of the cycle is the compression stroke, data is the same as in Figure 29

An example of torque calculation for multiple cylinders is shown in the figure below. Referencing to Table 2, Figure 19 and Figure 20, a 6-cylinder example is shown.

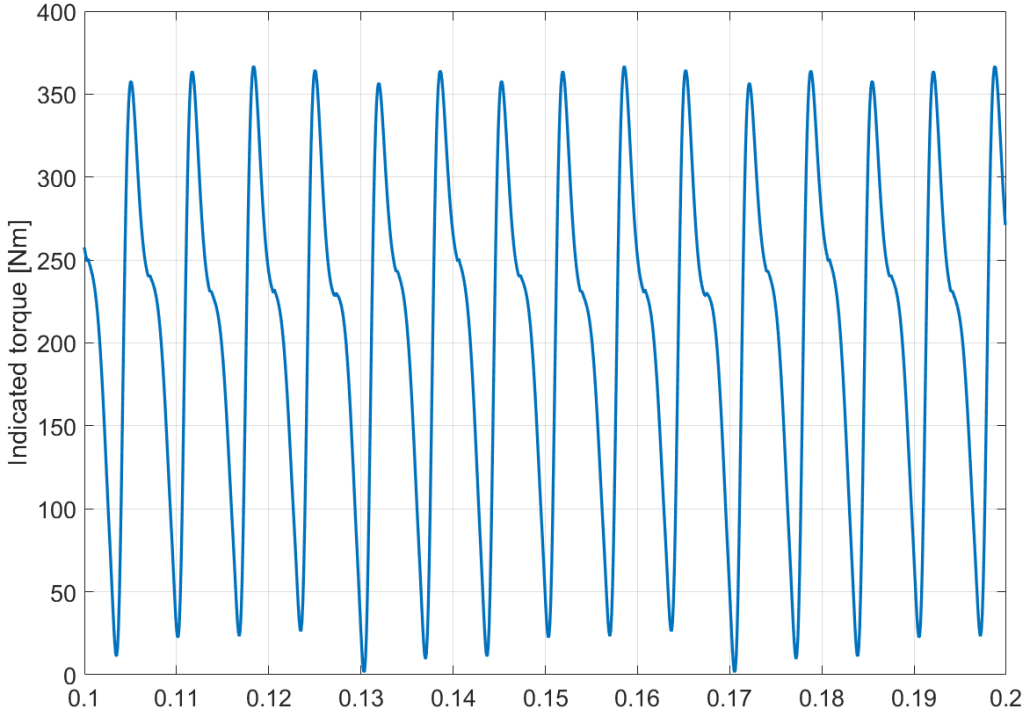


Figure 39. Indicated torque of a 6-cylinder engine at 3000rpm, data from Appendix A, Engine 3

As already mentioned, one cycle of a four-stroke engine lasts 40ms at 3000rpm. It can be seen from the figure above that there are exactly six peaks of indicated torque in the scope of 40ms, equivalent to the defined six cylinders. Individual torque peaks have different amplitudes despite the fact that the other five cylinder torques are just the delayed version of the first cylinder torque. The reason is that the above figure shows the transient state of the model, with variable engine speed and so it differs from Figure 37. Variable engine speed enters the delay blocks in Figure 19 and contributes to an even more realistic behavior of the model.

Because of the fluctuating behavior of the brake engine torque and inertia, engine speed has the equivalent behavior, as seen in figure below.

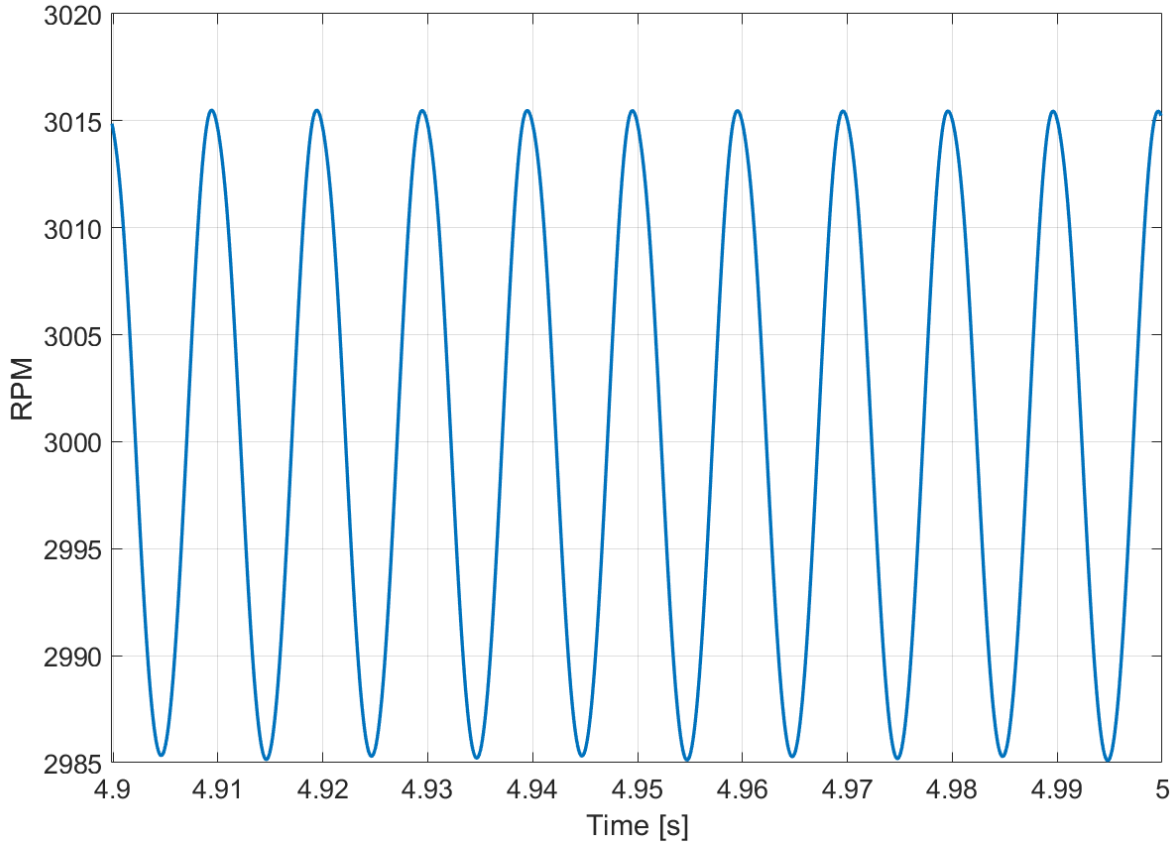


Figure 40. Engine speed oscillations at 3000rpm, data from Appendix A, Engine 1

The above figure was captured in the transient simulation. An adequate load was imposed to maintain the desired speed.

The effect and the purpose of the flywheel are shown next. According to the set of equations described in section 3.2.6, elastic connection between engine and testbed is defined. It is based on the dual-mass flywheel concept and the difference of the engine speed curve with or without the flywheel is shown in figure below.

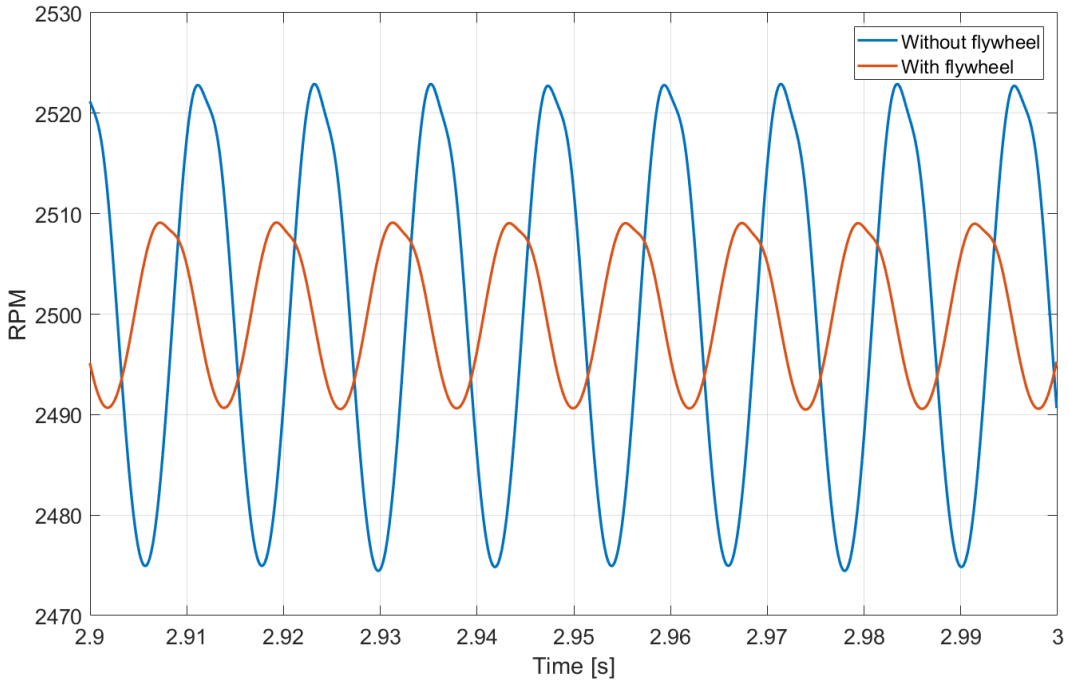


Figure 41. Effect of the dual-mass flywheel concept on the engine speed fluctuations

As one can see from the figure above, the amplitude of the engine speed fluctuations is reduced with the application of the dual-mass flywheel. The second (blue) curve represents the engine speed without the flywheel inertia, only the engine rotating inertia is considered, as defined in (52). If the dual-mass flywheel would happen to have a larger moment of inertia, the reduction would be even greater. Next, the engine torque fluctuations before and after the dual-mass flywheel would be considered.

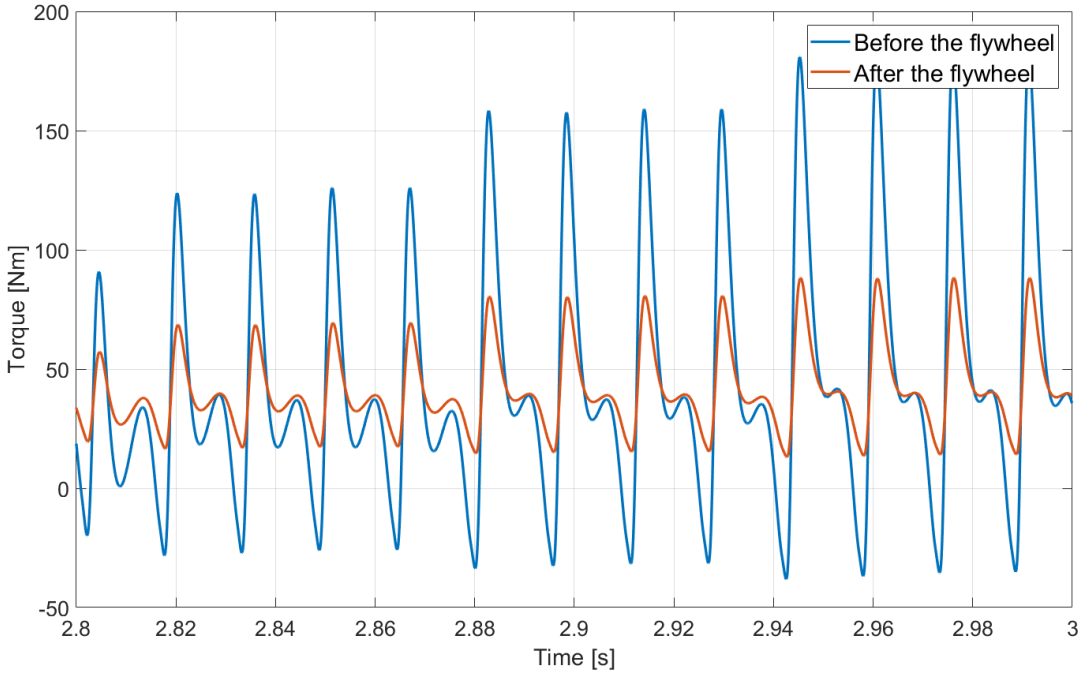


Figure 42. Engine torque fluctuations before and after the dual-mass flywheel, 4 cylinder engine

The engine has been imposed a load with the value of 40 Nm, and one can see from the figure above that the engine sustains the load torque before and after the flywheel. The mean torque before and after the flywheel is the same, as already explained in [9] while the oscillations have been reduced due to the flywheel inertia and its damping and stiffness factors. The amplitudes of the torque oscillations differ through the cycles as the engine speed controller tries to keep the engine speed at the desired value, despite the imposed load.

4. ENGINE CONTROL SYSTEMS

It was stated in the previous sections, many of the relevant control systems that exist within the car engine control unit (ECU) have been replaced with a look-up table or an approximation in order to reduce the model complexity. The developed model needs to be as general as possible to be able to approximately represent a diverse span of the ICE sizes and types.

- Boost pressure after the compressor was defined via a look-up table, disregarding the turbocharger (TC) dynamics and efficiencies. To properly define the TC dynamics, one would need to know the exact specifications of the discussed TC which would be impossible for a wide range of ICEs. With the look-up table approach, a good general approximation of the boost pressure is given that will satisfy the developed model needs.
- EGR was presumed non-existent, but it could be realized in a relatively simple way through another look-up table. It would define the residual combustion products fraction (γ) that would then be incorporated into the appropriate equations, but the EGR dynamics alone would also be ignored. The main reason is that the EGR itself was invented to reduce the engine pollutant emissions. The emissions content and amount is not the subject of this thesis.
- The equivalence ratio of the SI engine is presumed to be always equal to one, the value around the SI engine has the best performances. Modeling the A/F ratio control would introduce another, in this case irrelevant, dynamic to the developed model which would only further slow down the simulation.

Other control systems like fuel injection control, ignition control, knock control or coolant temperature control will also not be designed [1].

Engine control systems that are going to be designed and verified are the idle speed control (ISC) and cruise control. Both of them are relevant to the goals of the developed model – engine speed and torque fluctuations in various operating points. The ISC controls the engine behavior in idle, keeping the engine speed at the user-defined value while the cruise control system maintains the desired engine speed despite the imposed disturbances which can arise during the vehicle operation. Apart from being a model feature to be enabled during the simulation, cruise control also enables the user to have an insight into how would a real engine on testbed behave under certain conditions.

A couple of design approaches to the above-mentioned control systems will be discussed and the one with the best performance will be included in the final developed model version.

4.1. Idle speed control

During idling, the engine has to generate a torque which compensates its own combustion cycle losses, engine friction and the torque needed for the auxiliaries (water and oil pump, AC, etc.). The required torque, therefore, depends strongly on the varying loads and the engine state in the phases after start [1].

Because of the many disturbances, the idling speed has to be feedback controlled. The reference value for the speed should be as low as possible in order to save fuel and reduce emissions. However, noise and vibrations effects have to be considered, engine stalling especially must be prevented under all operating conditions.

The main control variable for the idle speed controller is the engine angular speed (ω) and the main manipulated variable is the fuel mass that ends up in the cylinder [1]. Depending if the engine is an SI or CI, the path to the desired fuel mass is different; control of the air flow through the intake system or control of the fuel injectors signal.

Various approaches have been suggested for designing a valid ISC for an SI or a CI engine. In [18], several designs are discussed and in [19] a detailed model of an SI engine ISC is described. In the above-mentioned designs, non-linear models (such as the developed model in this thesis) are linearized around the idle speed operation point which is known before running the simulation. As the desired idle speed and the important engine model parameters are defined by the final model user, linearization around the operating point and the controller design would have to be ran before the start of every simulation. That would slow down the simulation considerably and would not be possible to accomplish with the model eventually compiled to an FMU.

Also, ICE dynamics, that are described throughout the developed model, are so nonlinear that linearized perturbation equations and linear models have very limited validity, and as a result, closed loop controller designs based on linear models will inevitably lead to „gain scheduling“. Gain scheduling is a form of an adaptive control strategy and within it, controller gains are set depending on the defined variable values.

Because of the above reasons, linearization of the developed model is discarded and the control system will be designed for a non-linear model.

Three controllers will be compared within this section along with their performances.

- A simple PI controller, which can be used in almost any control system, whether it is linear or non-linear. The PI controller design was conducted heuristically.
- PI controller with an additional simple sliding mode control part.
- Sliding mode controller

4.1.1. PI control

A simple PI controller in the regular form is considered. It is well known that linear PI controllers, if suitably tuned, provide satisfactory results to many practical applications without requiring a detailed description of the system dynamics [24]. In the presence of strong non-linear effects, however, their performance is below par, and it is necessary to „re-tune“ the controller appealing to gain scheduling or adaptive procedures. In this thesis, the PI controller will serve as a reference point, its performance a setpoint which the other developed controllers will have to beat in performance.

$$u = K_P \cdot e + K_I \cdot \int e dt$$
$$e = \omega_d - \omega \quad \textbf{(54)}$$

where:

- u is the system input,
- K_P is the proportional gain,
- e is the tracking error,
- K_I is the integral gain and
- ω_d is the desired engine speed.

The derivative part of the general PID controller was not included in the current controller design. The engine speed fluctuations would drive the derivative part into great values, leading to an even more oscillating, and eventually unstable system.

Although there are several gain tuning procedures for the PID controllers (Ziegler-Nichols or an improved, so-called Good gain method [25]), neither of them has been able to provide a satisfactory set of gains, probably due to the nature of the model.

The proportional and the integral gains had to be tuned heuristically. Two sets of gains were found, one for an NA SI engine, and one for a TC CI engine. Two sets were needed because the paths from the system input (load signal) to the fuel mass, that affects the engine torque, are different in each case.

$$K_{P,NASI} = 10^{-4} \qquad K_{P,TCCI} = 10^{-3}$$
$$K_{I,NASI} = 3 \cdot 10^{-4} \qquad K_{I,TCCI} = 3 \cdot 10^{-3} \tag{55}$$

where:

- $K_{P,NASI}$ is the proportional gain of the NA SI engine PI controller,
- $K_{I,NASI}$ is the integral gain of the NA SI engine PI controller,
- $K_{P,TCCI}$ is the proportional gain of the TC CI engine PI controller and
- $K_{I,TCCI}$ is the integral gain of the TC CI engine PI controller.

These gain are, of course, not optimal for this system. If one would linearize the developed model around a desired operation point, a proper set of gains which would control the system with the desired performances (damping, overshoot) could be found. An excellent reference point can be found in [19].

But, as it is already mentioned, linearization of the model around every operating point (which will ultimately be set by the user) would be hard to incorporate in the model design, especially in the compiled FMU. In the following section, a nonlinear robust control system design will be described.

4.1.2. Sliding mode control introduction

Sliding mode control (SMC) is a form of nonlinear control which is capable of handling system nonlinearities and has robust characteristics [20]. Here robust means that the design methodology takes into account modeling uncertainties in the form of parameter uncertainties or drift as well as unmodeled dynamics. Model imprecision may come from actual uncertainty about the plant, or from the purposeful choice of a simplified representation of the system's dynamics [21]. Modeling inaccuracies can have strong adverse effects on nonlinear control systems. Therefore, any practical design must address them explicitly. The typical structure of

a robust controller is composed of a nominal part, similar to a feedback linearizing or inverse control law, and of additional terms aimed at dealing with model uncertainty.

SMC is a simple approach to robust control. It is based on the remark that it is much easier to control first order systems, so the higher order systems (n^{th}) are transformed into equivalent first-order systems. The cost is an extremely large control activity which then must be reduced through controller modification. Nevertheless, SMC provides a systematic approach to the problem of maintaining stability and consistent performance in the face of modeling imprecisions.

The first step in designing a sliding mode controller is to define the so-called „*sliding surface*" or „*sliding manifold*", which is usually defined as:

$$S(y,t) = \left(\frac{d}{dt} + \lambda_{SMC} \right)^{n-1} \cdot \tilde{y} \qquad \textbf{(56)}$$

$$\tilde{y} = y - y_d$$

where:

- S is the sliding surface,
- λ_{SMC} is a positive constant,
- y is the system output,
- y_d is the system desired state and
- $\tilde{y}$ is the tracking error.

The problem of tracking ($y = y_d$) is equivalent to that of the remaining on the sliding surface S for all $t > 0$. Indeed, $S = 0$ represents a linear differential equation whose unique solution is $\tilde{y} = 0$ [21].

The simplified, first-order problem of keeping the S at zero can now be achieved by choosing the control law such that outside of S, all system trajectories point to the S. The control law must satisfy the *sliding condition* which will be described later. Once the system trajectory has reached the sliding surface S, system behavior has entered into *sliding regime* or *sliding mode*. System trajectories are then defined by (56), making sliding surface S both a place and a dynamics. Visual representation of the SMC can be seen in the figure below.

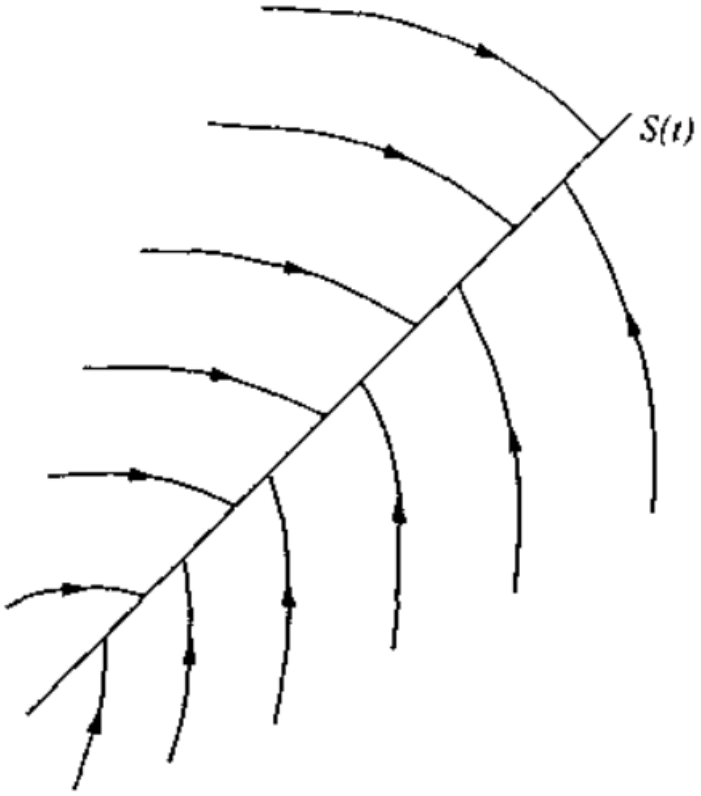


Figure 43. System trajectories converging onto sliding surface *S* [21]

After *S* has been defined, a feedback control law has to be selected. However, in order to account for the presence of modeling imprecisions and of disturbances, the control law has to be discontinuous across *S*. This inevitably leads to an undesired phenomenon known as *chattering*. Chattering involves high control activity and may excite high-frequency dynamics neglected in the course of modeling. The chattering is dealt with by smoothing the discontinuous control law.

The reason why the SMC has been selected in this thesis is that the dynamics and calculations that describe the torque calculation (Sections 3.1.7 and 3.2.2) contain numerous nonlinearities; signal delays and superposing, variable signal values and initial conditions depending on the system initial states, etc. The nonlinearities will have to be described with an unprecise equation and the control system needs to be able to respond robustly. Also, the developed control system needs to be applicable to a wide array of system parameters which will eventually be user-defined and sufficiently robust to unexpected loads and disturbances.

4.1.3. SMC design

The choice of the sliding surface *S* for the model developed in this thesis will be explained first. Because of the fluctuating behavior of the engine speed and even more fluctuating engine angular acceleration (engine speed derivative), their inclusion into the sliding surface would not be the best idea. Hence, the sliding surface is defined as proposed in [22]:

$$S = \left(\frac{d}{dt} + \lambda_{SMC} \right) \cdot \int_0^t \tilde{\omega} dt$$

$$S = \tilde{\omega} + \lambda_{SMC} \cdot \int_0^t \tilde{\omega} dt \quad \textbf{(57)}$$

$$\tilde{\omega} = \omega - \omega_d$$

Here, the sliding surface is defined as a linear combination of speed difference and integral of speed difference. The steady-state error is eliminated by the inclusion of the integral state [22].

As was mentioned before, the control law of the SMC consists of two parts. The first part is responsible for reaching the sliding surface and it has to contain all of the model uncertainties to ensure that the sliding surface will be reached. Once the sliding surface is reached, the second part of the control law takes place and keeps the system on the sliding surface. That's why the SMC is a variable structure control, it operates between two distinct control patterns. Based on [23], the control law is:

$$u = -K_{SMC} \cdot S - \rho \cdot sign(S) \quad \textbf{(58)}$$

where:

- K_{SMC} is a positive gain and
- ρ is the switching law gain
- *sign* is the signum function; has value 1 if the variable is positive, value -1 if the variable is negative

To repeat the equation (53):

$$J_E \cdot \dot{\omega} = T_I - T_F - T_{fly} \quad \textbf{(59)}$$

Indicated torque (T_I) is the input in the equation above, while the friction and flywheel torque (T_F and T_{fly}) can be considered as the external disturbances. The real system input, however, based on the developed model, is the load signal. It needs to be connected to the indicated torque via an algebraic expression. The load signal determines the fuel mass that will enter the cylinder and an estimated relationship between the fuel mass and the indicated torque can be made from [8]:

$$IMEP = \frac{Q_f \cdot \eta_i}{V_H} = \frac{m_f \cdot H_l \cdot \eta_i}{V_H}$$

$$T_I = \frac{IMEP \cdot z \cdot V_H}{\pi \cdot 4} = \frac{m_f \cdot H_l \cdot \eta_i \cdot z}{\pi \cdot 4} \quad \textbf{(60)}$$

$$m_f = \frac{T_I \cdot \pi \cdot 4}{H_l \cdot \eta_i \cdot z}$$

Since the designed controller should be a robust controller, indicated efficiencies will be estimated to some general values while every other variable in (60) is known. Next, a relationship between the fuel mass and the load signal must be established. Upper margin of the fuel mass needs to be derived.

For NA SI engines, that value will correspond to the case when the maximum amount of gas is inducted to the cylinder. That happens when the pressure drop is insignificant and the intake pressure is almost equal to the ambient pressure, around 1 bar.

$$m_{f,\max,NASI} = \frac{p_{i,\max} \cdot V_0}{R \cdot T_0 \cdot Z_0} \quad \textbf{(61)}$$

For TC CI engines, an empirical expression was found to approximate well the maximum fuel mass, in correlation with the sizing modification of the fuel mass look-up table in Figure 10.

$$m_{f,\max,TCCI} = 0.1 \cdot \frac{V_E}{z} \tag{62}$$

Load signal has the range [0,1].

$$LS = \frac{T_I \cdot \pi \cdot 4}{H_l \cdot \eta_i \cdot z} \cdot \frac{1}{m_{f,\max}} = u \tag{63}$$

where

- LS is the load signal, input to the model.

So redefining (63):

$$T_I = \frac{LS \cdot m_{f,\max} \cdot H_l \cdot \eta_i \cdot z}{\pi \cdot 4} = b \cdot LS = b \cdot u$$

$$b = \frac{m_{f,\max} \cdot H_l \cdot \eta_i \cdot z}{\pi \cdot 4} \tag{64}$$

$$u = \frac{1}{b} \cdot T_I$$

where:

- b is the system input coefficient.

To sum-up the expressions above, the signal flow explanation will be presented. Depending on the engine disturbances and the tracking error, the controller will calculate the desired engine torque the engine should generate in order to compensate the disturbances and reduce the tracking error. That desired torque needs to be converted to the load signal which is the system input. First, the estimated expressions that define the fuel mass needed for the desired torque are presented in (60). Calculated desired fuel mass from (60) then has to be converted to the load signal. For that to happen, the calculated fuel mass is divided with its maximum value, leading to the ratio that is within the range of the load signal, i.e. [0,1].

To ensure that the system trajectory would reach the sliding surface, the sliding condition needs to be fulfilled. The sliding condition can be set as a Lyapunov function and by performing the

Lyapunov function stability analysis, the value of the switching law gain (ρ) can be determined. The Lyapunov function candidate is:

$$V(S) = \frac{1}{2} \cdot S^2 \tag{65}$$

where:

- *V(S)* is the Lyapunov function.

Deriving the equation above and (57) (ω_d is a constant):

$$\begin{aligned} \dot{V}(S) &= S \cdot \dot{S} \\ \dot{S} &= \dot{\omega} + \lambda_{SMC} \cdot \tilde{\omega} \end{aligned} \tag{66}$$

where:

- $\dot{V}(S)$ is the Lyapunov funtion derivative and
- $\dot{S}$ is the sliding function derivative.

From (58), (59) and (64):

$$\begin{aligned} \dot{V}(S) &= S \cdot \left(\dot{\omega} + \lambda_{SMC} \cdot \tilde{\omega} \right) \\ &= S \cdot \left[\frac{1}{J_E} \cdot \left(b \cdot u - T_F - T_{fly} \right) + \lambda_{SMC} \cdot \tilde{\omega} \right] \\ &= S \cdot \left[\frac{1}{J_E} \cdot \left(b \cdot \left(-K_{SMC} \cdot S - \rho \cdot sign(S) \right) - T_F - T_{fly} \right) + \lambda_{SMC} \cdot \tilde{\omega} \right] \end{aligned} \tag{67}$$

Since:

$$sign(S) = \frac{|S|}{S} \tag{68}$$

then:

$$\dot{V}(S) = -\frac{b}{J_E} \cdot K_{SMC} \cdot S^2 - \frac{b}{J_E} \cdot \rho \cdot |S| + S \cdot \left[\frac{1}{J_E} \cdot \left(-T_F - T_{fly} \right) + \lambda_{SMC} \cdot \tilde{\omega} \right] \quad \textbf{(69)}$$

Next, an evaluation of the equation above needs to be performed. To ensure system stability the derivative of the Lyapunov function must be negative semi-definite [21]. Meaning it satisfies:

$$\dot{V}(S) \leq 0 \quad \textbf{(70)}$$

The function evaluation is performed with the help of the following axioms for the parameters that are not known.

$$\begin{aligned} &|a \cdot b| = |a| \cdot |b| \\ &|a + b| \leq |a| + |b| \end{aligned} \quad \textbf{(71)}$$

Then:

$$\begin{aligned} &\dot{V}(S) \leq -\frac{b}{J_E} \cdot K_{SMC} \cdot S^2 - \frac{b}{J_E} \cdot \rho \cdot |S| + |S| \cdot \frac{1}{J_E} \cdot T_F + |S| \cdot \frac{1}{J_E} \cdot T_{fly} + |S| \cdot \lambda_{SMC} \cdot |\tilde{\omega}| \\ &|\tilde{\omega}| = |\omega - \omega_d| \leq \omega + \omega_d \end{aligned} \quad \textbf{(72)}$$

Also from (53):

$$T_{fly} \leq \Delta\omega_{\max} \cdot D_{fly} + \Delta\alpha_{\max} \cdot C_{fly} \quad \textbf{(73)}$$

This leads us to the expression:

$$\dot{V}(S) \leq -\frac{b}{J_E} \cdot K_{SMC} \cdot S^2 + |S| \cdot \left(-\frac{b}{J_E} \cdot \rho + \frac{1}{J_E} \cdot T_F + \frac{1}{J_E} \cdot T_{fly} + \lambda_{SMC} \cdot \left(\omega + \omega_d \right) \right) \quad \textbf{(74)}$$

which needs to satisfy (71). The first part of the equation satisfies the condition; every part of *b* is larger than zero and the gain is chosen as positive. This leaves us with the second part of the equation, the expression on the parenthesis must smaller than zero. This leads to the expression for the switching law ρ:

$$\rho \geq \frac{1}{b} \cdot \left[T_F + T_{fly} + J_E \cdot \lambda_{SMC} \cdot \left(\omega + \omega_d \right) \right] \tag{75}$$

and thus completing the control law design.

To eliminate chattering, a technique proposed in [21] is applied. It consists of designing a boundary layer that smooths the *sign(S)* function. The *sign(S)* in (58) is replaced with the saturation function *sat(S)*.

$$sat(S) = \begin{cases} 1, & S > L \\ \dfrac{S}{L}, & |S| \leq L \\ -1, & S < -L \end{cases} \tag{76}$$

where:

- L is the boundary layer width.

4.1.4. PI Control with an additional simple SMC part

In addition to the previously described PI controller and SMC, a third possible control law is presented. A fusion between the PI and Sliding Mode control. The sliding surface *S* is chosen to be equivalent to the defined tracking error in (54).

$$S = \omega - \omega_d \tag{77}$$

Based on [26], the control law is designed as:

$$\begin{aligned} u &= u_{PI} - \rho \cdot sign(S) \\ e &= -S \end{aligned} \tag{78}$$

where:

- u_{PI} is the PI control part of the system input

In the first part of the control law, previously described PI controller is used. The tracking error in (54) is defined contrary to the switching surface in (77) so the sign of *S* has to be changed before it is forwarded to the PI part of the controller.

The control design then proceeds in the same way as in the previous section:

$$V(S) = \frac{1}{2} \cdot S^2$$

$$\dot{V}(S) = S \cdot \dot{S}$$

$$\dot{S} = \dot{\omega}$$

$$\dot{V}(S) = S \cdot \dot{\omega}$$

$$= S \cdot \left[\frac{1}{J_E} \cdot \left(b \cdot u - T_F - T_{fly} \right) \right]$$

$$= S \cdot \left[\frac{1}{J_E} \cdot \left(b \cdot \left(u_{PI} - \rho \cdot sign(S) \right) - T_F - T_{fly} \right) \right] \quad \textbf{(79)}$$

$$\dot{V}(S) \leq 0$$

$$\dot{V}(S) \leq \frac{b}{J_E} \cdot |u_{PI}| \cdot |S| - \frac{b}{J_E} \cdot \rho \cdot |S| + |S| \cdot \frac{1}{J_E} \cdot T_F + |S| \cdot \frac{1}{J_E} \cdot T_{fly}$$

$$\dot{V}(S) \leq |S| \cdot \left(\frac{b}{J_E} \cdot |u_{PI}| - \frac{b}{J_E} \cdot \rho + \frac{1}{J_E} \cdot \left(T_F + T_{fly} \right) \right)$$

The final equation above needs to be less or equal to zero. The switching law ρ is then defined as:

$$\rho \geq \frac{1}{b} \cdot \left(T_F + T_{fly} \right) + |u_{PI}| \quad \textbf{(80)}$$

To eliminate chattering, the same approach as before is used.

4.1.5. Results and performances

Designed controllers are tested on various engine sizes and desired engine speeds. The results of the tests are shown and their performances commented.

The PI controller gains were kept constant for the solo PI control, and for the PI+SMC fusion control law. The boundary layer width was not kept constant for the pure SMC and the PI+SMC fusion control laws due to the different dynamics of the controllers.

The model was disturbed with the engine load signal as seen on the figure below.

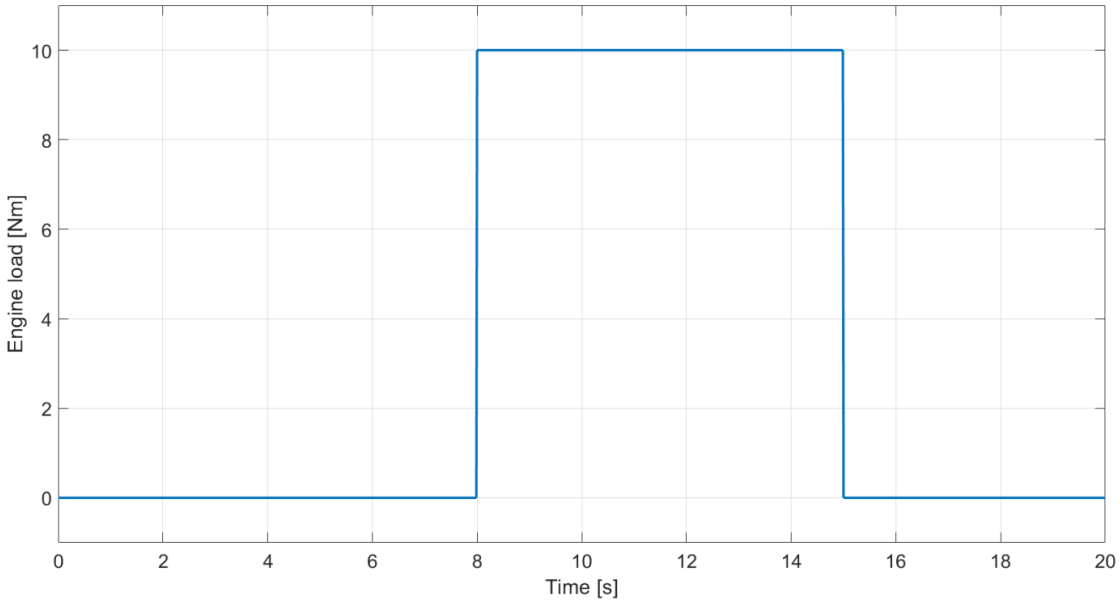


Figure 44. Engine load acting upon the flywheel

Because the calculated engine speed signal is very oscillatory, comparing the three control laws on one figure would be very messy. The signal mean value is calculated and shown instead. It is calculated at the end of every engine cycle and kept constant throughout the next cycle. System input is also shown in order to display the „cost“ of the control signal.

Two measures of performance are given:

- Integral of Absolute Error (IAE):

$$IAE = \int |e| dt \tag{81}$$

- Integral of Squared Error (ISE):

$$ISE = \int e^2 dt \tag{82}$$

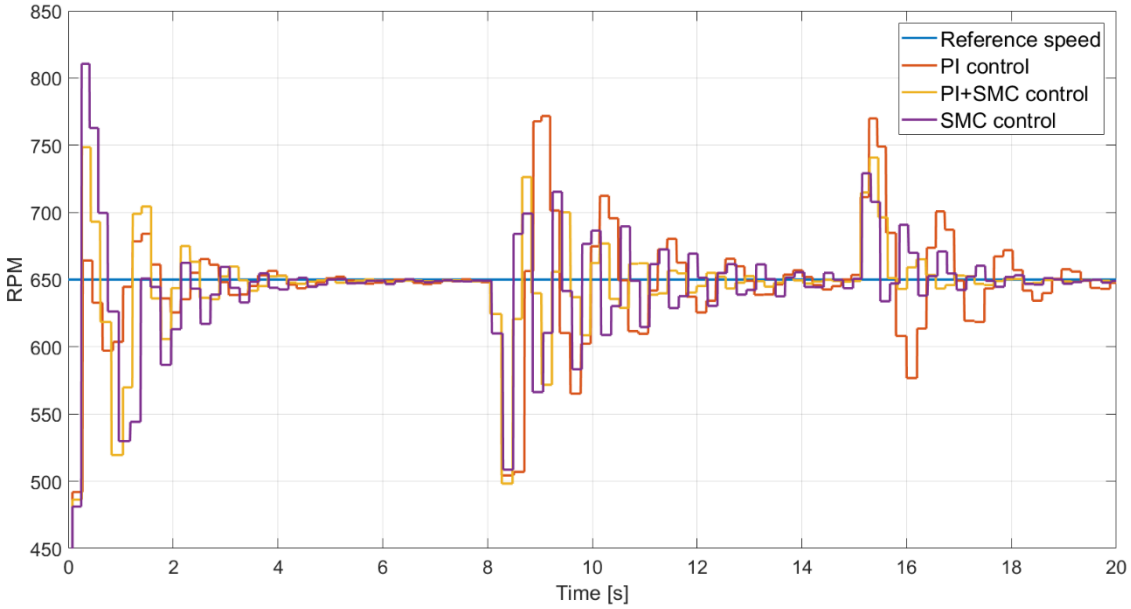


Figure 45. ISC response of Engine 3, data from Appendix A, various control systems

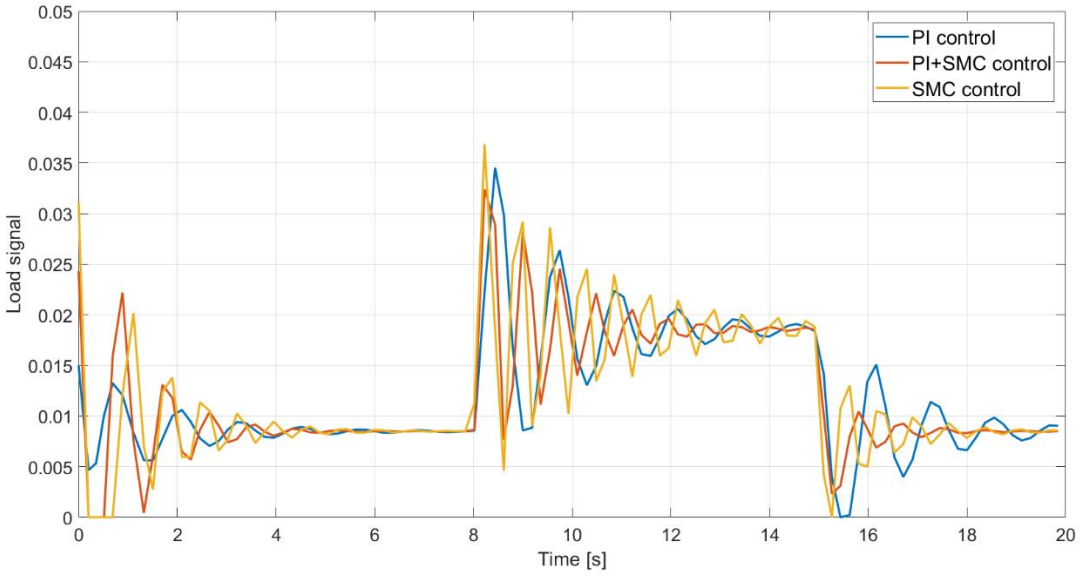


Figure 46. Control signal for Engine 3, data from Appendix A, various control systems

Table 3. Performance of designed control systems, ISC, Engine 3, data from Appendix A

	IAE	ISE
PI control	49.61	318.55
PI+SMC control	37.85	210.13
SMC control	42.57	257.22

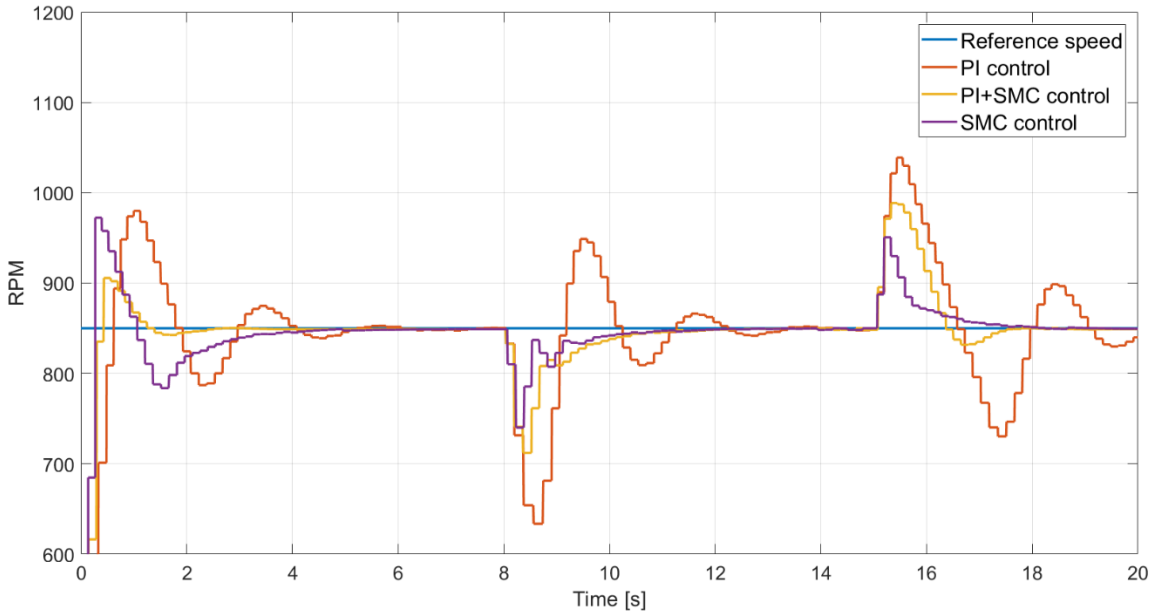


Figure 47. ISC response of Engine 4, data from Appendix A, various control systems

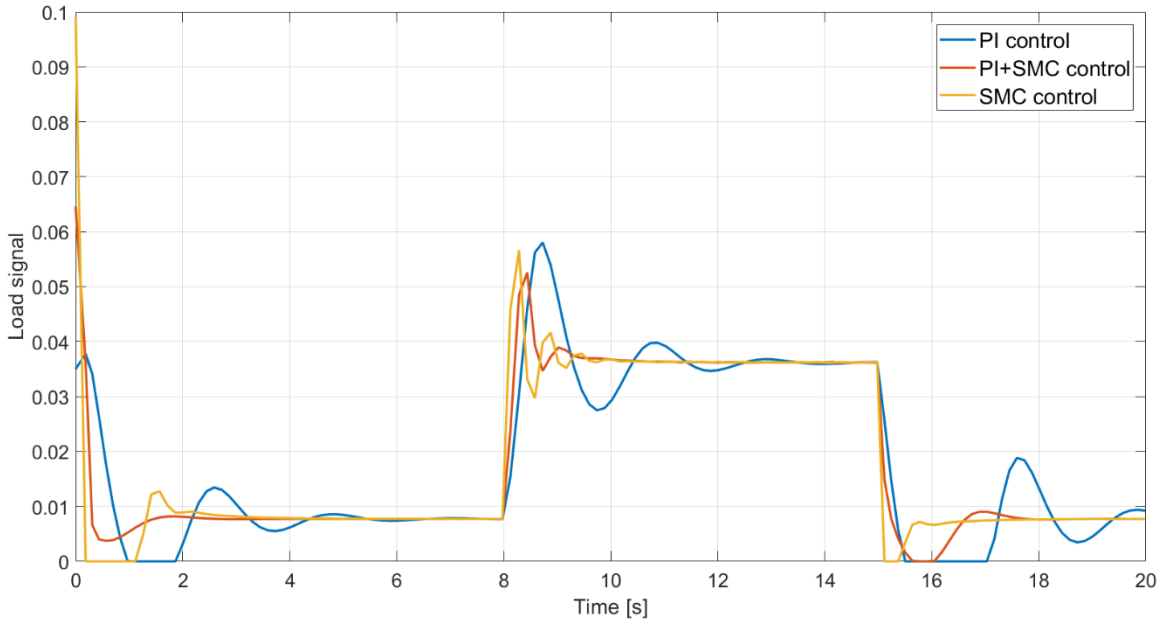


Figure 48. Control signal for Engine 4, data from Appendix A, various control systems

Table 4. Performance of designed control systems, ISC, Engine 4, data from Appendix A

	IAE	ISE
PI control	92.52	1115
PI+SMC control	44.51	423.27
SMC control	41.53	323.74

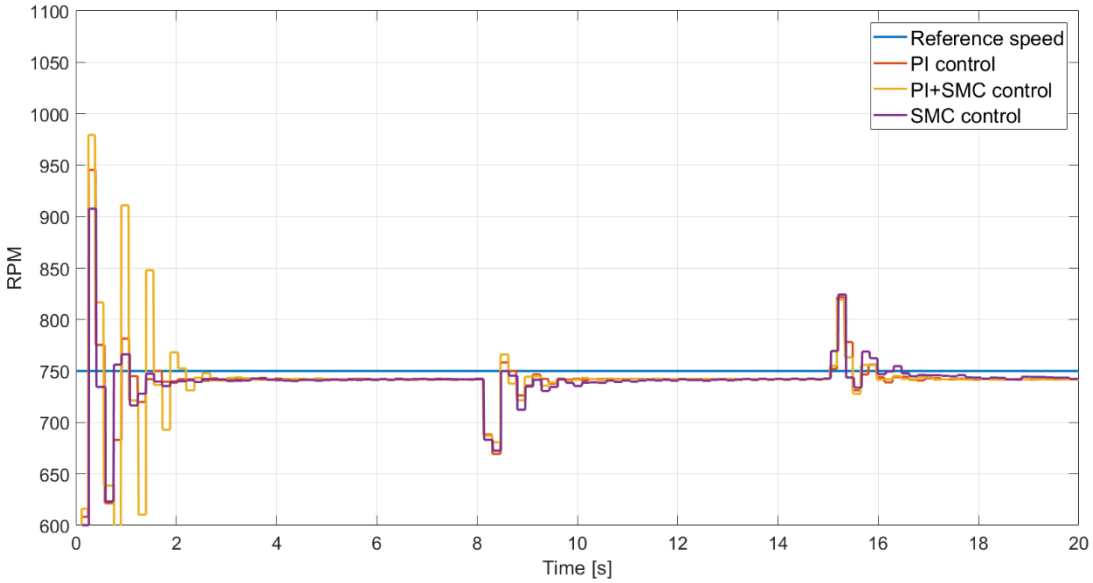


Figure 49. ISC response of Engine 2, data from Appendix A, various control systems

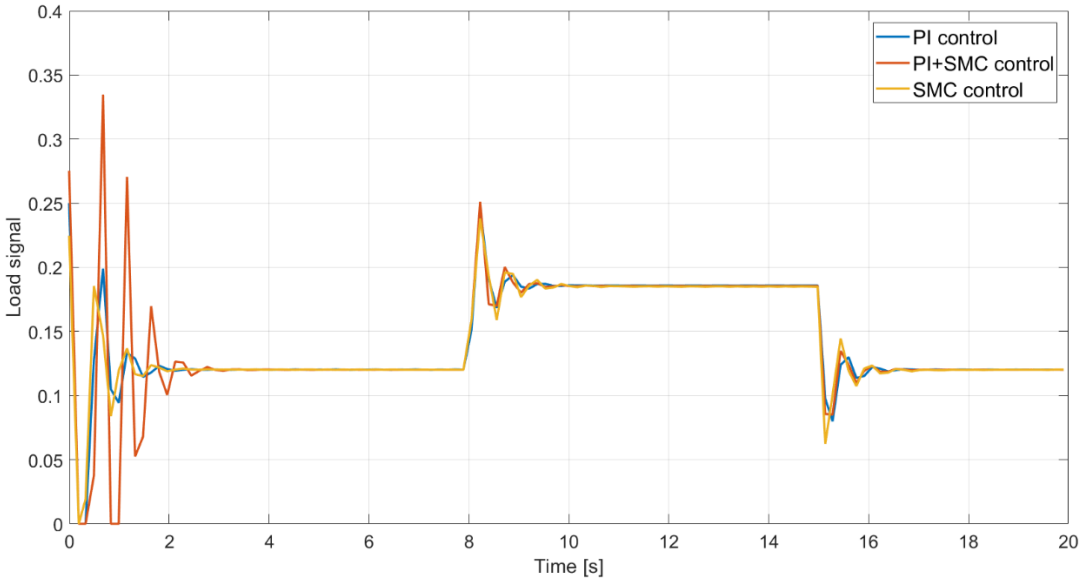


Figure 50. Control signal for Engine 2, data from Appendix A, various control systems

Table 5. Performance of designed control systems, ISC, for Engine 2, data from Appendix A

	IAE	ISE
PI control	111	878
PI+SMC control	115	1043
SMC control	108	856

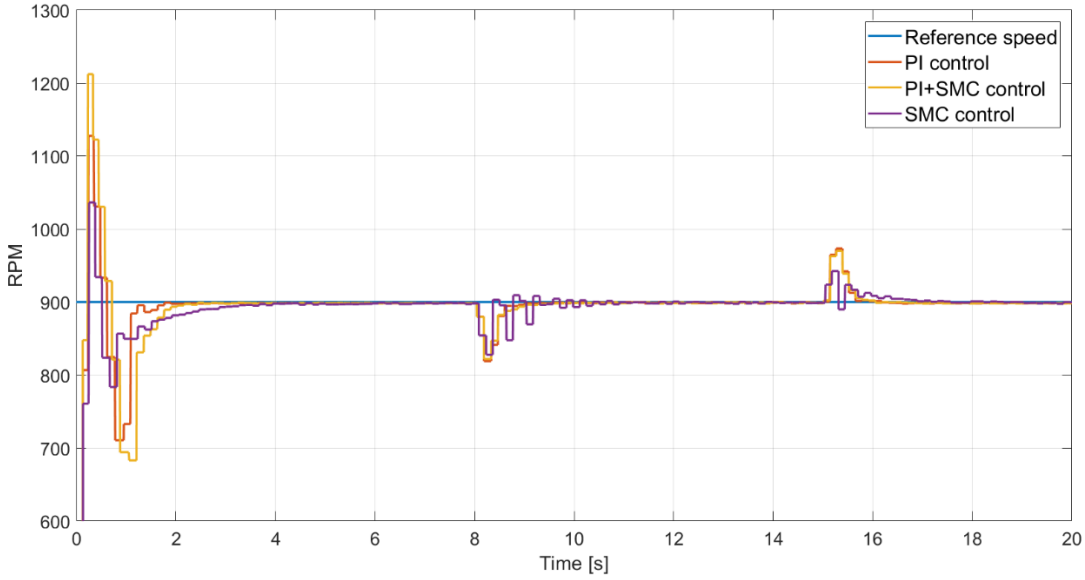


Figure 51. ISC response of Engine 5, data from Appendix A, various control systems

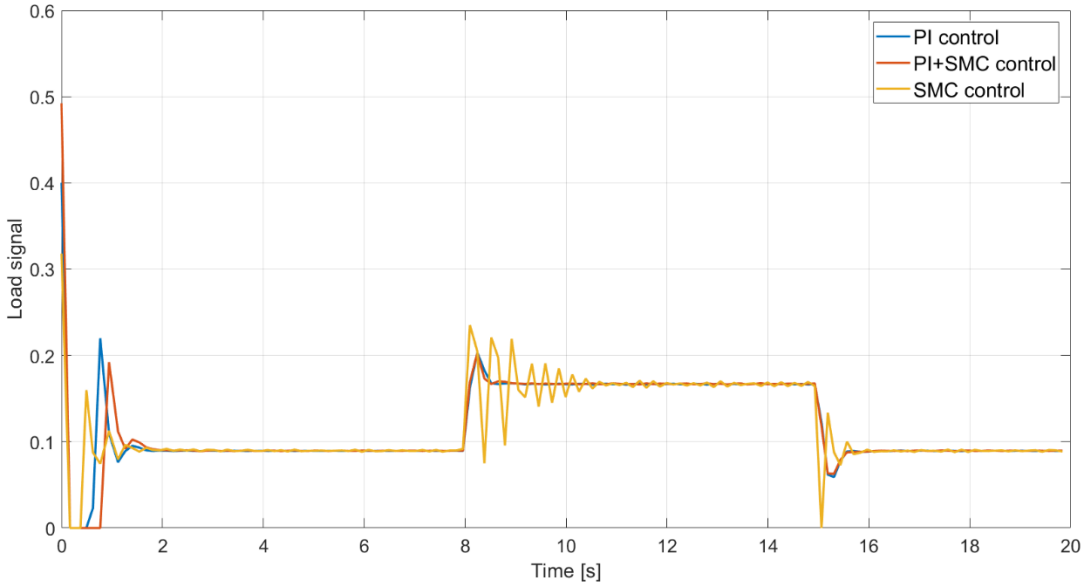


Figure 52. Control signal for Engine 5, data from Appendix A, various control systems

Table 6. Performance of designed control systems, ISC, Engine 5, data from Appendix A

	IAE	ISE
PI control	104	1011
PI+SMC control	109	1188
SMC control	99	863

Previously designed control systems were validated on two engine types, four engine sizes and four different reference speeds.

It is important to emphasize that the controller parameters do not change depending on the engine size. Once the engine type and the controller type is selected, the control system operates under the same parameters, independently of the engine size. Therefore, one can conclude that the developed control systems are robust to:

- the model parameters deviations that occur with the change of engine size,
- the non-linear dynamics that have not been taken into account during controller design,
- imposed loads and
- desired idle speed variations.

The type of the controller that is going to be included in the developed model now needs to be selected based on the performance factors. An additional performance factor could be evaluated; fuel mass spent. But the fuel mass spent during the observed test cycle has insignificant variations and the choice of the controller will be based on the two performance factors; IAE and ISE.

Integral of Absolute Error will be taken as a primary evaluation factor. Integral of Squared Error penalizes the larger errors more (larger deviation from the reference) and it will be evaluated when the values of the IAE are similar.

In the case of the Idle Speed Control for the Naturally Aspirated Spark Ignition engine, the fusion between the PI and SMC control is better in one case, while in the other case the SMC has the lower IAE factor.

In the case of the Idle Speed Control for the Turbocharged Compression Ignition engine, the SMC control undeniably leads with performance. The IAE factor is relatively similar to all three control designs, but the ISE factor shows that the overall engine speed deviation is the smallest with the SMC control.

In order to simplify the model execution and since the SMC performance is also satisfying with the NA SI engine, SMC is chosen as the default controller type for the Idle Speed Control system.

4.2. Cruise Control

Cruise control is a vehicle control system that is designed to maintain the desired vehicle velocity in order to increase the comfort of the driver and the passengers. The driver sets the desired velocity and the vehicle accelerates until the velocity is reached. The system that enables this, apparently simple, feature is just another form of engine speed control. The vehicle velocity is rigidly (if all power clutches are engaged) connected to the engine speed with a variable transfer ratio that depends on the current gear. Therefore, controlling the engine speed, vehicle velocity changes accordingly, assuming that the transmission stays in the same gear. Cruise control system needs to be able to withstand all of the loads imposed on the engine during the drive cycle. Whether it's an incline, a sudden gust of wind, change of the driving surface or a simple acceleration, the cruise control system needs to respond appropriately and accurately. The task of the cruise control system is to maintain a constant engine speed, despite all disturbances, which translates to a constant vehicle velocity.

In this thesis, the developed control system could be simply called „engine speed control system“ because, in reality, the cruise control system has more features, but also more responsibilities. The reason why the cruise control system is being designed within this thesis is to enable a detailed insight into the engine behavior in a desired operation point. Desired engine speed can be reached and arbitrary loads imposed on the engine. Then, engine speed and torque shape can be observed and evaluated.

Since a robust engine speed controller has already been developed for the idle speed control, now is the chance to test its robustness to a variety of engine speeds and loads. The control system design has already been conducted in the previous section and will not be repeated.

The engine has been given a reference speed and was loaded with a discontinuous load as shown in the figure below, along with the brake mean engine torque. The test has been conducted only on one engine size, but the behaviour is similar throughout the tested batch.

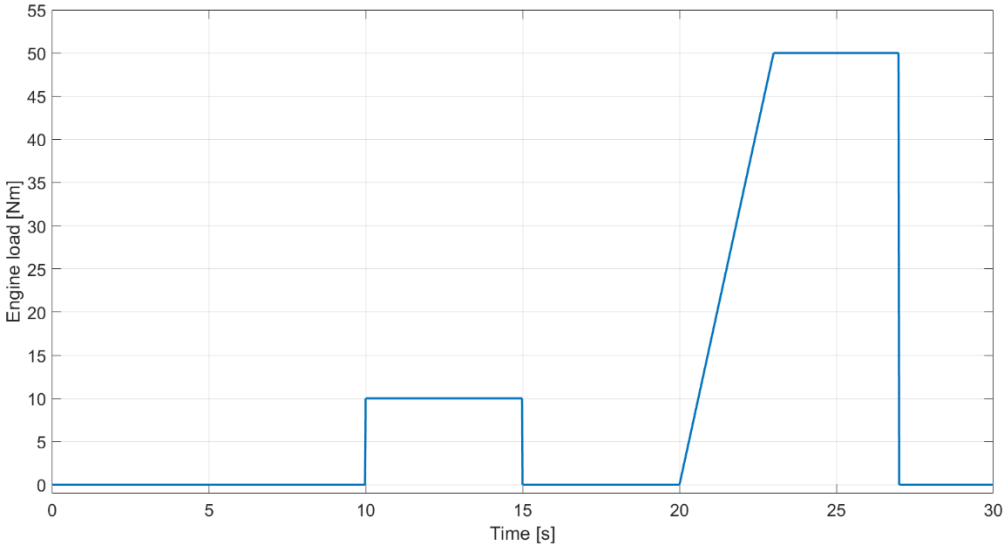


Figure 53. Imposed engine load during the simulation

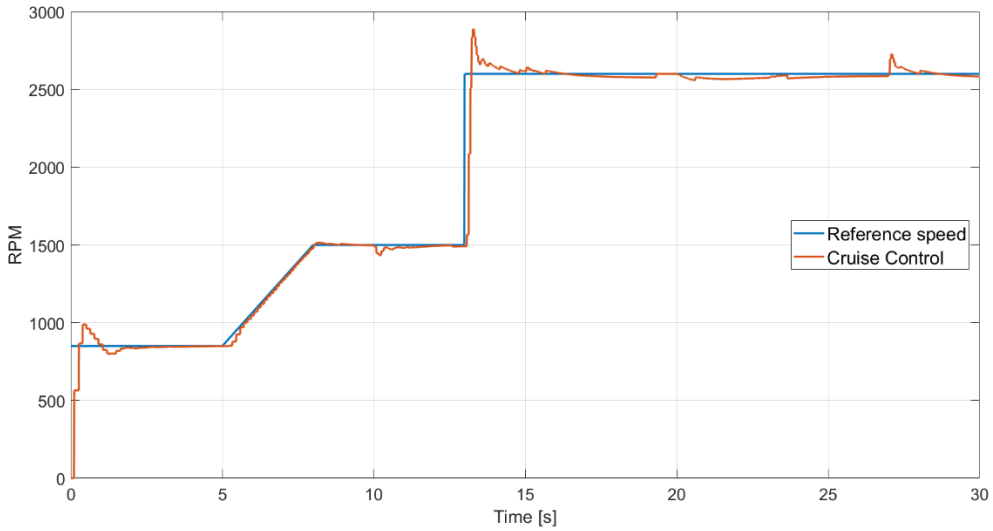


Figure 54. Cruise control system performance

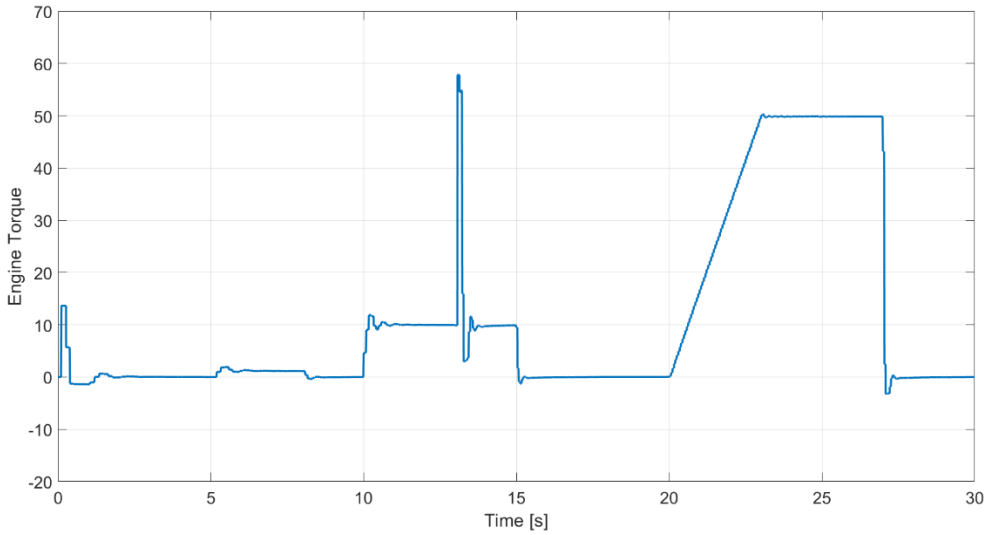


Figure 55. Brake mean engine torque

The tested engine generates a maximum torque of about 135Nm at 3000rpm, and it was tested with a maximum load that equals about 40% of the maximum torque. Engine managed to follow the reference speed with small deviations even during the load increase. The reference speed overshoot after the sudden increase of the reference speed (at 13s) is the result of the SMC. The overshoot could be reduced, but then the SMC performance under disturbances would deteriorate and it has been evaluated that the disturbance resistance is more important.

5. FMU COMPILATION

Functional mock-up interface (FMI) has become an industry standard for model exchange. A simulation model designed in most of the numerous simulation software can, with the appropriate tools, be compiled into a Functional mock-up unit (FMU). The tool for the FMU compilation is usually supplied with the simulation software but there is a growing number of the open-source FMU compilation tools that can generate the FMU from the code or a model of a certain type.

FMU's advantage lies in the fact that the designed model can be exchanged and/or sold without giving out the know-how and the hours invested in it. It serves as a black-box from which the user can only see the inputs and the outputs of the system. Some model parameters, defined by the model creator, can also be modified. FMU enables the user to perform a co-simulation between the FMU and the tool that supports the FMI.

AVL fmi.Lab is a tool developed by the AVL that can compile the FMU from the Simulink models according to the latest FMU standard (2.0). A custom part of the Simulink blocks library is developed and it contains the blocks that replace the model inputs and outputs. Model inputs are defined by the model operation. Model outputs can extract any relevant signal to be observed once the model is compiled.

A tool that supports the FMI also needs to be present at the user's desktop. Most of the simulation software used today support the FMI integration within their models.

Model inputs:

- Load signal,
- T or N model type (Section 3.2.7),
- Engine load (T model type) and
- Engine speed (N model type).

Some of the model outputs (creator of the FMU can define as many outputs out of his model as he wants, the question is only if they are all relevant):

- Engine speed (T model),
- Engine torque (N model),
- Cylinder pressure, engine speed and torque mean values, equivalence ratio etc.

The model can be parametrized in a way that allows the user to change some of the model parameters. By changing the parameters, model properties connected to the defined parameters are also modified. The choice of the parameters in this model is:

- General model parameters:
    - Engine type: 1 for NA SI engine, 2 for TC CI engine,
    - Idle speed [rpm],
    - Flywheel inertia [kg m^2] and
    - Flywheel damping [Nm s/rad]
- Engine size:
    - Cylinder diameter [m],
    - Engine displacement [m^3],
    - Number of cylinders and
    - Compression ratio.
- Advanced combustion parameters:
    - Vibe shape parameter *m*,
    - Combustion duration and
    - Firing angle.

AVL tool for office co-simulation is called AVL Model Connect. It supports multiple third-party software (Matlab\Simulink, AMESim, GT Suite, Kuli, CarMaker, CarSim etc.) and most of the AVL simulation software (Cruise, Cruise M, Boost, VSM etc.). It enables a co-simulation between the supported software on a large scale. For example, a user would like to evaluate the vehicle's performance on a certified driving cycle. Vehicle information and the connection to the environment can be designed in AVL Cruise, detailed engine model in GT Suite, thermomanagement system in Kuli, virtual driver in Simulink and the driveline in AMESim. Their model inputs and outputs are all connected in the Model Connect and simulated as a whole. The process of setting up the co-simulation is slightly more complicated, but that is not the subject of this thesis. FMU of the developed model in this thesis is shown in the figure below, in the Model Connect environment, along with its parameters.

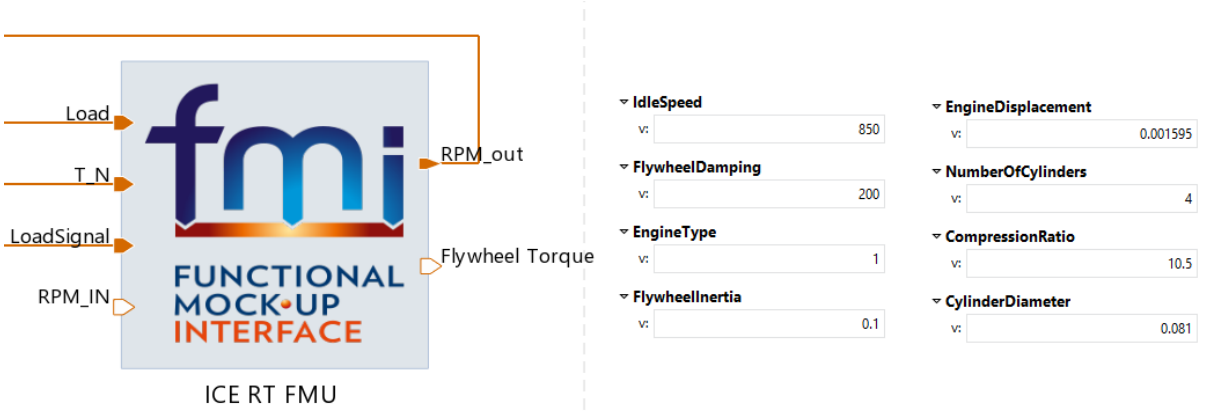


Figure 56. FMI in the Model Connect environment along with the main model parameters

The FMU is connected in T mode; engine load is input to the FMU while the speed is output from the FMU and to the rest of the model. The rest of the model consists of the vehicle specifications and driveline in Cruise and the virtual driver is designed in Simulink. Vehicle's performance is shown in the figure below where it tracks the desired velocity of the Worldwide Harmonised Light Vehicle Test Procedure (WLTP) very good, and the model is powered by the engine developed in this thesis. WLTP is the latest certified vehicle test cycle and the developed engine is tested on the first part of the cycle (first 400s).

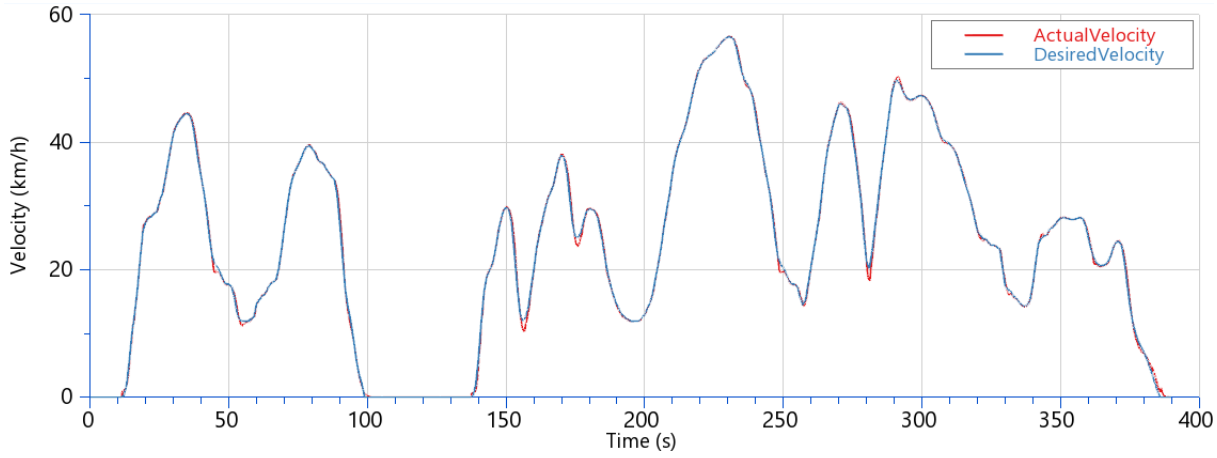


Figure 57. Vehicle velocity profile, WLTP

6. CONCLUSION

The task of this thesis was to design a real-time capable internal combustion engine model with the accompanying control systems. The designed model had to reproduce engine speed and torque fluctuations precisely and with adequate accuracy. That feature would distinguish the model from the more common mean value models that calculate only the mean value of the engine variables. Simulation results from the developed model would provide reference points and reduce the setup time of a real engine on a real engine testbed.

First, the accuracy and model type were chosen. A fine combination of theoretical and experimental modeling was needed for the model to calculate satisfying results, while also remaining real-time capable.

The traces model was designed first, engine variables and calculations being a part of the crank-angle domain. Cylinder geometry relations, combustion model, initial conditions and torque calculations were described and the model results were validated with a certified software. The model was transferred to the time domain through a transient model where the model variables are now time-dependent. Necessary modifications were made along with the definition of the rest of the engine parameters, e.g. the engine friction and inertia.

The idle speed control system was developed next. Different types of possible controllers were considered; an ordinary PI controller, PI + Sliding Mode Controller and only a Sliding Mode Controller (SMC). The SMC proved to have the best performance among the tested controllers, and in a variety of engine types and sizes. It was selected as the default idle speed controller and later included within the cruise control strategy. The cruise control system was realized as a reference speed tracker and served as another benchmark test for the developed controller.

Finally, the model was compiled as a Functional Mock-up Unit (FMU), an industrial standard for model exchange. Important model parameters that determine the engine type and size were made available for the user to modify to his preferences. The compiled FMU's performance was tested in the AVL Model Connect environment.

The thesis goals were accomplished. A real-time capable internal combustion engine model along with the accompanying control systems was developed and its performance and accuracy were verified on the certified software.

The cylinder pressure was verified against the simulation results of an equivalent cylinder in the AVL Cruise M environment. The data for the NA SI and TC CI engine across the engine sizes, different engine speeds and different load signals don't deviate more than 10-15%, which

is deemed satisfactory and accurate enough for the required purpose. The calculated indicated torque, that results from the cylinder pressure acting on the piston and the piston inertia forces, was verified against the data from AVL Excite, with the equivalent piston and conrod masses. The results match almost perfectly leading to the conclusion that the engine indicated torque is calculated well.

The traces model was transferred to the transient model with some approximations which proved to be accurate. Engine model performed well in transient operation and under various conditions, disturbances and parameters. Engine friction and inertia was described. Elastic connection with the testbed was realized through the concept of a dual-mass flywheel which reduced the engine speed and torque fluctuations.

The sliding mode control proved to have the best performance among the tested controllers and has been selected for the default controller of the developed model. It had the best evaluation factor scores which vouched for good controller performance and responded well to a different array of reference idle speeds and different engine types and sizes. It also had the lowest speed deviations on imposed disturbances, compensating them efficiently. It was also used for the cruise control system of the model. Cruise control with the SMC proved to be robust to the disturbance and reference deviations, tracking the reference speed efficiently.

The model was compiled to FMU and successfully incorporated into a co-simulation in the AVL Model Connect environment. It was simulated as a T and as an N model, and both versions performed well, interacting with the other co-simulation models appropriately

Possible improvements of the model might include more engine types (turbocharged spark ignition engine or a naturally aspirated compression ignition engine) or support for more engine configurations (V configuration). The model could also expand to a more theoretical basis, replacing some of the look-up tables with calculated variables, but the real-time capability has to be ensured.

Although the thesis is completed, the work on the model is not. Compiling the model into FMU was just the first step of simulating the real behavior of the engine on the testbed. The model has to be compiled into another format (.ecp), which can be run within the AVL Testbed Connect environment where the model will eventually emulate the real engine performance on the testbed. With the model real-time capability ensured, further improvements of the model in the desired directions will not pose much of a problem.

REFERENCES

[1] Iserman R.: Engine modeling and control, Springer, 2014.

[2] https://www.avl.com/documents/10138/2056996/AVL+Testbed , AVL Testbed environment, page visited November 16th, 2018.

[3] Guzella L., Onder C.H.: Introduction to modeling and control of internal combustion engine systems, Springer, 2010

[4] Sjekavica M.: Modeling and control of a modern turbocharged diesel engine, 2009.

[5] Deur J., Hrovat D., Petrić J., Šitum Ž.: A control oriented polytropic model of SI engine intake manifold, ASME, 2003.

[6] AVL Boost team: Boost theory, AVL, 2018.

[7] Heywood J.B.: Internal combustion engine fundamentals, McGraw-Hill, Inc., 1988.

[8] Mahalec I., Lulić Z., Kozarac D.: Internal combustion engines, Lecture notes, University of Zagreb, 2012.

[9] Mahalec I., Lulić Z., Kozarac D.: Engine design, Lecture notes, University of Zagreb, 2015.

[10] Krishnan S.: Combustion engines, Lecture notes, University of Alabama, 2003.

[11] Kozarac D.: Overview of the ICE combustion models, Lecture notes, University of Zagreb, 2018.

[12] Demirel Y.; Green energy and technology, Springer, 2012.

[13] Klein M., Erkisson L.: A comparison of specific heat ratio models for cylinder pressure modeling, Linkopings Universitet, 2004.

[14] Nayeri M.H.: Cylinder-by-cylinder torque model of an SI-engine for real-time applications, Master's thesis, Linkopings Universitet, 2005.

[15] Shiao Y., Pan C., Moskwa J.J.: Advanced dynamic spark ignition engine modeling for diagnostics and control, University of Wisconsin – Madison, 1994.

[16] Hendricks E., Sorenson S.C.: Mean value modeling of spark ignition engines, International congress and exposition, Detroit, 1990.

[17] Hoag K., Dondlinger B.: Vehicular engine design, Springer, 2016.

[18] Hrovat D., Sun J.: Models and control methodologies for IC engine idle speed control design, Ford Research Laboratory, 1997.

[19] Deur J., Ivanović V., Pavković D., Jansz M.: Identification and Speed control of SI engine for Idle Operating Mode, University of Zagreb and Ford Motor Company, 2004.

[20] Kjergaard L., Nielsen S., Vesterholm T., Hendricks E.: Advanced nonlinear engine idle speed control systems, Technical University of Denmark, 1994.

[21] Slotine J.J.E., Li W.: Applied Nonlinear Control, Prentice Hall, 1991.

[22] Kao M., Moskwa J.J.: Nonlinear Diesel Engine control and Cylinder Pressure Observation, Universitiy of Wisconsin, 1995.

[23] Kasać J.: Control of technical systems, Lecture notes, University of Zagreb, 2007.

[24] Ortega R., Astolfi A., Barbanov N.E.: Nonlinear PI Control of Uncertain Systems: An alternative to parameter adaptation, 2002.

[25] Haugen F.: The Good Gain method for simple experimental tuning of PI controllers, Telemark university college, 2012.

[26] Kuo T.C., Huang Y.J., Chen C.Y., Chang C.H.: Adaptive Sliding Mode Control with PID Tuning for Uncertain systems, Ching Yun University, Taiwan and Yuan-Ze University, Taiwan, 2008.

APPENDICES

A Engine model parameters definition

B Indicated cylinder pressure validation

C Indicated cylinder torque validation

Appendix A

In this appendix, model parameters values will be defined.

Engine 1 parameters:

NA SI engine.

$D = 0.081m$

$V_E = 0.001595m^3$

$z = 4$

$\varepsilon = 10.5$

Engine 2 parameters:

TC CI engine.

$D = 0.081m$

$V_E = 0.001968m^3$

$z = 4$

$\varepsilon = 19$

Engine 3 parameters:

NA SI engine.

$D = 0.085m$

$V_E = 0.002996m^3$

$z = 6$

$\varepsilon = 12$

Engine 4 parameters:

NA SI engine.

$D = 0.0745m$

$V_E = 0.000999m^3$

$z = 3$

$\varepsilon = 10$

Engine 5 parameters

TC CI Engine

$D = 0.084m$

$V_E = 0.001496m^3$

$z = 3$

$\varepsilon = 16.5$

If the NA SI Engine is selected for the simulation, these are the default values for other model parameters.

$H_l = 43.5 \cdot 10^6 \frac{MJ}{kg}$

$Z_0 = 14.5$

$\alpha_c = 55°$

$m = 2$

$\alpha_0 = -20°$

$T_0 = 300K$

If the TC CI Engine is selected for the simulation, these are the default values for other model parameters.

$H_l = 42.8 \cdot 10^6 \frac{MJ}{kg}$

$Z_0 = 14.7$

$\alpha_c = 70°$

$m = 1$

$\alpha_0 = -10°$

$T_0 = 330K$

General model parameters

These are the general model parameters, which do not change.

$\lambda_c = \frac{1}{3.5}$

$C = -6.9078$

$R = 287 \frac{J}{kg \cdot K}$

$T_e = 1100K$

$p_h = 10^5 Pa$

Heat loss parameters

$C_1 = 2.28$
$C_2 = 0.00324$
$T_{TDC} = 555K$
$T_{BDC} = 355K$
$T_h = 590K$
$T_p = 615K$

SMC parameters

$\lambda_{SMC} = 1$
$K_{SMC,SI} = 0.001$
$K_{SMC,CI} = 0.01$
$L = 100$

Appendix B

In this appendix, model validation is performed. The data from the model are compared to the data from the certified software, AVL Cruise M. A couple of the cases are considered, differing in the load signal value and engine type.

NA SI Engine

Parameters as defined in the previous section.

Load signal = 0

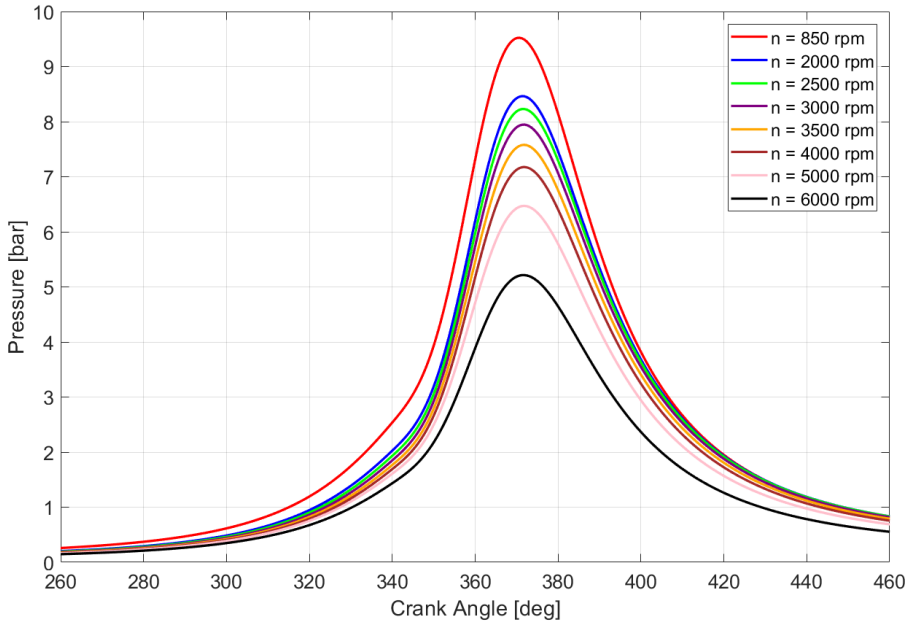


Figure B.1. Cylinder pressure trace through various engine speeds, Engine 1, data from Appendix A, load signal = 0, thesis model results

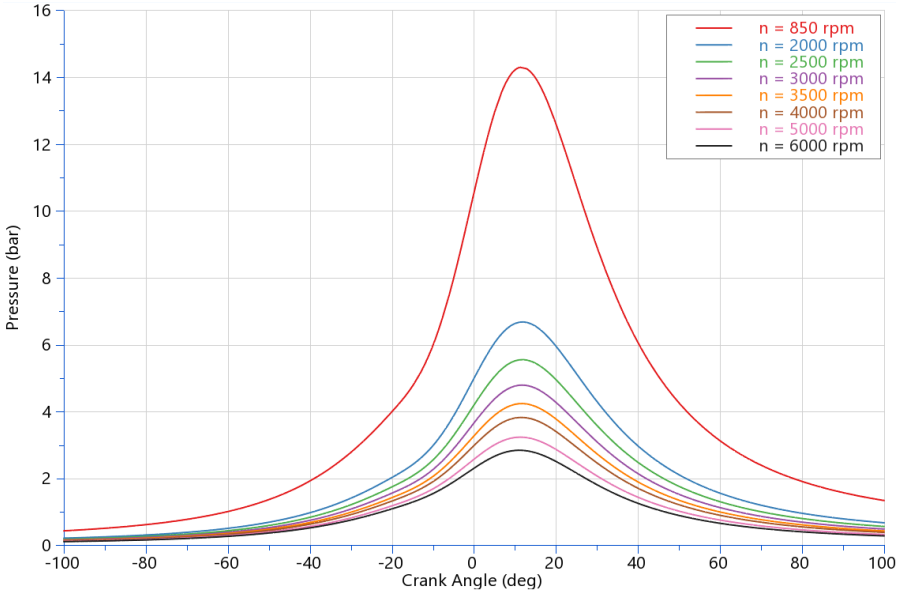


Figure B.2. Cylinder pressure trace through various engine speeds, Engine 1, data from Appendix A, load signal = 0, AVL Cruise M results

Load signal = 0.2

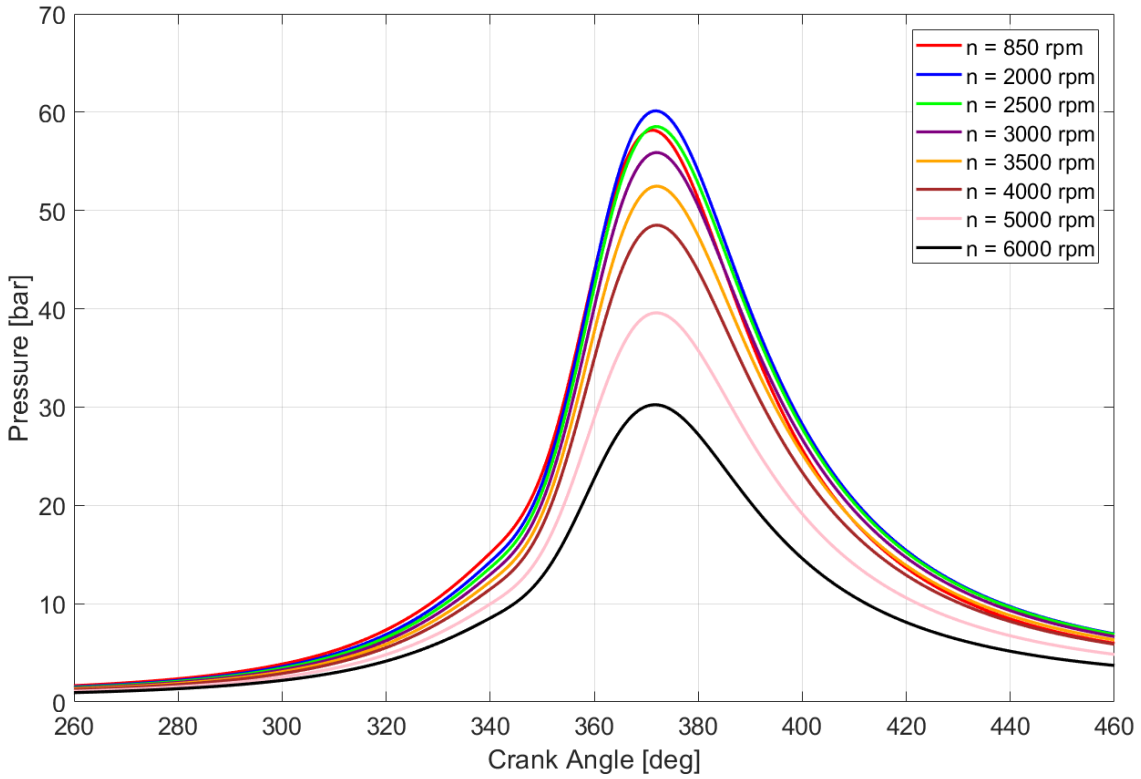


Figure B.3. Cylinder pressure trace through various engine speeds, Engine 4, data from Appendix A, load signal = 0.2, thesis model results

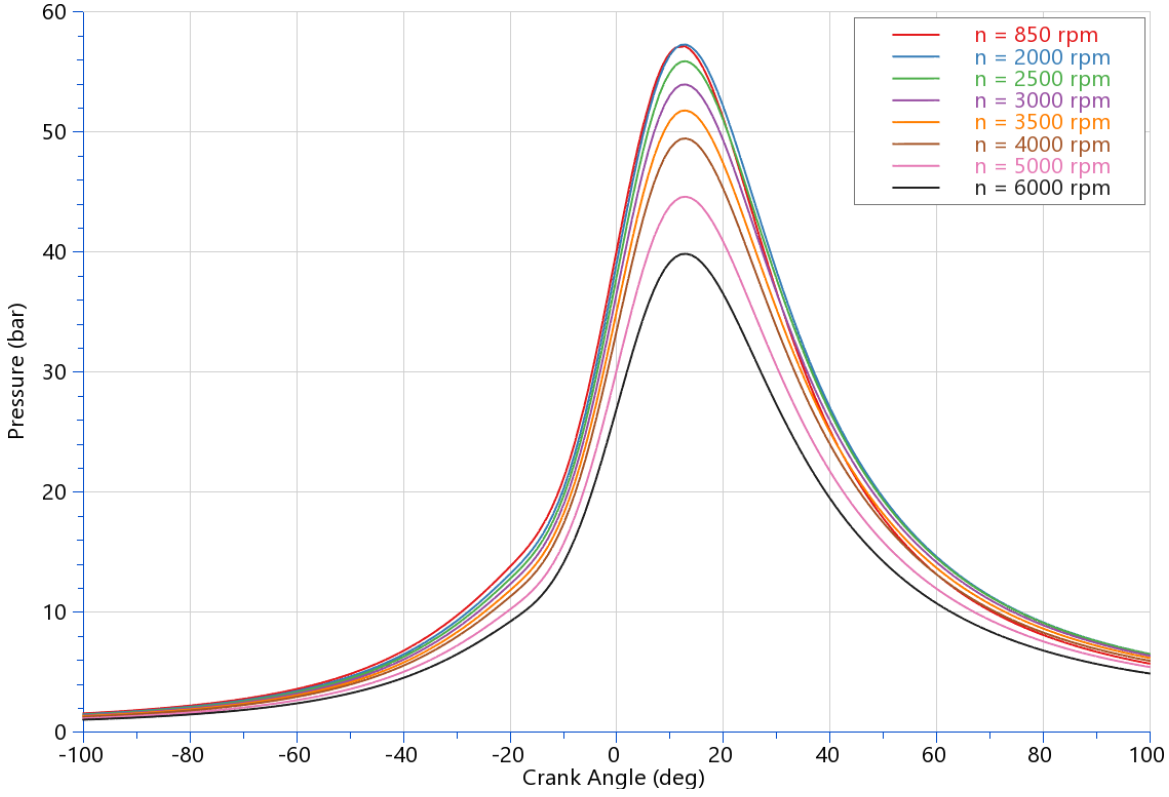


Figure B.4. Cylinder pressure trace through various engine speeds, Engine 4, data from Appendix A, load signal = 0.2, AVL Cruise M results

Load signal = 1

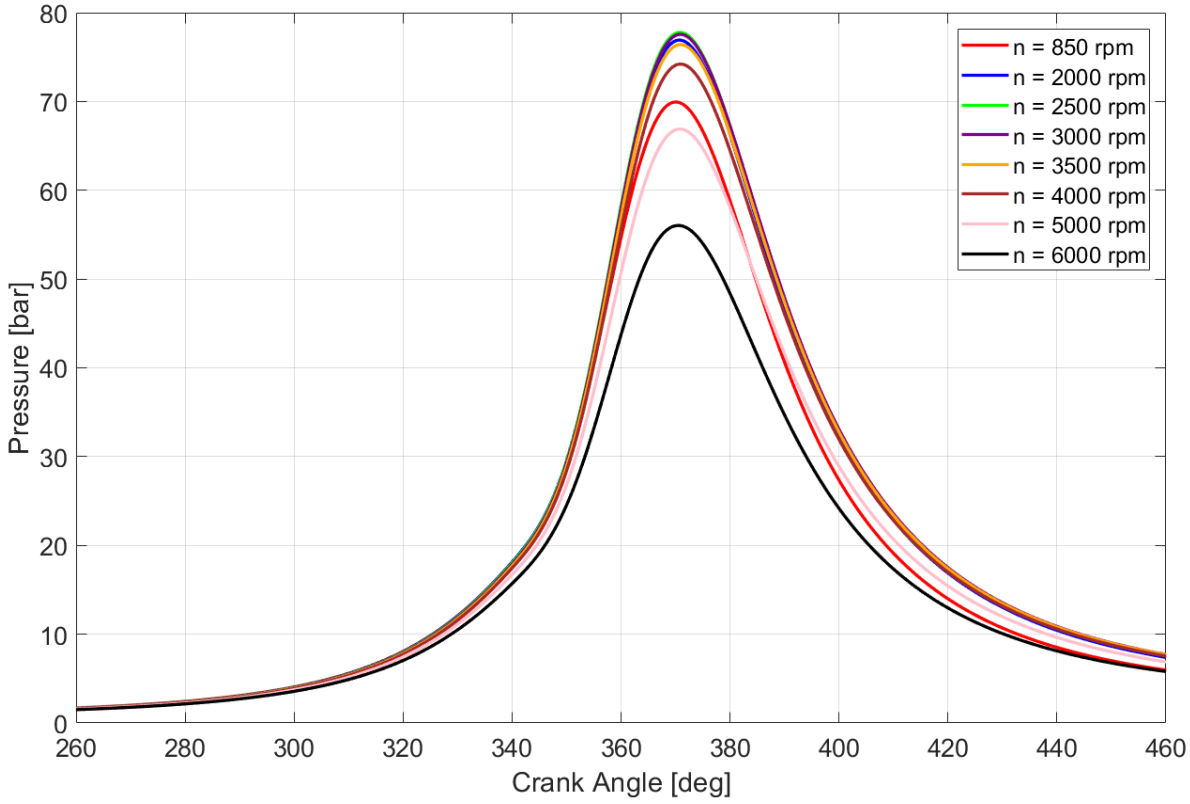


Figure B.5. Cylinder pressure trace through various engine speeds, Engine 3, data from Appendix A, load signal = 1, thesis model results

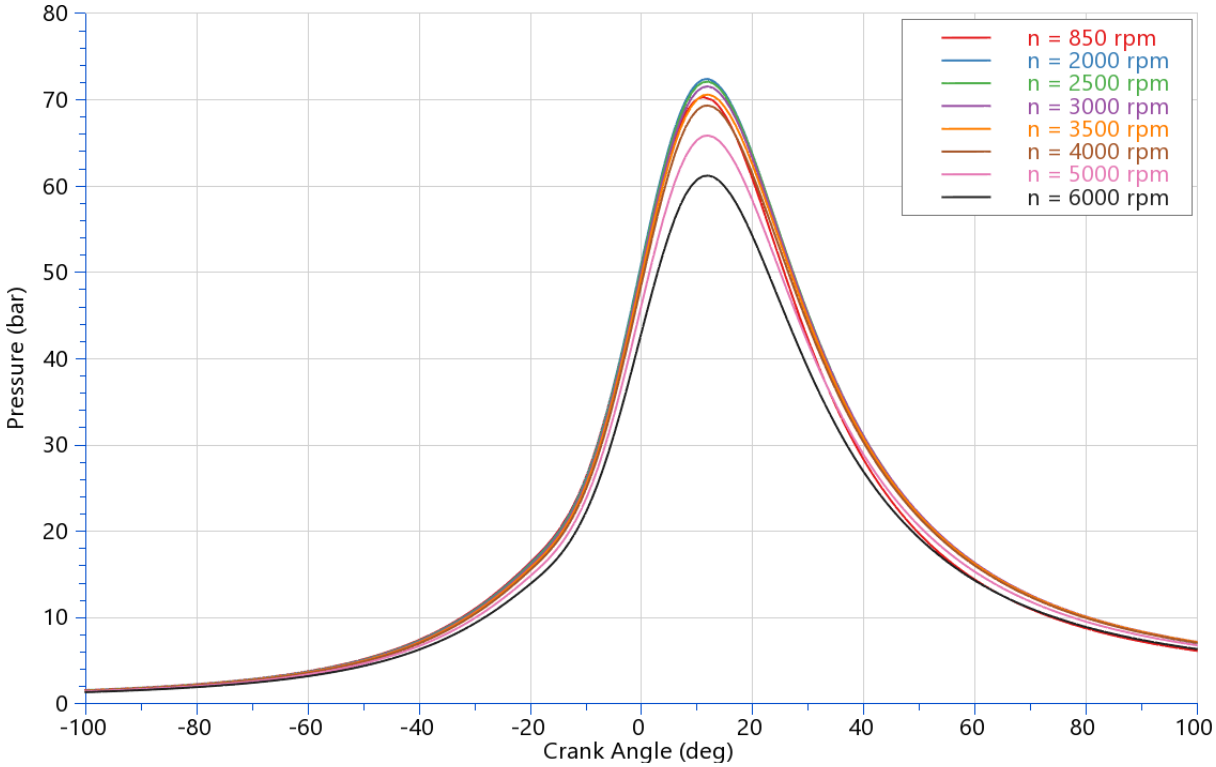


Figure B.6. Cylinder pressure trace through various engine speeds, Engine 3, data from Appendix A, load signal = 1, AVL Cruise M results

TC CI Engine

Parameters are as defined in the previous section

Load signal = 0.3

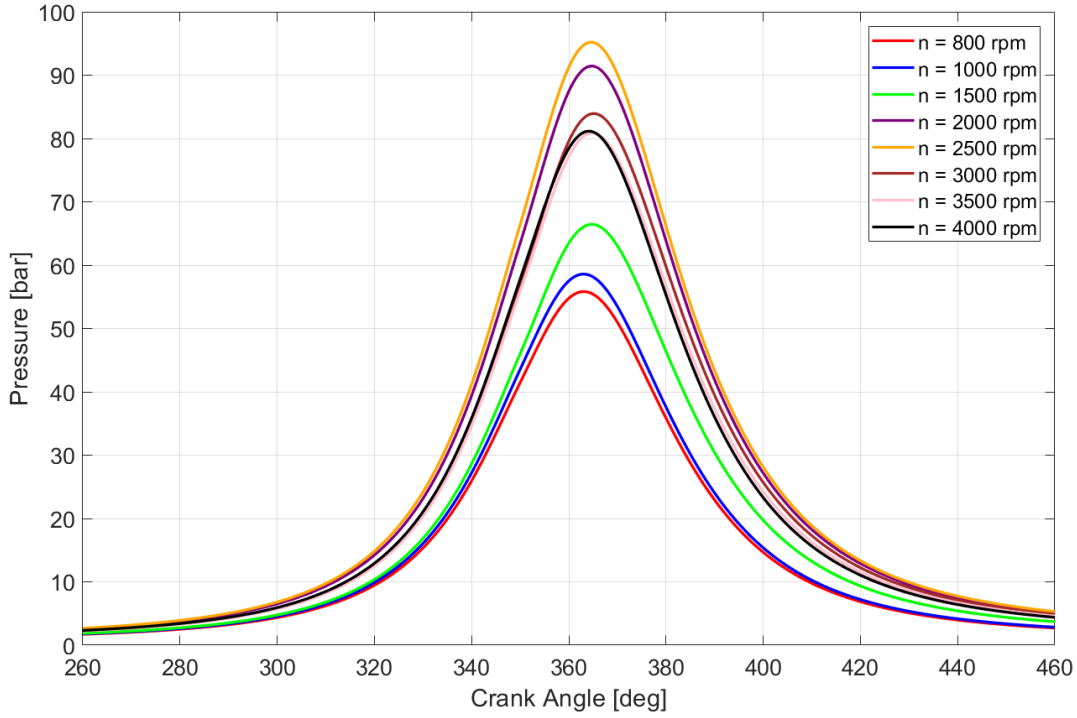


Figure B.7. Cylinder pressure trace through various engine speeds, Engine 2, data from Appendix A, load signal = 0.3, thesis model results

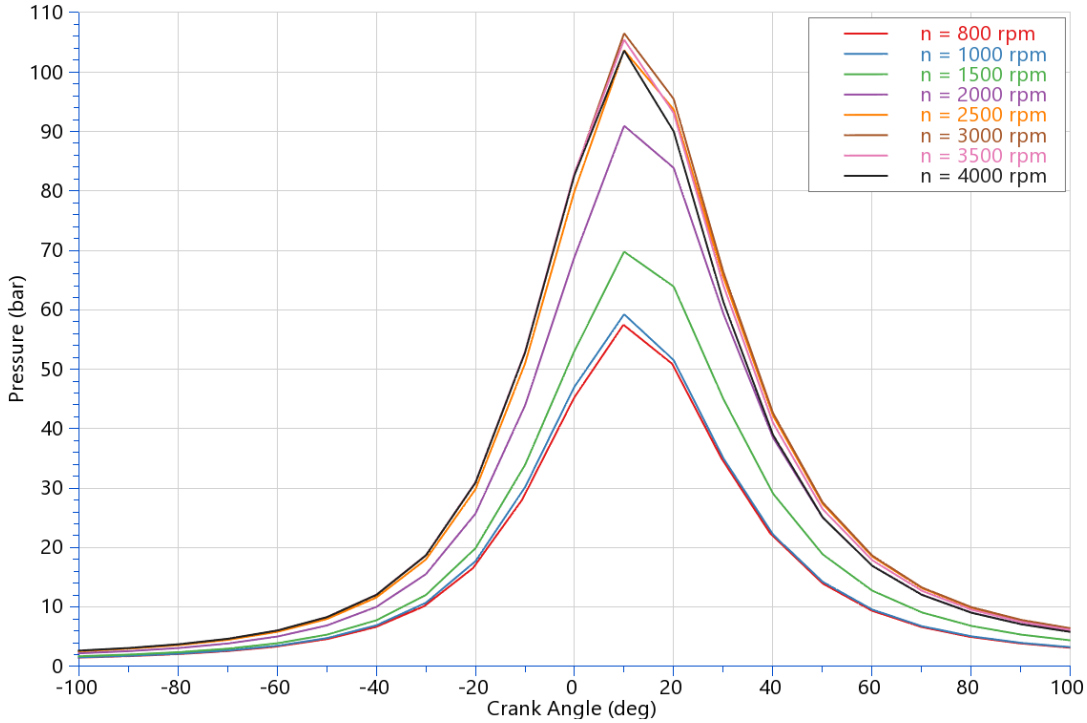


Figure B.8. Cylinder pressure trace through various engine speeds, Engine 2, data from Appendix A, load signal = 0.3, AVL Cruise M results

Load signal = 0.6

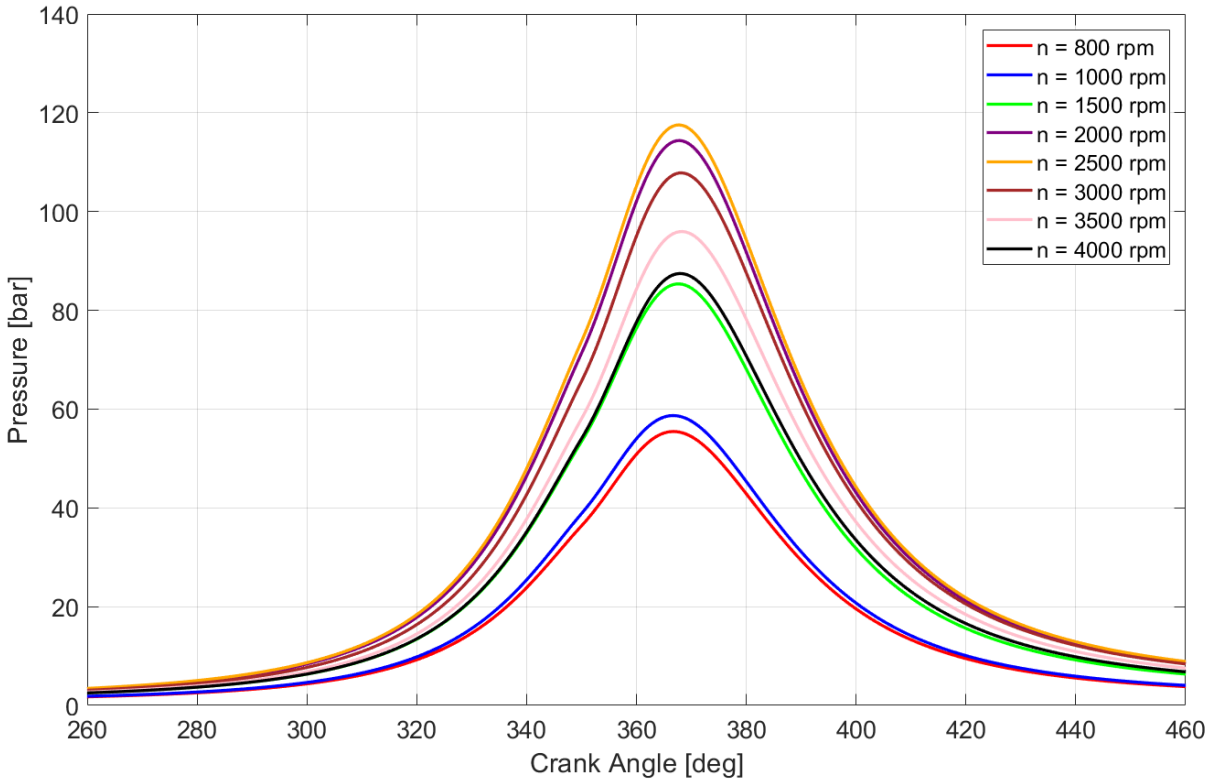


Figure B.9. Cylinder pressure trace through various engine speeds, Engine 5, data from Appendix A, load signal = 0.6, thesis model results

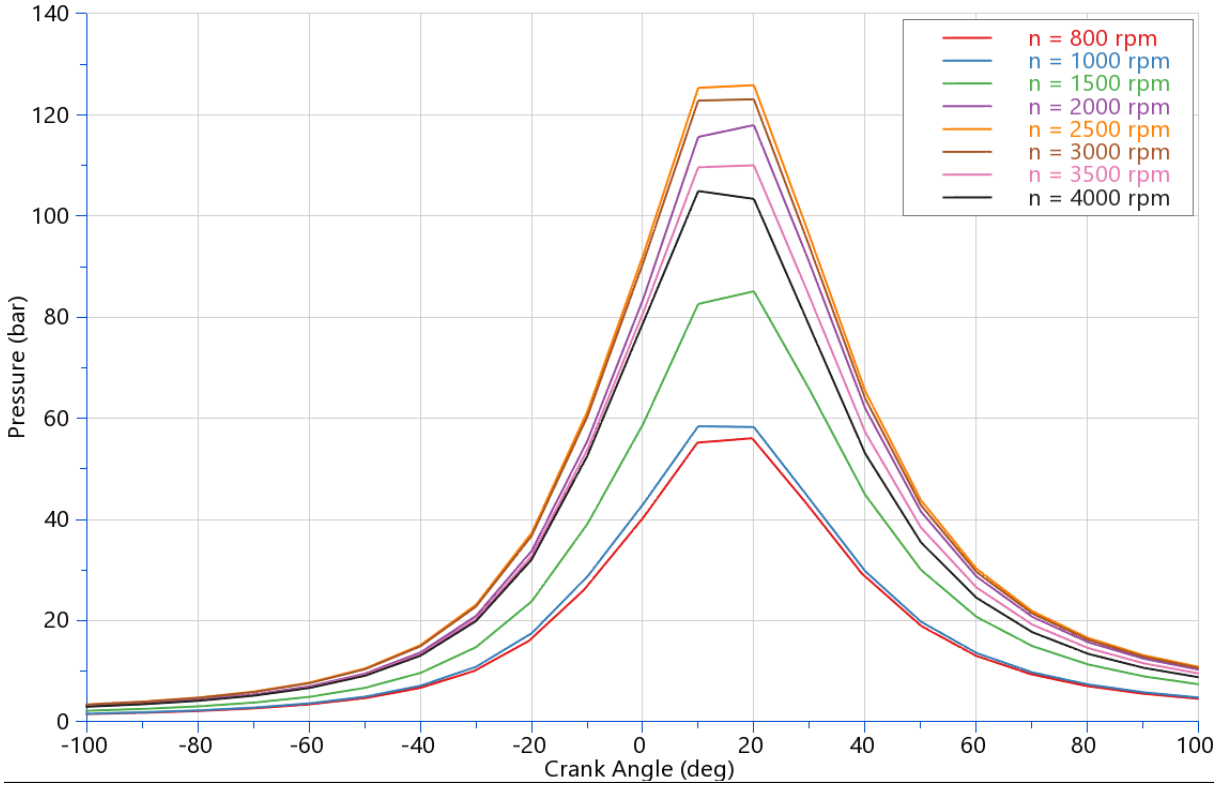


Figure B.10. Cylinder pressure trace through various engine speeds, Engine 5, data from Appendix A, load signal = 0.6, AVL Cruise M results

Appendix C

In this appendix, results validation of the indicated torque from one cylinder will be performed. The data from the thesis model will be compared to the certified software, AVL Excite.

NA SI Engine

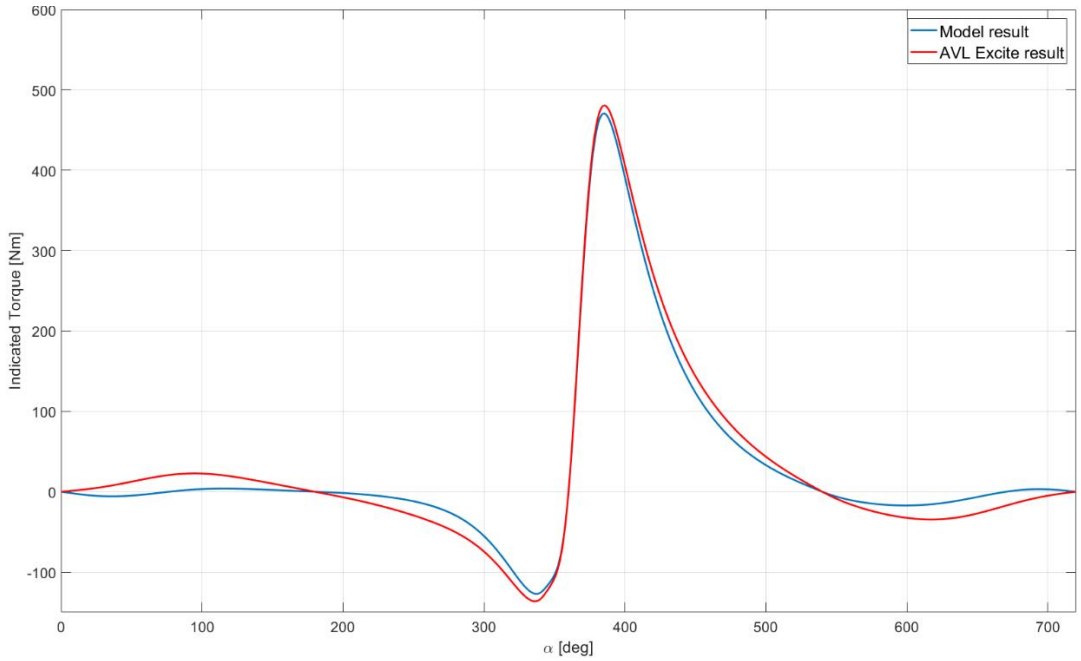


Figure C.1. Indicated torque one cylinder trace, Engine 1, data from Appendix A, load signal = 1, engine speed = 850rpm, thesis model result and AVL Excite result comparison

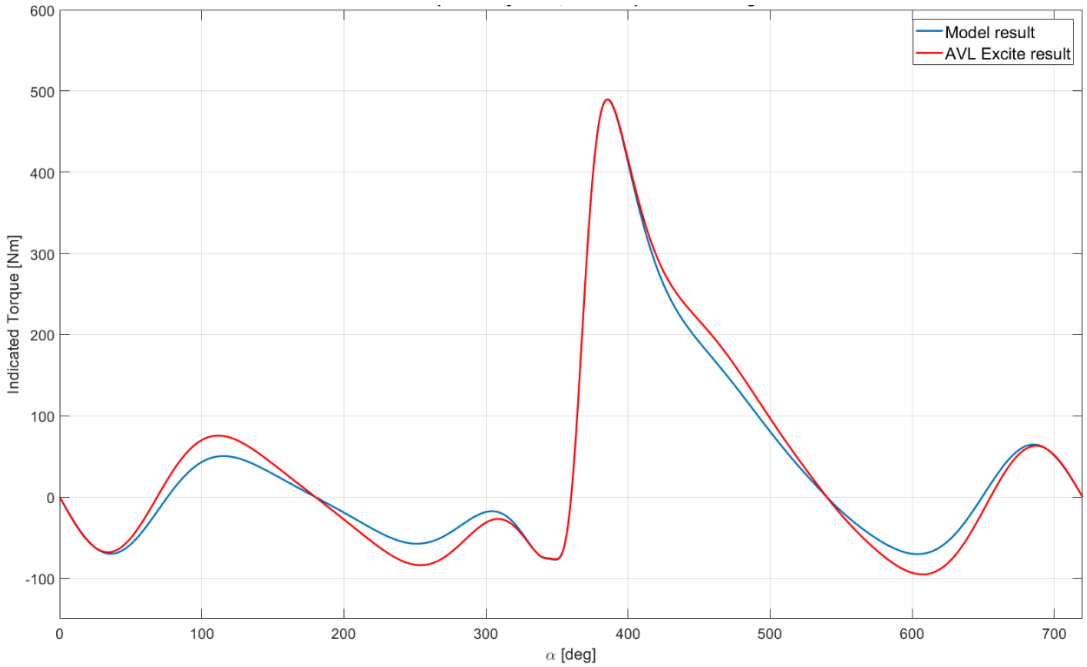


Figure C.2. Indicated torque one cylinder trace, Engine 1, data from Appendix A, load signal = 1, engine speed = 3000rpm, thesis model result and AVL Excite result comparison

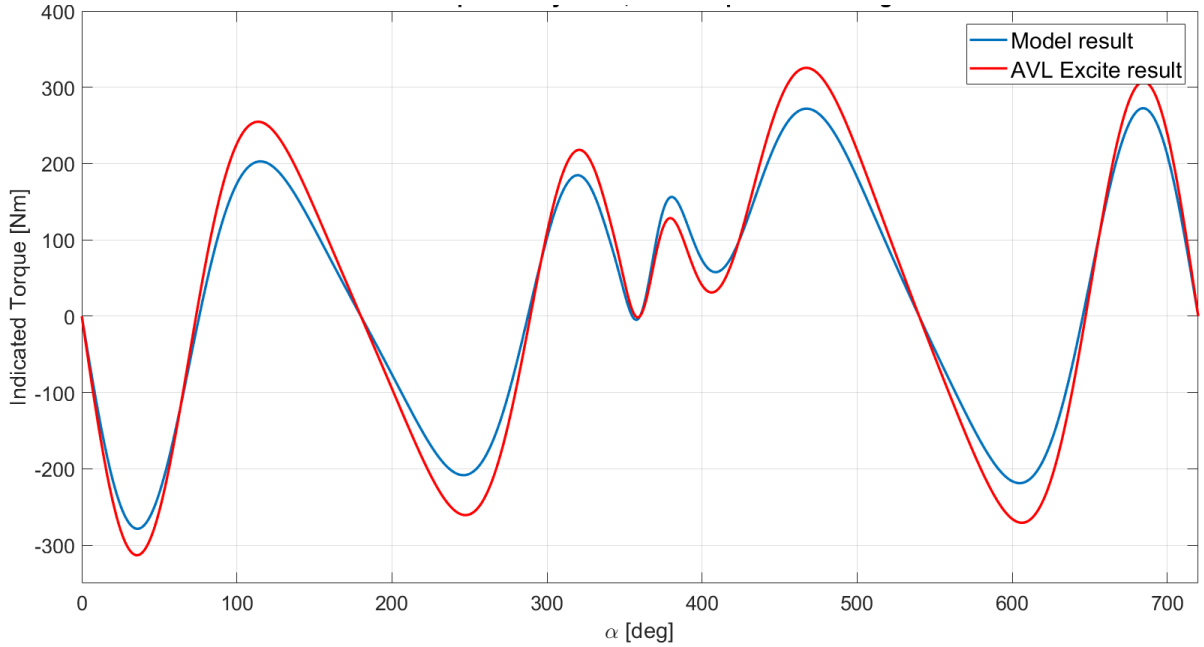


Figure C.3. Indicated torque one cylinder trace, Engine 1, data from Appendix A, load signal = 1, engine speed = 6000rpm, thesis model result and AVL Excite result comparison

TC CI Engine

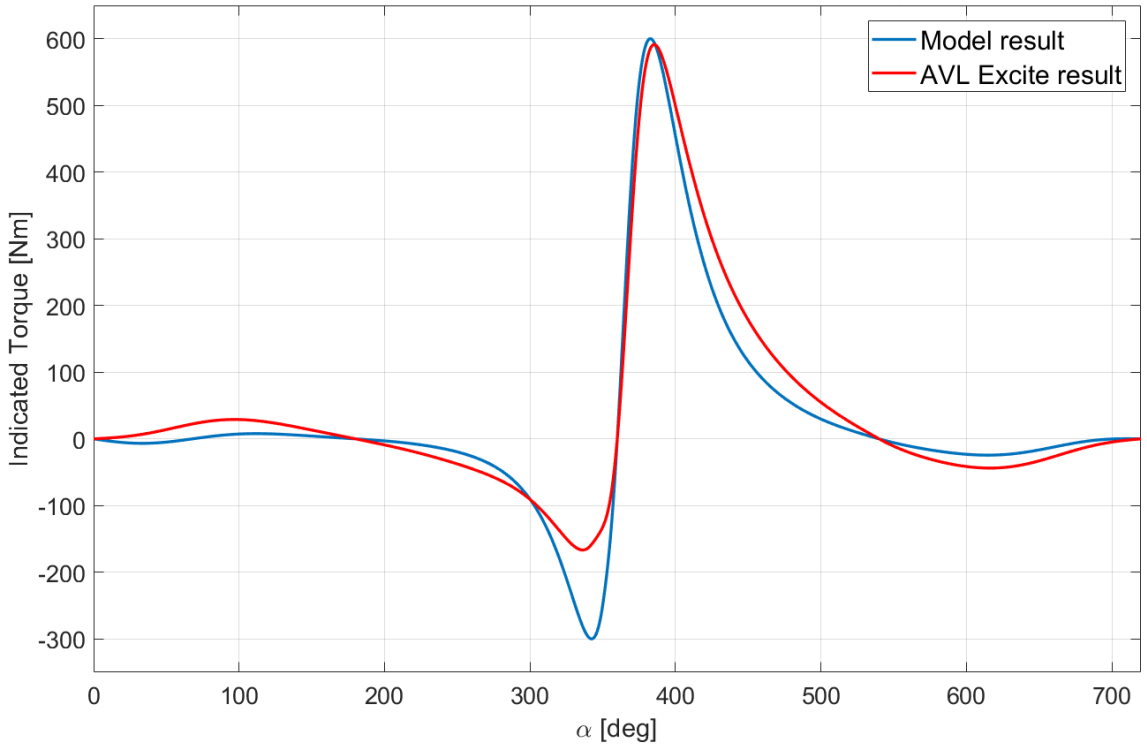


Figure C.4. Indicated torque one cylinder trace, Engine 2, data from Appendix A load signal = 1, engine speed = 850rpm, thesis model result and AVL Excite result comparison

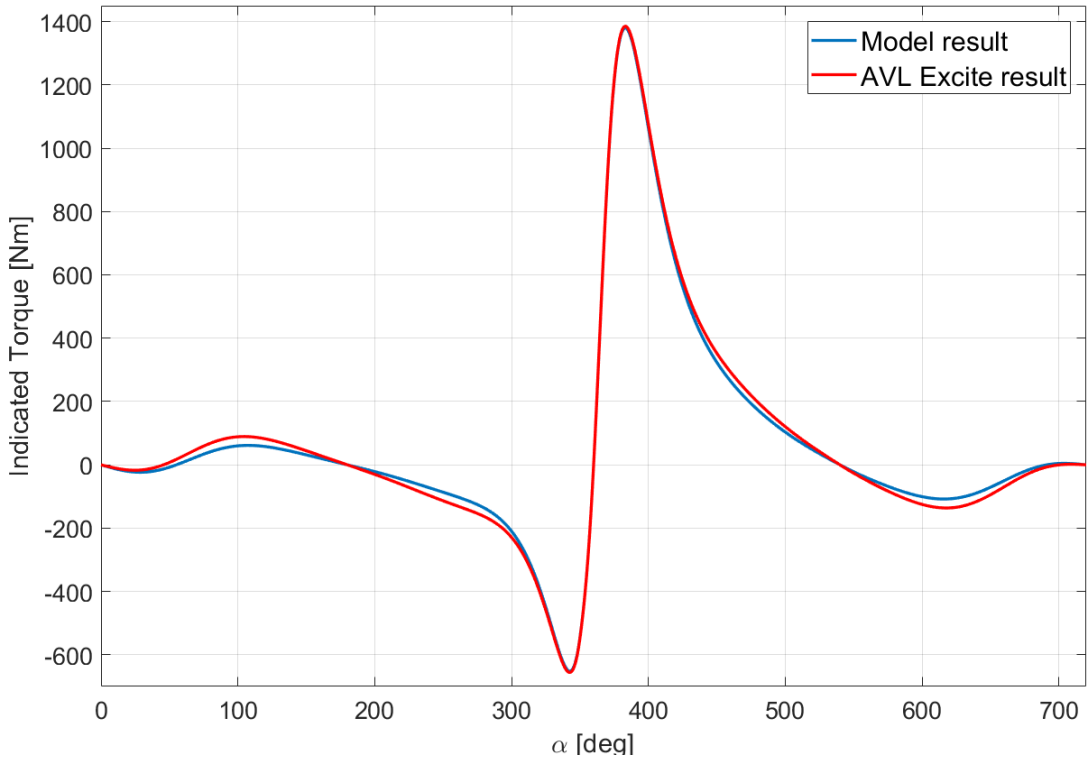


Figure C.5. Indicated torque one cylinder trace, Engine 2, data from Appendix A, load signal = 1, engine speed = 2000rpm, thesis model result and AVL Excite result comparison

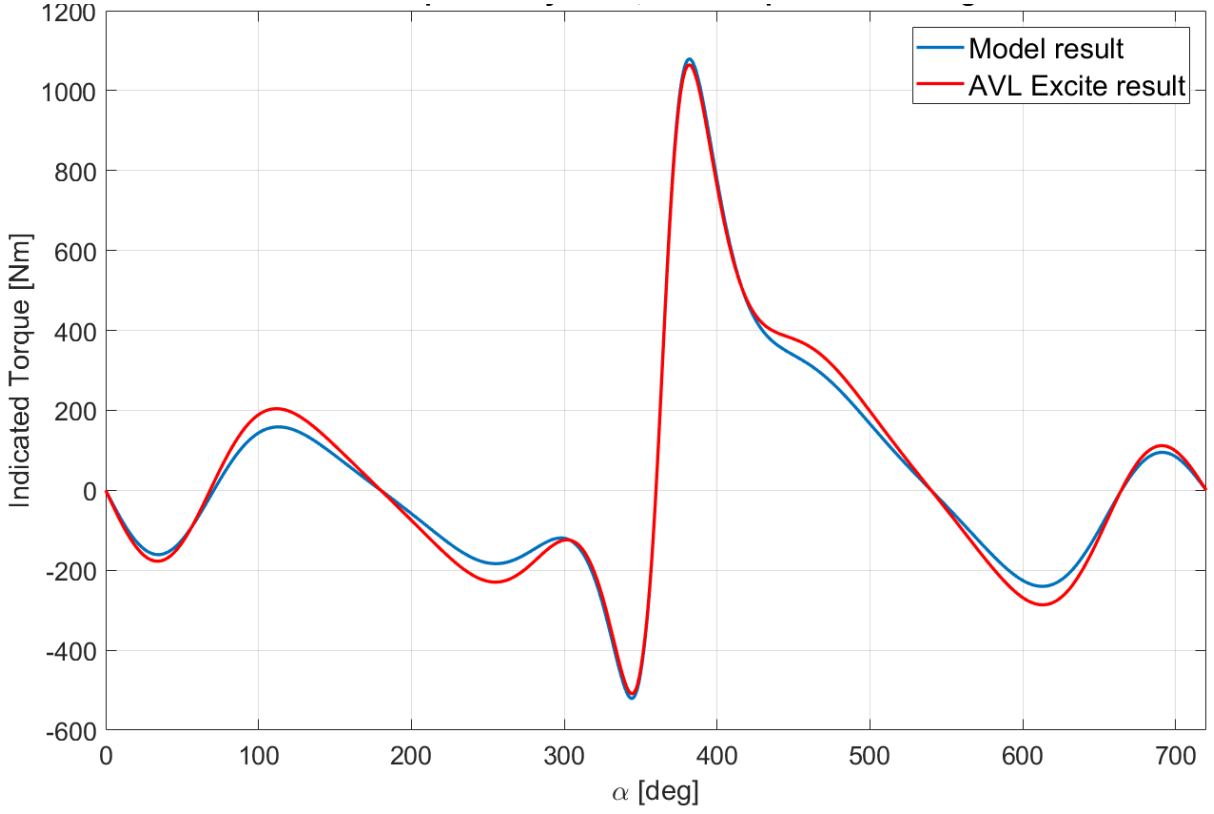


Figure C.6. Indicated torque one cylinder trace, Engine 2, data from Appendix A, load signal = 1, engine speed = 4000rpm, thesis model result and AVL Excite result comparison